Characterizing the Efficacy of Ice Recrystallization Inhibitors as a Novel Cryoprotectant for Lung Cryopreservation

by

Larissa J. Lautner

A thesis submitted in partial fulfillment of the requirements for the degree of

Master of Science

Department of Surgery
University of Alberta

Abstract

Although lung transplant remains the only option for patients suffering from end-stage lung disease, donor lung supply is currently insufficient to meet demand. While many lungs become available for transplant, most are discarded due to failure to meet physiologic or compatibility criteria. Many lungs are currently unutilized due to short preservation times, with lungs surviving only 6-8 hours on ice. Successful cryopreservation of lungs would allow for extended storage to help ameliorate this problem; however, many challenges must be overcome before this can occur.

The growth of existing ice at the expense of new ice nucleation is called ice recrystallization, and it is one of the major causes of freezing injury, as it results in osmotic stress and mechanical damage to cellular membranes, intercellular connections, and intracellular organelles. Previous research has demonstrated that ice recrystallization can be controlled through the use of small-molecule ice recrystallization inhibitors (IRIs). Therefore, the research performed for this thesis aimed to assess the utility of these IRIs as novel cryoprotectants for lung cryopreservation. It was hypothesized that IRIs would not be cytotoxic and would be capable of controlling intra- and extra-cellular ice growth resulting in improved cellular survival following cryopreservation of type II pneumocyte monolayers and rat lung tissue, when compared to DMSO-treated controls.

The first objective of this work assessed the ability for IRIs to reduce intracellular ice grain size and improve post thaw survival, without cytotoxicity, in the immortalized type 2 pneumocyte cell line BEAS-2B. Short- and long-term cytotoxicity of two IRI compounds was compared to the commonly used cryoprotectant, DMSO, through the use of the metabolic assay reagent alamarBlue™. Intracellular ice grain size was quantified after cells treated with IRIs, with or without the addition of DMSO, were cryofixed and stained with SYTO13 and observed under fluorescent microscopy. Post-thaw membrane integrity and metabolism was assessed following intracellular ice nucleation and recrystallization in samples treated with DMSO, with or without the

addition of one IRI. These experiments indicated that one IRI, (2-fluorophenyl)-C6-azido-D-gluconamide (2FA), was non-toxic and reduced intracellular ice grain size when used alone. However, no reduction of intracellular ice grain size was observed when 2FA was added to DMSO, which corroborated with the finding that post-thaw survival was not improved by 2FA addition to DMSO.

The second objective of this work set out to develop low-cost subnormothermic techniques for *ex vivo* rat lung perfusion to assess the cytotoxicity of 2FA and ability for 2FA to reduce extracellular ice growth resulting in improved post-thaw cell membrane integrity and tissue structural integrity, when compared to DMSO-treated controls. After rat lungs were perfused subnormothermically with 2FA in STEEN solution™, toxicity was assessed through the perfusion of 0.4% (w/v) trypan blue prior to fixation, paraffin-embedding, sectioning, eosin staining, and visualization under light microscopy. The ability for 2FA to reduce extracellular ice grain size was assessed using tissue cryofixation after a 1 h hold at -20 °C. Post-thaw cell membrane integrity and tissue morphology was assessed by perfusing rat lungs with 0.4% (w/v) trypan blue and 10% (v/v) DMSO, with or without the addition of 2FA, freezing to -20°C, and thawing in a 37 °C water bath. The addition of 2FA was found to improve post-thaw alveolar cell membrane integrity and tissue morphology when compared to DMSO treatment alone.

This work successfully demonstrated that one IRI, 2FA, is not cytotoxic and reduces intra- and extra-cellular ice grain size in pneumocyte monolayers and rat lungs, respectively, when used alone. While previous work has demonstrated intracellular ice control by IRIs, this work expands on previous findings by demonstrating a reduction in extracellular ice grain size within lung tissue and revealing the limitations of intracellular ice control by IRIs when used with DMSO. In addition, this is the first work to assess ice-allowing cryopreservation of lungs. Given the underrepresentation of lungs in the whole organ cryopreservation literature, the techniques described here may be utilized by other researchers to assess cryoprotectant efficacy, in terms of

cytotoxicity, ice control, and post-thaw cell membrane integrity and tissue morphology. Therefore, this work contributes to the fields of cryobiology and organ preservation, as it expanded upon the uses and limitations of IRIs and developed low-cost techniques for the analysis of whole rat lung cryopreservation.

Preface

The research project, of which this thesis is a part, received research ethics approval from the University of Alberta Research Ethics Board, Project Name "Organ Preservation Techniques", AUP00003409, October 16th, 2019.

A large portion of Chapter 1 has been published as L.J. Lautner, D.H. Freed, J. Nagendran, and J.P Acker, "Current techniques and the future of lung preservation", *Cryobiology*, https://doi.org/10.1016/j.cryobiol.2020.04.009 [117]. I was responsible for the manuscript composition, D.H. Freed assisted with manuscript revision, and J. Nagendran, and J.P Acker were the supervisory authors who assisted in concept formation and manuscript revision.

The technique utilized for cryofixation in Chapter 3 has been published as L. Lautner, N. William, and J.P. Acker, "High subzero cryofixation: A technique for observing ice within tissues", *Cryobiology,* https://doi.org/10.1016/j.cryobiol.2020.05.008 [118]. I assisted in the development of the experimental design, performed the data collection and analysis, composed the abstract, results, and discussion sections of the manuscript, and assisted in manuscript revision. N. William assisted in the development of the experimental design, processed the experimental specimens, composed the introduction and methods sections of the manuscript, and assisted in manuscript revision. J.P. Acker was the supervisory author and he assisted in concept formation and manuscript revision.

Acknowledgments

I am exceptionally grateful for the support and guidance of several individuals who made this work possible.

First, I would like to thank my fantastic supervisors, Dr. Jason Acker and Dr. Jayan Nagendran, for their mentorship and support throughout this degree. Dr. Jason Acker's influence has greatly improved the quality of the research I conduct, as he has patiently guided me through the complexity of cryobiology research. Dr. Jayan Nagendran has offered strong encouragement and enthusiasm every step of the way. Together, they have offered a source of inspiration and have challenged me every day to become a better scientist.

I would like to express my gratitude to Sayed Himmat for helping me through the process of animal ethics and teaching me how to perform small animal surgery. His support, patience, and encouragement throughout my degree have made an exceptional difference.

I would like to thank the members of my thesis defense and committee, including Dr. Kieran Halloran, Dr. Jason Acker, Dr. Jayan Nagendran, and Dr. Grace Lam for their time and thoughtful review which has greatly improved the quality of my work.

I am thankful to all the members of the Acker/Elliott Labs, past and present, who have offered support and inspiration, including, but not limited to, Anusha Sajja, Wenhui Li, Tracey Turner, Carly Olafson, Olga Mykhailova, April Xu, and Leah Marquez-Curtis.

I am grateful for the opportunity to have worked alongside Nishaka William; whose project paralleled my own. His work ethic, optimism, and support inspired me to work harder each day.

Lastly, I would like to thank my parents, Adrianne, Chuck, and Arthur, my brother, Eric, and all my friends and family who have offered encouragement and support throughout this degree.

Table of Contents

Tables

Figures

List of abbreviations

AFP : antifreeze proteins

DCD : donated after circulatory death

DMSO : Dimethyl Sulfoxide (Me_2SO)

ECMO : extracorporeal membrane oxygenation

EVLP : *Ex vivo* lung perfusion

HUVEC: human umbilical vein endothelial cells

H&E: hematoxylin and eosin

IRI : Ice Recrystallization Inhibitor

IVC: inferior vena cava

LA : left atrium

PA : pulmonary artery

PCLS : precision cut lung slices

PVP : polyvinyl pyrrolidone

2FA : (2-fluorophenyl)-C6-azido-D-gluconamide

4ClA: N-(4-chlorophenyl)-D-gluconamide

1. Introduction

The first long-term successful single-lung transplant was performed in 1983 in Toronto after more than two decades of unsuccessful attempts or short-term survival in humans[177]. Since then, thousands of lung transplants have taken place currently resulting in a high 1 year survival rate[39; 146; 201]. However, the need for additional lungs is still high, with 5-year survival rates dropping to less than 60% in the UK and United States, and less than 70% in Canada [39; 146; 201]. Given the high rate of graft failure, retransplantation is common thus causing an additional increase in lung demand. This results in an unacceptable incidence of death on the waitlist, with over 11% of patients on the Canadian lung transplant waiting list in 2018 dying before receiving a lung[39]. While many lungs become available for transplant, a large number of these lungs are unutilized due to failure to meet physiological or compatibility criteria. Therefore, research to improve organ utilization and organ preservation times is greatly needed.

In the following sections, the two current methods of lung preservation, static cold preservation and normothermic *ex vivo* lung perfusion (**EVLP**), will be reviewed. Following this, the potential use of cryopreservation to increase preservation times leading to improved donor lung utilization will be discussed. Since cryopreservation is not currently utilized as a lung preservation method, a review of the various challenges faced in cryopreservation, and the current cryoprotectants used to mitigate cryoinjury will be discussed. The qualities of the lung which make it amenable to cryopreservation will be discussed in conjunction with a review of the research developments published to date. Finally, the hypothesis and objectives of this thesis will be presented.

1.1 Current Lung Preservation Methods

1.1.1 Static Cold Preservation

Inherent to a discussion of organ preservation is the concept of cooling organs to reduce the harmful effects of metabolic activity under ischemic conditions. Cold static preservation has been used for decades to allow lung survival during transport to the recipient. However, cold static preservation ultimately causes cellular damage and demise for a variety of reasons (Figure 1.1). As temperatures drop, aerobic metabolism is reduced due to inhibited activity of enzymes involved in pyruvate oxidation and the citric acid cycle[124]. This results in failure of necessary membrane

proteins to maintain ionic balance[30] and the development of cellular acidosis as anaerobic metabolism produces lactate[92]. Iron stores are released as cells become acidotic and enable the production of harmful reactive oxygen species[167]. Failure of membrane proteins to maintain ionic balance results in a net increase of intracellular sodium chloride[4] and calcium[207]. This increase in intracellular osmolality causes swelling of the cell as water enters[4]. Additionally, the rapid increase in intracellular calcium causes mitochondrial cytochrome C release[155] and facilitates calcium-dependent phospholipases and proteases which can cause cytoskeletal disorganization and cleavage of pro-apoptotic proenzymes[97; 111; 156]. These changes can ultimately lead to cellular necrosis or apoptosis [23; 24; 30].

To reduce damage caused by ionic imbalance, organs undergoing cold static preservation are flushed with preservation solutions. In whole lung preservation, a low-potassium dextran solution, called Perfadex® (XVIVO Perfusion, Goteborg, Sweden), is often used, and the lungs are inflated with oxygen to reduce ischaemic injury[219]. While this improves lung quality, cold static preservation only allows for short term storage. Some studies indicate that lungs transplanted after undergoing cold static preservation for longer than 5 hours result in poorer recipient outcomes[184], while other studies have reported that there is no difference in recipient outcomes for up to 9 hours[81]. Regardless, in current practice, lungs are only used if cold static preservation is less than 8 hours[219].

1.1.2 *Ex vivo* Lung Perfusion (EVLP)

A more recent advance in lung preservation, which has shown great potential, is *ex vivo* lung perfusion (EVLP). EVLP offers a variety of advantages over static cold preservation, since it allows for greater evaluation of the donor lungs and treatment of donor lungs prior to transplant[53; 144; 186]. This is particularly desirable with the reduced evaluation time afforded in lungs donated after circulatory death (**DCD**) or in the transplant of high-risk donor lungs which may require treatment prior to transplant[53; 134; 144].

EVLP was first used to evaluate lung suitability for transplant in 2000 when Steen and colleagues demonstrated the usefulness of this approach in lungs DCD[186; 187]. Following their work, the same method was used to repair and transplant lungs that had been deemed unacceptable for transplant[188]. Prolonged normothermic EVLP was then performed successfully in 2008 in Toronto by Cypel and colleagues with their protocol for EVLP becoming the standard protocol in many facilities thereafter[50]. Further research by this group then demonstrated that

12-hour normothermic EVLP can improve the quality of lungs as measured by lung oxygenation, rates of edema formation, epithelial tight junction integrity, and metabolic function[52]. This demonstrated that much of the damage incurred in cold static preservation as a result of hypothermia and hypoxic metabolic reactions can be avoided through normothermic EVLP.

In EVLP, a perfusing solution enters the lung through the pulmonary artery (**PA**) cannula, exits the lungs through the left atrium (**LA**) opening or cannula, and enters the perfusing circuit[50]. The general components of the EVLP circuit are common among all modern EVLP protocols (Figure 1.2), as the circuit is composed of a reservoir, a pump, a membrane de-oxygenator attached to a heat exchanger and gas source, and a leukocyte filter[53; 188]. The leukocyte filter is used to reduce cytokine-induced lung injury[100] and immunogenicity[189], although its importance has recently been called into question[123]. A flow probe is present between the leukocyte filter and PA, while a temperature probe is present between the membrane deoxygenator and leukocyte filter[53; 188]. STEEN solution™ (XVIVO Perfusion, Goteborg, Sweden), is the most common perfusate used in EVLP[6; 28; 50; 52; 53; 54; 55; 56; 134; 139; 144; 178; 202; 219; 227]. STEEN solution™ contains human serum albumin, which prevents edema by maintaining optimal colloid pressure[46; 110], and dextran 40, which prevents endothelial damage and inhibits coagulation and platelet aggregation[116; 223]. In addition to these benefits, STEEN solution™ has antioxidant capabilities through NOX2 downregulation in platelets, polymorphonuclear leukocytes, lymphocytes, monocytes, and endothelial cells[43; 152].

In addition to the perfusing circuit, a ventilator is attached to the endotracheal tube to maintain the desired ventilation. While such a method of positive pressure ventilation is standard in EVLP, studies have reported the addition of negative pressure ventilation using a sealed organ chamber with a turbine-driven ventilator[1; 34]. This research has revealed the benefit of negative pressure ventilation by demonstrating its ability to reduce lung inflammation and edema when compared to positive pressure ventilation methods[1; 34]. Three main EVLP protocols currently exist, and vary in terms of the perfusion setup, perfusion flow rate, perfusate used, and ventilation settings (Figure 1.2). These differences and clinical outcomes have been discussed thoroughly by some review articles[8; 203], but a general comparison of the main differences is presented in Figure 1.2.

1.1.2.1 Treatment of Damaged Lungs by *EVLP*

A large body of research has demonstrated the ability of EVLP to maintain lungs sufficiently to allow for treatment of a variety of conditions. Initial EVLP research by the Toronto group demonstrated that lungs marginally rejected due to reduced PaO_2/FIO_2, pulmonary edema, poor lung compliance, or high-risk history can be successfully treated by EVLP leading to successful transplant outcomes[53]. Further research by this group then studied the effect of IL-10 gene therapy on lungs deemed unsuitable for transplant[51]. In this research, the IL-10 therapy improved the integrity of the alveolar-blood barrier function, increased anti-inflammatory cytokine expression, and improved function, as measured by arterial oxygen pressure and pulmonary vascular resistance[51]. EVLP has also been used to treat more specific conditions, including infection[10; 144] sepsis-induced injury[134], gastric-acid aspiration damage[145], and pulmonary embolism[122; 125].

Given that various studies have indicated that donor lungs have a high rate of bacterial contamination[29; 176] that may compromise recipient outcomes[5; 15], the ability to use EVLP to treat infected lungs prior to transplant is valuable. While broad-spectrum antibiotics are currently used to prevent pneumonia in lung recipients, EVLP allows for antibiotic dosage at higher levels without damage to other organs[144]. Research on this topic has demonstrated that high-dose antibiotic treatment during EVLP can reduce microbial load significantly[10; 144] and allows for improved pulmonary oxygenation and reduced pulmonary vascular resistance[144]. Therefore, EVLP with extensive antibiotic treatment has the potential to reduce post-transplant pneumonia in clinical practice. Similarly, EVLP has been used in conjunction with germicidal light-based therapies to rid donor lungs of the hepatitis C virus[80]. Ultimately, research such as this demonstrates that EVLP allows for flexibility in treatment of lung infections which can improve donor lung utilization.

Related to these findings, it has been demonstrated that EVLP can improve lung quality in cases of acute respiratory distress syndrome brought on by sepsis[134]. Unfortunately, very few therapeutic options currently exist for those afflicted with severe acute respiratory distress syndrome, with extracorporeal membrane oxygenation (**ECMO**) or ventilation with low tidal volumes and prone positioning being the most common treatment methods[179; 198]. In a porcine model of acute respiratory syndrome secondary to sepsis induced by lipopolysaccharide exposure, 4 hours of normothermic EVLP resulted in improved oxygenation and dynamic lung compliance[134]. While this research was intended for the treatment of patients experiencing acute

respiratory distress syndrome, it also demonstrates the potential for EVLP to repair critically damaged lungs for the purposes of transplantation[134].

While infection is a common reason to reject a lung for transplantation, many donor lungs are rejected due to damage by gastric-acid aspiration[145]. When gastric-acid is aspirated, as commonly seen in brain-damaged donors, damage to the epithelium occurs leading to failure of surfactant production[166]. Therefore, EVLP treatment which includes the addition of pulmonary surfactant could allow for increased lung function making the lungs suitable for transplantation[145]. This has been studied in a porcine model of gastric-acid aspiration which demonstrated that EVLP could repair the damaged lungs when combined with pulmonary lavage and pulmonary surfactant administration[145]. Pre-transplant, lung improvement was observed through improved static lung compliance and reduced inflammatory interleukins, secretory phospholipase, and pulmonary vascular resistance[145]. Post-transplant outcomes were also improved when compared to non-treated or lavage-only controls, as demonstrated by increased PaO_2/FiO_2 and static compliance[145]. Therefore, lungs that would be rejected for transplant due to evidence of gastric acid aspiration or lungs accepted for transplant with suspected gastric-acid aspiration can be treated by EVLP with lavage and surfactant administration. This has the potential to increase the donor pool and improve the quality of lungs donated.

Interestingly, pulmonary embolism, which would usually warrant rejection of a lung for transplantation, can be sufficiently repaired for transplant through the use of EVLP. There are at least two case reports of pulmonary embolism in donor lungs being successfully treated, allowing for their successful transplant[122; 125]. To repair the lungs, thrombi were removed during a retrograde flush, and thrombolysis was performed through the administration of alteplase during EVLP[122; 125]. The lungs were then transplanted into a human recipient who had no reported incidence of primary graft dysfunction and was doing well at the time of publication[122; 125]. This clearly demonstrates how EVLP can be utilized to repair lung damage.

1.1.2.2 Challenges in Extended *EVLP*

While EVLP has provided promising outcomes through its ability to repair lungs deemed unacceptable for transplant, the safe duration of EVLP is not currently known since very little clinical research has been performed with extended EVLP runs. While it is known that EVLP can safely maintain lungs for 12 hours[1; 50; 144; 219], one study observed an increase in pro-inflammatory cytokines as EVLP progressed[129]. This research assessed the presence of 4

cytokines in the perfusate of lungs undergoing EVLP and determined that cytokines increased by a statistically significant amount over time[129]. However the presence of increasing perfusate cytokines does not directly demonstrate lung damage that could impair transplant, and the small sample size of 14 reduces the validity of the conclusions[129]. In contrast to this study, a larger scale study assessing over 900 lung transplant patients in Toronto concluded that extended EVLP runs result in patient outcomes comparable to cold static perfusion or short EVLP runs[219]. While this study provides evidence that transplants after extended preservation times are as successful as transplants after shorter preservation times, it did not directly study the relationship between EVLP duration and patient outcomes[219]. Rather, it included all lungs preserved for transplantation during the period of study, with only 135 transplanted lungs undergoing EVLP[219]. Also, the outcomes of survival and primary graft dysfunction were assessed at 72 hours post-operatively and may, therefore, not be indicative of comparable long-term outcomes[219]. In addition, the lungs preserved for greater than 12 hours had a mean preservation time of just 14.6 hours[219]. Therefore, the ability for EVLP to preserve human lungs for extended durations of time is uncertain and further research is required to elucidate the effect of increased EVLP time on lung quality and patient outcomes. Some research has begun this investigation in a porcine model and has demonstrated maintenance of lung quality for as long as 24 hours when negative pressure ventilation is used[34]. If further research demonstrates that this method is successful in a human model, it would significantly improve preservation times over current standards.

1.2 Cryopreservation

Successful cryopreservation would allow for much greater storage durations than static cold preservation and EVLP. Although storage at any temperature below normothermic can be classified as cryopreservation, cryopreservation is often defined as preservation occurring below 0 °C. As temperatures are lowered, the reduction of metabolic activity allows for longer storage since the harmful effects of metabolic activity occurring under ischemic conditions are mitigated. Since metabolism decreases by approximately 2 fold for every 10 °C reduction in temperature[25], cryopreservation has the potential to store organs for exceedingly long periods of time depending on the temperature of storage. However, cryopreservation is complicated by many challenges which exist at the cell, tissue, or whole organ level. While many review articles have discussed such challenges[120; 194], the cellular and structural morphology of the lung offers unique challenges.

Therefore, a review of general cryobiology theory will be discussed first, followed by a discussion regarding the specific challenges facing lung cryopreservation.

1.2.1 Cryoinjury

While cellular cryoinjury is exceedingly complex and unique, it is often split into two categories based upon the freezing rate selected. This concept is based upon Mazur's two-factor hypothesis [131], in which it is theorized that slow cooling injury results in damage due to increasing solute toxicity from dehydration, while rapid cooling injury is due to intracellular ice formation.

In slow cooling, extracellular ice nucleation occurs initially as water molecules bond to form a crystalline structure[138] and solutes are excluded from the developing ice lattice[104]. This causes an increase in extracellular solute concentration in the unfrozen space compared to normothermic physiological conditions[104] resulting in cell shrinkage as water exits the cell [226]. The amount and rate of water which leaves a cell is related to the permeability of the plasma membrane to water which is strongly affected by temperature[103; 130; 133]. When intracellular dehydration is severe, solute toxicity[1; 97; 111; 155; 156] and structural damage[121] may lead to cellular demise.

In contrast, when cells are cooled too rapidly, intracellular ice formation occurs since the cells do not have sufficient time to dehydrate, leading to intracellular supercooling and spontaneous nucleation [131]. Intracellular ice formation is highly associated with lethal cell damage[132]; however, many cells can survive intracellular ice formation[102] especially when it is controlled[157]. The damage incurred during intracellular ice formation may be due to mechanical damage to membranes[75], the formation of gas bubbles[140], or osmotic effects during rewarming[71; 142].

However, the terms slow cooling and rapid cooling are relative and the actual rates of cooling that would be slow or rapid for a given cell type is dependent upon various cell characteristics. For instance, the membrane characteristics of a cell may influence the amount of water which effluxes during dehydration or influence the cells susceptibility to membrane damage from dehydration or intracellular ice formation. The amount of water within a cell that is capable of freezing may also differ between cell types, therefore altering the susceptibility of cells to cryoinjury.

In addition to the damage that may occur during the cooling phase of cryopreservation, damage may also occur as a cell is re-warmed from a frozen state. As cells are warmed from a cryopreserved state, intracellular and extracellular ice may become larger in size, thus causing mechanical damage and increased solute concentration. This process is called ice recrystallization, and it occurs during warming because smaller ice particles have higher surface free energies that are conducive with ice formation if sufficient time is allowed[79]. Therefore, rapid warming helps to reduce ice recrystallization[106; 159; 193]. However, ice recrystallization cannot completely be avoided by modifying the warming rate and may play a role in the substantial cell death that results from many cellular and tissue cryopreservation techniques[69; 159; 220].

When considering tissue level or organ level cryoinjury, the difficulties facing cellular cryopreservation are exacerbated by the variety of different cell types, the presence of cellular interactions, and heat and mass transfer limitations. Each cell type may have its own optimal cryoprotectant combination and concentration, duration of cryoprotectant exposure, and rate of cooling and warming[61; 133]. Therefore, the various types of cell within a tissue or organ may not all be compatible with the same cryoprotectant protocol. In addition, the physical size of an organ and the way the cells are organized may also mean that certain cells will have greater exposure to the cryoprotectants and temperature changes than others[143]. Therefore, damage due to inconsistent warming and cooling rates, ice formation, or cryoprotectant toxicity may not be uniform [143; 224]. Lastly, organs have complex cell to cell and cell to matrix interactions through various tight and communicating junctions. If ice was to grow within a tissue, the potential for severing of intercellular junctions and cell-matrix connections increases[13; 91], thus resulting in a loss of tissue functionality.

1.2.2 Cryoprotectants

In order to mitigate cryoinjury, cryoprotectants are utilized. Cryoprotectants are solutes which allow for heightened post-thaw recovery when added to cell medium when compared to untreated controls[105]. Glycerol was the first cryoprotectant used to preserve cells[78] with its cryoprotective ability discovered in 1949 by Polge and colleagues[158; 183]. Many cryoprotectants have been developed since the discovery of the cryoprotective effects of glycerol, and the mechanisms of cryoprotection are varied.

1.2.2.1 Traditional Cryoprotectants

Traditional cryoprotectants are often classified by their ability to permeate cells. Permeating and non-permeating cryoprotectants are often used in combination to limit cytotoxicity and prevent multiple types of damage since they function through different means[61; 104].

Permeating cryoprotectants, such as dimethyl sulfoxide (Me_2SO; **DMSO**), glycerol, and propylene glycol[61; 104], reduce the freezing point and act as a secondary solvent for solutes[79]. Therefore, in slow cooling conditions, they prevent damage due to increasing solute concentrations as cells dehydrate[79].

Non-permeating cryoprotectants dehydrate cells prior to freezing since they have high osmotic coefficients and remain in the extracellular space[79]. They therefore reduce the amount of intracellular and interstitial water which can freeze, thus limiting the probability of ice nucleation[79]. Non-permeating cryoprotectants include polymers, such as polyvinyl pyrrolidone (**PVP**) or hydroxyethyl starch, and various sugars, such as trehalose and sucrose[61; 104].

Given that permeating and non-permeating cryoprotectants function through different means, a great deal of cellular damage may be mitigated through their combined use. This has been demonstrated experimentally by an abundance of research, which use various combinations of ethylene glycol, DMSO, sucrose, glucose, and trehalose to cryopreserve cells[69; 77; 89; 114; 115; 141; 170].

1.2.2.2 Non-Traditional Cryoprotectants

Other cryoprotectants have been used in cryopreservation research that do not function in the same way as the traditional cryoprotectants described above. One such cryoprotectant class, antifreeze proteins (**AFP**), has been derived from various organisms that are naturally freeze tolerant[60]. Some of these proteins are non-colligative, as they adsorb to developing ice particles and prevent ice recrystallization[60]. As a result, these proteins are able to induce thermal hysteresis, which is the depression of the freezing point below the melting point[58; 60]. AFPs have allowed for improved survival during hypothermic storage in a variety of different cells and tissues including oocytes[12], embryos[93], insulinoma cells[101], neurons[175], liver cells[88], and whole rat hearts[9].

AFPs have also been used to preserve oocytes[98], spermatozoa[147; 164; 225], and embryos[147] at lower temperatures. A variety of AFPs have been identified, with fish AFPs usually

binding to the prism plane of a developing ice nuclei[168], while some arthropod AFPs bind to both the prism and basal planes of developing ice nuclei[154]. Fish AFPs are used as cryoprotectants more often than arthropod AFPs[12; 88; 93; 98; 101; 147; 164; 175; 225]; however, the failure of these proteins to prevent basal plane ice growth can cause damage[94; 173]. Therefore, use of arthropod AFPs provides one research avenue to potentially improve cryopreservation outcomes[60; 86]. Research on such arthropod AFPs has improved smooth muscle and endothelial cell viability during cryopreservation[86; 204], and allowed for extended sub-zero preservation of kidneys[197].

The ability of AFPs to prevent ice recrystallization has inspired the development of synthetic molecules that can control the growth of ice, called ice recrystallization inhibitors (IRIs)[19; 40; 157; 199]. These small carbohydrate derivatives are more suitable to large-scale production than AFPs derived from fish or arthropods, and their small size allows them to permeate into cells to control ice growth, unlike AFPs[20; 42]. The small size and functionality of these molecules is due to their hydrophobic moieties (aryl chains) which substitute the functional tripeptide groups in antifreeze glycoproteins[20; 199].

Such IRIs have been used to successfully cryopreserve hematopoietic stem cells [31] and red blood cells allowing for improved survival and protection during transient warming events[32; 41]. Further research with these IRIs on human umbilical vein endothelial cells (HUVEC) and red blood cells has demonstrated that IRIs are also capable of permeating cells allowing for control of intracellular ice growth[157]. Therefore, IRIs have the potential to be a useful cryoprotectant in organ cryopreservation due to their low toxicity, cell permeability, and control of ice growth. This would allow for long exposure times leading to uniform permeation which prevents ice from growing to a damaging size intra- and extra-cellularly.

1.2.3 Whole Organ Cryopreservation Strategies

Several methods have been attempted to enable whole organ cryopreservation at various temperatures of storage, including vitrification, high sub-zero preservation methods, and partial freezing. These methods have been formulated to consider various types of cryoinjury and cryoprotectant toxicities; however, each method has disadvantages. As shown in Figure 1.3, the majority of whole organ cryopreservation research has occurred at high sub-zero temperatures in livers, kidneys, and hearts, while lung cryopreservation research is underrepresented in the scientific literature.

1.2.3.1 Vitrification

Since a great deal of the damage incurred in cryopreservation may occur as a result of ice formation, the ability to cryopreserve without ice formation would be ideal[67]. The concept of freezing without harmful ice formation is called vitrification and is the basis of many cryopreservation techniques[89; 114; 115; 141; 170]. In vitrification, the solvents cool and enter a solid glass-like state as a result of high viscosity without crystalline structure formation[216]. In order for this to occur, solvents must be cooled at a rate that is fast enough to increase the viscosity of the fluid sufficiently to impede ice lattice formation and allow for a stable solid state of water[72]. Cryoprotectants can aid in this process by reducing the rate of cooling required to achieve vitrification to a feasible level. Due to advances in cryoprotectant research, vitrification methods are promising in the field of organ preservation[67]. Vitrification is currently the most common form of cryopreservation in reproductive sciences with oocytes, spermatozoa, and embryos primarily being cryopreserved by vitrification[89; 114; 115; 141; 158; 170]. But other cell types, such as monocytes[191] and cell lines[217] have also been vitrified. More important to a discussion on organ preservation, a variety of tissues have been successfully vitrified including cornea[14], skin[76], islet of langerhans[99], liver slices[214], whole mouse ovaries[135], and vascular grafts[185]. In theory, whole organ vitrification is possible; however, only one case of successful whole organ vitrification of a rabbit kidney has been reported and has not been replicated[68].

While vitrification may seem ideal, vitrification in whole organ cryopreservation is complicated by the toxicity of the large amount of cryoprotectants required, difficulty in removing the cryoprotectant solution, and the current inability to warm rapidly enough to prevent devitrification ice formation[61; 66; 67]. For these reasons, control of, rather than prevention of, ice formation is another potential means of achieving whole organ cryopreservation.

1.2.3.2 High Sub-Zero Organ Preservation

Other techniques have been studied to prevent ice formation during cryopreservation. Unlike vitrification, these methods are performed at high sub-zero temperatures and include supercooling, isochoric freezing, and liquidus tracking.

Supercooling techniques utilize high concentrations of cryoprotectants to supress the freezing point and allow for ice-free sub-zero cryopreservation. Initial research has indicated that

this improves organ recovery or allows for longer durations of storage when compared to static cold preservation methods[27; 33; 57; 107; 150; 192]. The most promising supercooling outcomes have been observed in rat livers [27; 33]. This method allowed for 4-day rat liver perfusion followed by successful transplant[27; 33]. This research has also been extended to human livers, and has demonstrated that human liver preservation can be extended to 27 hours through supercooling via *ex vivo* perfusion[57]. Preliminary research has analyzed supercooling preservation of hearts and lungs; however, no post-thaw functional analysis has been performed to date[107; 150].

Liquidus tracking is another technique which utilizes a high concentration of cryoprotectants[153]. However, in this technique, cryoprotectant concentrations are gradually increased as cooling commences such that the equilibrium freezing point is matched[70; 153; 206]. Therefore, ice nucleation is avoided, and cryoprotectant toxicity is mitigated. This technique has been successfully demonstrated in articular cartilage, although no other tissue or organ research has been performed using this technique to date[153; 206].

Isochoric freezing varies from supercooling and liquidus tracking in that pressure is applied through the maintenance of volume during freezing to reduce damaging hypertonicity of solutions and ice formation[162; 174]. Although preliminary research studying isochoric methods to preserve hearts demonstrated that the increasing pressure causes tissue damage[205], an experimental thermodynamic model utilizing a multiphase isochoric freezing technique has been validated in a simple solution-based model[160]. In addition, recent research has demonstrated maintenance of pancreatic islet viability at -3 °C for 3 days without the use of any cryoprotectants using an isochoric freezing strategy[161]. Therefore, future research is warranted to assess the utility of this technique for organ preservation.

While ice-free sub-zero preservation is promising, the duration of preservation at high sub-zero temperatures is less than that possible through lower temperature storage since metabolic activity continues to occur at high sub-zero temperatures. However, metabolism has been found to decrease by approximately 2 fold for every 10 °C reduction in temperature[25], so any decrease in temperature will increase preservation times beyond normothermic storage.

1.2.3.3 Partial Freezing

Although no recent publications exist for organ cryopreservation techniques which allow ice formation to occur, some researchers have proposed the allowance of ice formation in a

targeted way to facilitate lower temperature storage[196]. Such researchers are currently studying the use of non-permeating cryoprotectants and ice nucleating agents in addition to permeating cryoprotectants to encourage ice nucleation in the vasculature of rat livers[196]. Although this may seem counter-intuitive, the cellular dehydration afforded by the use of non-permeating cryoprotectants may allow for localized freezing such that intracellular and intercellular ice is minimized. This would allow for lower temperatures of storage than that possible through supercooling thus allowing for longer storage times[196]. In addition, if ice nucleation can remain innocuous in the vasculature, this technique would result in less damage than that caused by spontaneous ice nucleation occurring during devitrification. Therefore, partial freezing is an interesting research direction for organ cryopreservation.

1.2.4 Lung Cryopreservation

1.2.4.1 Cellular- and Tissue-level Cryopreservation Challenges and Research

Lungs are unique to many other organs of the body in terms of their diversity of cell types. The lung is composed of over 40 different cell types, each with their own characteristics relevant to cryobiology[74]. While all cells of the lung serve a valuable purpose, a large amount of these cell types are resident immune cells whose function after cryopreservation for transplant purposes would be undesirable. Therefore, the major classes of cells whose function post-thaw would be important for lung function include airway epithelial cells, alveolar epithelial cells, salivary gland cells of the bronchi, interstitial connective tissue cells, and cells of the blood vessels[74]. Each of these classes of cells includes various cell types, each with their own membrane permeability characteristics which affects their susceptibility to cryoinjury and, in turn, protection by cryoprotectants.

This complexity has been investigated at a preliminary level through the cryopreservation of lung tissue and subsequent culture of specific cells isolated from the tissue post-thaw. For example, work by Roth and colleagues in 1992 demonstrated that fibroblast, dendritic, epithelial, and macrophage cell cultures could be derived from 5 mm^2 lung tissue cryopreserved in a 10% (v/v) DMSO solution frozen at a rate of -1 °C/min to -70 °C and stored in liquid nitrogen for up to 1 year [172]. This work was further expanded by Baatz *et al* (2014), who created a technique to cryopreserve 0.5-0.75 cm^2 lung tissue blocks for the purposes of biobanking specimens for delayed analysis[16]. In this method, lung tissue undergoes pseudo-diaphragmatic expansion using a

syringe-pump and a cryoprotectant solution whose components are not disclosed, prior to freezing at rate of -1 °C/min to -80 °C[16]. They demonstrate that this method allows for robust post-thaw tissue analysis involving cell culture of vascular endothelial cells, type II pneumocytes, and fibroblasts in addition to tissue morphological analysis and other molecular analysis[16]. While this method allows for the delay in analysis of patient samples, its relevance to lung cryopreservation for the purposes of organ banking is very limited. Although it can be concluded that many cells survive the cryopreservation process when lung tissue is prepared and frozen in the manner depicted in this paper, the composition of cells which survive, and the functionality of the tissue post-thaw is unknown.

While individual cell survival is one large consideration in organ cryopreservation, the ability for these cells to interact is additionally important for the function of a tissue. Within the lung, various tight junctions compartmentalize the lung. Should these connections be compromised by ice formation and growth, thawed lungs would suffer from edema incompatible with lung functionality [215]. In addition to these tight junctions, the communicating gap junctions of lung epithelium allow for the passage of signaling molecules and metabolites to regulate production of pulmonary surfactant and control cell attachment in response to stress[109].

Some research has assessed post-thaw tissue function through the use of precision cut lung slices (**PCLS**) [171; 210]. This research sought to increase storage durations of PCLS since PCLS only survive for approximately 2-5 days in tissue culture, but it additionally demonstrates the potential for maintained tissue function following lung cryopreservation[18; 171; 210]. In this research, PCLS were frozen to -80 °C in a 10 % DMSO solution using a Mr. Frosty Freezing Container. While simple in design, this cryopreservation protocol allowed for maintained cell survival, as measured by an LDH assay, and function, as determined by ciliary activity, maintained airway contraction when exposed to contractile agonists, and functional phagocytosis by resident immune cells[18]. This clearly demonstrates the capacity for maintained lung tissue function following cryopreservation; however, the small size of PCLS ensures uniform cryoprotectant exposure and freezing that is unlikely to occur in larger scale models. Additionally, the LDH assay does not allow for differential cell survival, so it remains unclear if some cells survive at a greater rate than others during this process. Therefore, its translatability to whole lung cryopreservation is limited.

1.2.4.2 The Potential for Whole Lung Cryopreservation

While the challenges at the cellular and tissue level make whole lung cryopreservation daunting, various qualities of the lung make it an interesting subject for cryopreservation research. For example, many of the challenges facing large organ cryopreservation exist due to the density of the tissue resulting in heat and mass transfer limitations. These challenges are much smaller in the lung, given its large air spaces and vascular properties. For instance, *ex vivo* perfusion allows for much faster perfusion of the lung when compared to other organs due to the low density and expansive vasculature. This would allow for more rapid perfusion of cryoprotectants, thus allowing for a reduction in normothermic exposure to molecules which may cause cytotoxicity. Temperature changes can also occur more rapidly in the lung due to its air space, thus reducing heat transfer limitations. Since EVLP has been shown to improve lung quality, it could additionally be used pre- and post- cryopreservation to improve lung quality and facilitate cryoprotectant delivery.

Although the characteristics of the lung make a variety of different cryopreservation strategies a possibility, lung cryopreservation is underrepresented in the organ cryopreservation literature (Figure 1.3). Currently, only one publication has studied the cryopreservation of whole lungs [150]. In this sole publication, rat lungs were supercooled to –2 °C for 17 hours through the suspension in a cryoprotectant-free preservation solution, called ET-Kyoto [150]. This treatment group was then compared to storage at 4 °C for 17 hours or to fresh controls during reperfusion in an *ex vivo* perfusion circuit[150]. This analysis provided promising results which demonstrated that supercooling maintained lung function comparably to fresh controls, in terms of tidal volume, arterial oxygen tension, and weight gain[150]. ATP levels were additionally improved when compared to the 4 °C treatment group[150]. While these results are encouraging, only an abstract has been published furthering this work to a transplant model but with shorter storage durations[151]. Therefore, further research on lung supercooling to assess long term feasibility for transplants would be a welcome addition to the literature.

In addition to supercooling research, vitrification or partial freezing are potential avenues for lung cryopreservation research. Vitrification in whole organ preservation is currently complicated by the toxicity of the large amount of cryoprotectants required, difficulty in removing the cryoprotectant solution, and the current inability to warm rapidly enough to prevent devitrification ice formation [61; 66; 67]. These problems are significantly reduced in lung tissue due to its reduced density and rapid perfusion which would allow for a reduction in normothermic exposure to toxic cryoprotectants and current heat and mass transfer limitations. However, some of

the methods currently being studied to enable devitrification, such as nanoparticle rewarming[82; 180], may not be feasible in the lung due to its complicated architecture. Therefore, a partial freezing protocol may be of interest for lung cryopreservation given the large air spaces of the lung in which ice has the potential to form innocuously. Although no publications currently exist for successful human organ cryopreservation techniques which allow ice formation to occur, some researchers have proposed the allowance of ice formation in a targeted way in liver cryopreservation[196] and an ice-allowing cryopreservation method for sheep whole ovary cryopreservation has been successful[37]. Therefore, a similar approach may be fruitful in lung cryopreservation given its unique morphology.

1.3 Conclusion

Although static cold preservation has allowed for an abundance of successful lung transplants over the last few decades, its inability to halt metabolism reduces storage of lungs to 8 hours[219] (Figure 1.1). The development of normothermic EVLP greatly improves upon static cold preservation by allowing for the improvement of lung quality with storage durations up to 12 hours[50; 144; 219]. However, the limitations of EVLP are currently unknown, and the lack of donor lung utilization warrants the pursuit for a preservation method which increases storage times. Although successful cryopreservation would allow for longer storage times, lungs remain underrepresented in the organ cryopreservation literature (Figure 1.3). The low density of the lung and the ability to improve lung quality with *ex vivo* lung perfusion offer unique advantages over other organs for cryopreservation research, thus warranting further study.

As described previously, the large air spaces of the lung and the complexity of the vasculature likely make lungs most amenable to an ice-allowing cryopreservation protocol utilizing an *ex vivo* perfusion circuit. Therefore, this research sought to study the cryopreservation of lungs in an ice-allowing manner following subnormothermic perfusion. Since the control of ice growth would be of the utmost importance in an ice-allowing organ cryopreservation protocol, the utility of IRIs as a novel cryoprotectant for lung cryopreservation was studied.

1.4 Hypothesis

IRIs are not cytotoxic and are capable of controlling intra- and extra-cellular ice growth resulting in improved cellular survival following cryopreservation of type II pneumocyte monolayers and rat lung tissue when compared to DMSO-treated controls.

1.5 Objectives

Objective 1. Determine the cytotoxicity of IRIs and the ability for IRIs to reduce intracellular ice grain size resulting in improved post-thaw survival over DMSO-treated controls, in the immortalized type 2 pneumocyte cell line BEAS-2B.

- Question 1: What is the short- and long-term cytotoxicity of IRIs to BEAS-2B cells?
  - In order to assess this, confluent BEAS-2B monolayers were exposed to increasing concentrations of, or increasing duration of exposure to, two IRIs. alamarBlue™, a metabolic assay reagent, was then used to analyze cell metabolism after treatment, and the data from each condition was normalized to media-treated positive controls. This was compared to the toxicity of a commonly used cryoprotectant, DMSO. Cells undergoing extended exposure to IRIs or DMSO were re-plated to assess their ability to replicate after extended exposure. This data was also normalized to the media-treated controls.
- Question 2: Can IRIs permeate BEAS-2B cells and reduce intracellular ice grain size?
  - After BEAS-2B monolayers were treated with IRIs, cells were placed on an VIAfreeze™ controlled-rate freezer (GE Healthcare) pre-cooled to -80 °C for 30 minutes prior to fixation on dry ice. The cells were then stained with SYTO13 and intracellular ice was visualized by fluorescent microscopy. Mean ice grain size was calculated using image analysis software and compared to DMSO-treated or cryoprotectant-free controls.
- Question 3: Does the ice control afforded by IRI use improve post-thaw survival over DMSO-treated controls in conditions which cause intracellular ice?
  - BEAS-2B monolayers treated with 8% DMSO, with or without IRIs, were frozen at a rate of -90 °C/min to -25 °C and thawed at a rate of +90 °C/min using a cryomicroscope. This was completed with or without a transient warming event to exacerbate intracellular ice growth. Post-thaw survival was assessed immediately using SYTO13 and ethidium bromide and after 24 h recovery using SYTO13 and ethidium bromide or the metabolic

assay reagent alamarBlue™. Cryoprotectant use in each experimental condition was compared. In conditions where alamarBlue™ is used, this data was normalized to unfrozen controls.

Objective 2. Determine the cytotoxicity of IRIs to lung cells during *ex vivo* subnormothermic perfusion of rat lungs, as well as the ability of IRIs to reduce extracellular ice grain size and improve cell survival and structural morphology of rat lungs after -20°C cryopreservation

- Question 1: Can a low-cost subnormothermic rat *ex vivo* lung perfusion system be developed?
  - Surgical techniques for the procurement of rat lungs were developed. Following this, an inexpensive system for ex vivo perfusion using a syringe pump, tubing, a beaker, and parafilm was developed. Techniques for assessment of cytotoxicity were then validated.
- Question 2: Are IRIs cytotoxic in rat lungs during subnormothermic perfusion?
  - One IRI, 2FA, was added to STEEN Solution™ and subnormothermically perfused. 0.4% (w/v) trypan Blue in STEEN Solution™ was then perfused, and the lung was formalin-fixed, paraffin-embedded, sectioned, and stained with eosin. The number of membrane-permeable cells was quantified and compared to STEEN Solution™ controls.
- Question 3: Do IRIs control extracellular ice growth, when compared to cryoprotectant-free controls, in rat lungs after subnormothermic perfusion and 1 hour storage at -20°C?
  - The ability for 2FA in STEEN Solution™ to control extracellular ice growth, as compared to STEEN Solution™ controls, was assessed by freezing the lungs at a chamber rate of -5 °C/min to -20°C in a CryoMed™ Controlled-Rate Freezer (Thermo Scientific™), holding the lungs at -20°C for 1 h, and cryofixation using a low-temperature fixative.
- Question 4: Do IRIs improve post-thaw cell membrane integrity and tissue morphology of rat lungs when compared to DMSO-treated controls after subnormothermic perfusion and 1 hour storage at -20°C?
  - Rat lungs were perfused subnormothermically with 10% (v/v) DMSO and 0.4% (w/v) trypan blue in STEEN Solution™, with or without the addition of 2FA. The lungs were then frozen at a rate of -5 °C/min to -20°C, held for 1 h at -20 °C, and thawed to 37 °C prior to formalin-fixation, paraffin-embedding, sectioning, and staining with eosin. The number of dead cells in both conditions was quantified and compared.

1.6 Figures

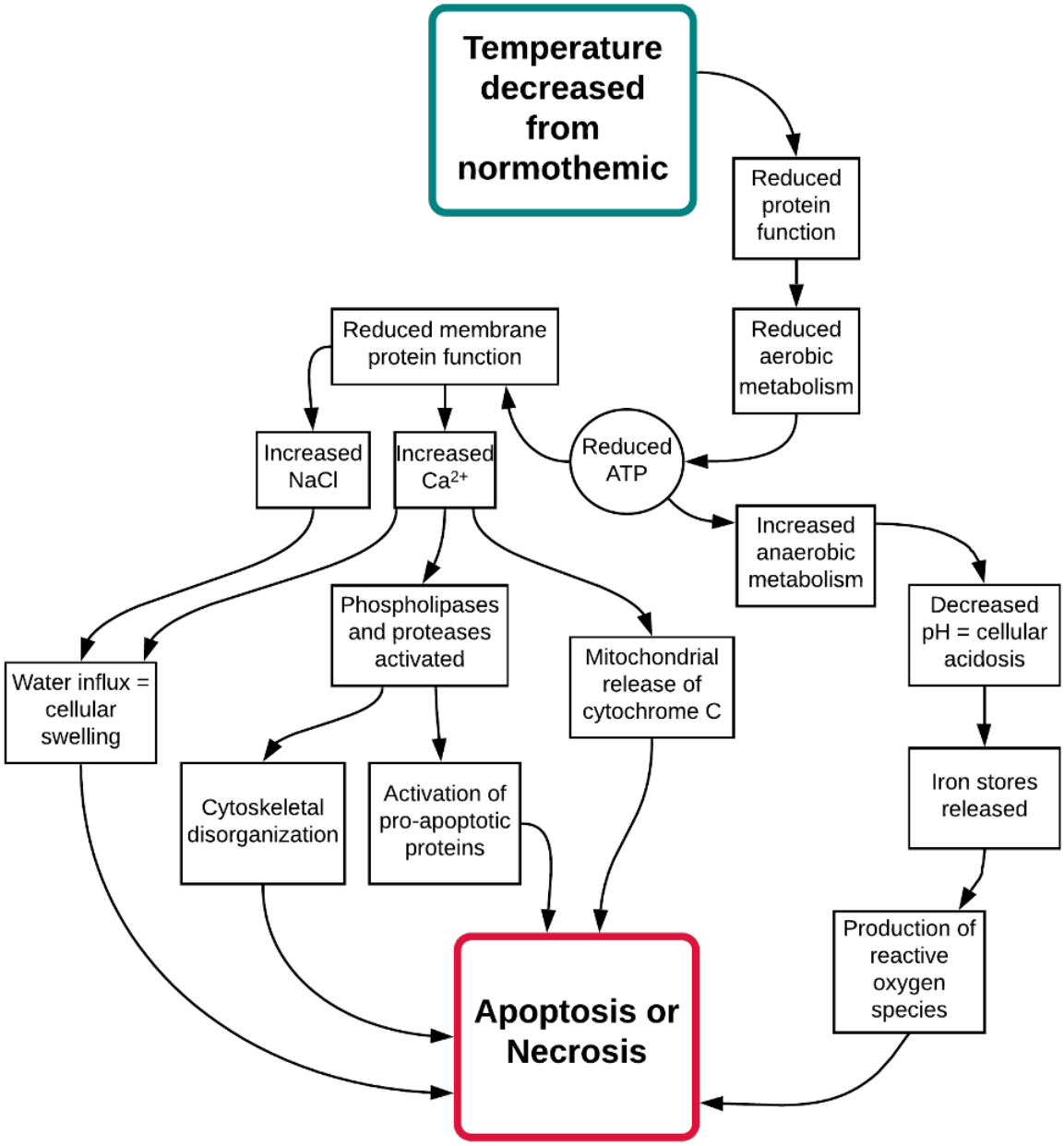

Figure 1.1 Causes of cellular damage and demise during static cold preservation

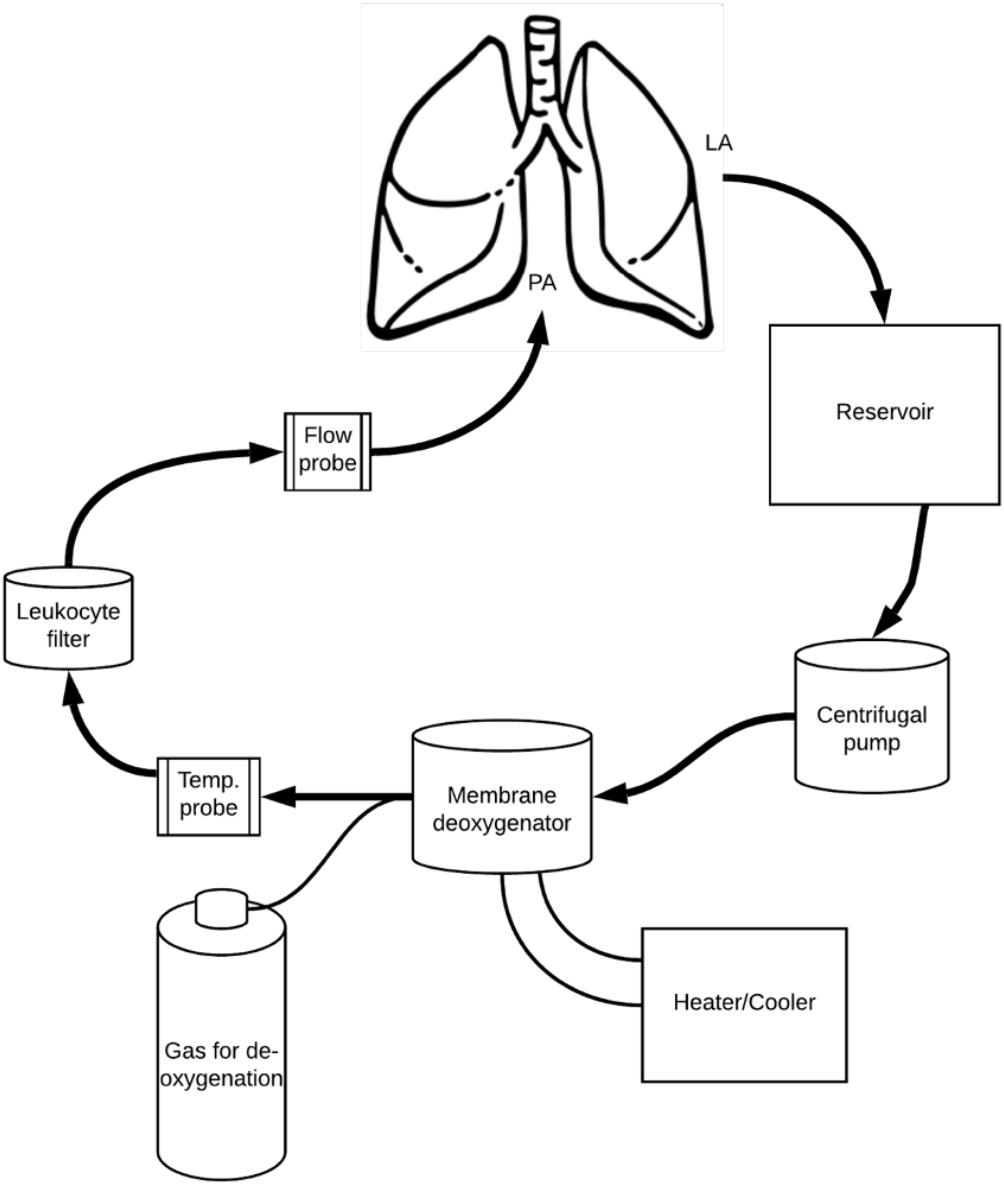

	Perfusate	Target flow	Open or closed left atrium	Ventilation (Breaths per minute)
Toronto [50]	STEEN	40 % Cardiac Output	Closed	7
Lund [119; 213]	STEEN + RBC (Hct 10-15%)	100 % Cardiac Output (4-6 L/min)	Open	15-20
Organ Care System (OCS) [136; 209]	STEEN or Perfadex + RBC (Hct 15-25%)	2-2.5 L/min	Open	10

Figure 1.2 The generalized EVLP circuit and the major differences in EVLP protocols.

	Number of patients on Canadian waitlist 2018 [38; 39]	Canadian transplant waitlist deaths 2018 N (%) [38; 39]	Duration of organ survival using static cold preservation [17]	Challenges in Cryopreservation			Publications on Whole Organ Cryopreservation Research	
				Number of cell types	Heat and mass transfer limitations (tissue density)	Ability to repair organ post-thaw	Vitrification	High subzero methods
Liver	424	76 (17.9%)	12-18 h	~8 [7]	High	Highly regenerative in vivo; no ex situ regeneration [85]	[180]	**Ice free:** [27; 33; 57; 137; 192] **Ice allowing:** [195; 196]
Kidney	2626	83 (3.2%)	48 h	>40 [47]	High	No	[64; 65; 68; 108]	**Ice free:** [127; 137; 190; 212] **Ice allowing:** [35; 59; 96; 112]
Heart	95	6 (6.3%)	4-6 h	~12 [182]	High	No	[82]	**Ice free:** [107; 137; 149; 205] **Ice allowing:** [63; 149; 208]
Lungs	193	23 (11.9%)	6-8 h	>40 [74]	Low	Ex situ perfusion can improve lung quality [51; 53; 144]		**Ice free:** [150]

Table 1.1 Transplantable organ demand, cryopreservation challenges, and published cryopreservation research

2. Characterizing IRI Efficacy in BEAS-2B Cell Monolayer Cryopreservation

2.1 Introduction

Cryoprotectants are a required component of most cell, tissue, or organ cryopreservation protocols, as they mitigate the damaging effects of ice formation and growth[61]. However, many cryoprotectants are known to have cytotoxic effects, both short- and long-term, and certain functional concentrations[23; 61; 66; 69]. Therefore, when exploring the use of a novel cryoprotectant, the concentration which is used must be carefully assessed to balance toxicity and functionality.

Although IRIs have been shown to control intracellular ice growth in HUVEC cells and improve red blood cell survival during cryopreservation[32; 157], their toxicity, permeability, and ability to control intracellular ice in lung cells is unknown. Therefore, the dose- and time-dependent cytotoxicity of IRIs to lung cells must first be characterized, followed by an assessment of their permeability and ability to reduce intracellular ice grain size. The optimal concentration and durations of exposure can then be selected in a way which balances cytotoxicity and efficacy. Following this, the ability for IRIs to improve post-thaw survival, by means of reducing intracellular ice growth, can be assessed.

Furthermore, it was hypothesized that IRIs would not be cytotoxic and would be capable of permeating cells and reducing intracellular ice grain size resulting in improved survival of type II pneumocytes under freezing conditions which stimulated intracellular ice formation and growth, when compared to DMSO-treated controls. The following questions were assessed to study this hypothesis:

- Question 1: What is the short- and long-term cytotoxicity of IRIs to BEAS-2B cells?
  - Time- and dose-dependent toxicity of the IRIs in type II pneumocytes was first assessed to determine the acceptable concentrations and duration of exposure lung cells may be exposed to IRIs. Both short- and long-term toxicity of the IRIs was assessed since other research has demonstrated that cryoprotectants may cause molecular damage resulting in delayed onset cytotoxicity[69].
- Question 2: Can IRIs permeate BEAS-2B cells and reduce intracellular ice grain size?
  - The ability for IRIs to reduce intracellular ice grain size was assessed through the use of a permeating nucleic acid stain and freezing of the cells in such a way as to cause intracellular ice formation. Under these conditions, intracellular ice may be visualized as unstained

fractions within cells and ice grain size may then be quantified from images of the cells. While a reduction in intracellular ice grain size would not prove that IRIs are capable of permeating lung cells, it provides support for this component of the hypothesis. The ability of IRIs to reduce intracellular ice grain size was assessed with or without the presence of permeating cryoprotectants and at different concentrations.

- Question 3: Does the ice control afforded by IRI use improve post-thaw survival over DMSO-treated controls in conditions which cause intracellular ice formation and growth?
  - Considering that intracellular ice formation and recrystallization is one of the known causes of cellular demise during cryopreservation [44; 48; 83; 131; 165], the inhibition of recrystallization by IRIs may confer a survival benefit under freezing conditions which cause intracellular ice formation and growth. As described in Chapter 1, rapid freezing rates often result in intracellular ice formation since the cell does not have sufficient time to dehydrate prior to reaching a temperature low enough to cause intracellular nucleation[131]. Transient warming events may then be used to increase intracellular recrystallization since the heightened temperatures in a frozen state increase the surface free energy of ice nuclei conducive with recrystallization[21; 79]. Therefore, plunge-freezing events, with or without a transient warming event, were performed and cell metabolism and membrane integrity were assessed post-thaw.

The results of this chapter will expand the current IRI literature by assessing a new cell type for use with IRIs and by better defining the toxicity of IRIs, as no IRI research has characterized long-term cytotoxicity. In addition, the results of this chapter will allow for determination of the value of studying IRIs in whole lung cryopreservation.

2.2 Materials and Methods

2.2.1 Cell Culture

BEAS-2B cells (ATCC® CRL-9609™) were selected for all experiments within this chapter as they are an immortalized type II pneumocyte cell line originating from the phenotypically normal type II pneumocytes of a human. Type II pneumocytes cover approximately 7% of the alveolar surface and make up approximately 15% of the cells of the lung[49]. They are the progenitor cell from which type I pneumocytes arise, and they produce the pulmonary surfactant of the lung[45]. This surfactant allows for a reduction of surface tension within the lung and helps improve immune response during lung infection[45]. Therefore, in whole organ cryopreservation, type II pneumocyte integrity would be of the utmost importance even though many other cell types reside in the lung. In all experiments, BEAS-2B cells were studied in confluent monolayers. This was selected over a suspension method as it allowed for ease of analysis using the metabolic assay reagent, alamarBlue™ (Invitrogen), and better represents cell to cell and cell to matrix connections found within lung tissue. It additionally allows for quantification of intracellular ice which is difficult to achieve through suspension analysis.

In all experiments, BEAS-2B cells (ATCC® CRL-9609™) were thawed and cultured with BEGM media (ATCC® PCS-300-040™) in T150 culture-treated flasks (Corning) within an incubator set to 37 °C and 5% CO_2. If coverslips were required for the experiment, cells were plated on 12 mm glass coverslips (VWR) within a 24-well culture plate that had been pre-treated with a plate-coating solution composed of 0.01 mg/mL fibronectin, 0.03 mg/mL bovine collagen type 1, and 0.01 mg/mL bovine serum albumin for 48 h. In all cases, media was replaced every 2-3 days, cells were monitored for signs of differentiation and discarded if differentiation occurred.

2.2.2 Cell Viability Assays

Determining viability of cells following cryoprotectant exposure and cryopreservation is critical for interpreting the efficacy and toxicity of IRIs. Many options exist for determining cell viability, including various types of membrane integrity assays and metabolic assays[84]. However, each viability assay has its advantages and disadvantages and the results of one assay may not corroborate with another[163]. Therefore, it is preferred to use a variety of different viability assays when assessing cellular demise or proliferation[163]. For this reason, toxicity assessments

were completed using the metabolic assay reagent alamarBlue™ (Invitrogen), and post-thaw assessments utilized this reagent in addition to the membrane integrity dye, ethidium bromide.

Although the alamarBlue™ assay is commonly used to determine cell viability, validation of this assay in BEAS-2B cells was performed to confirm the ability of alamarBlue™ to differentiate different concentrations of BEAS-2B cells for viability assessments. To assess this, BEAS-2B cells were plated in a 96-well plate in replicates of 4 for the following concentrations: 4 000, 8 000, 12 000, 16 000, 20 000, 24 000, 28 000, 32 000, and 36 000 cells/cm^2. BEGM media was added to ensure that each well contained a final volume of 150 µL. After 2 hours of 37 °C 5% CO_2 incubation, 15 µL of alamarBlue™ was added to create a 10% (v/v) alamarBlue™ in media solution in each well. Absorbance at 570 nm and 600 nm was then obtained, using a SpectraMax® Plus384 Absorbance Microplate Reader (Molecular Devices), every hour for 6 hours, and again at 24 hours. Percent alamarBlue™ reduction was determined using the following equation (Equation 1), where the negative control contains 10% (v/v) alamarBlue™ in BEGM media without cells. The correlation between number of cells plated and alamarBlue™ reduction was calculated for each duration of exposure using GraphPad Prism 8. A $p < 0.05$ was considered to be statistically significant.

Equation 1.

$$\text{Percent alamarBlue™ reduction} = \frac{[(117216)(A) - (80586)(B)]}{[155677\ (C) - (14652)(D)]}\ x100$$

Where A is the absorbance of the test well at 570 nm, B is the absorbance of the test well at 600 nm, C is the absorbance of the negative control well (10% (v/v) alamarBlue™ in BEGM media without cells) at 600 nm, and D is the absorbance of the negative control well at 570 nm.

In addition to the alamarBlue™ assay, membrane integrity of cells was assessed for experiments involving post-thaw survival. Membrane integrity was determined by cell impermeability to ethidium bromide through the addition of a 50 uM SYTO13 and 20 uM Ethidium Bromide in PBS to cells. In all cases, cells were observed under fluorescent microscopy (Nikon eclipse 80i). Images were merged using NIS Elements AR 3.2 image analysis software (Nikon) and the percentage of cells that were membrane impermeable to ethidium bromide was calculated using the Viability3 program for automated cell counting (Custom software: Version 3.2, The Great Canadian Computer Company, Spruce Grove, AB, Canada).

2.2.3 Cytotoxicity of IRIs

The following two IRIs were studied in BEAS-2B cell monolayers[26] to determine their short- and long-term cytotoxicity as compared to a commonly used cryoprotectant, Me_2SO (DMSO). DMSO was only studied at a concentration of 10% (v/v), since it is most commonly used at this concentration for the prevention of cryoinjury and is considered to have an acceptably low cytotoxicity at this concentration for cell cryopreservation.

1) N-(2-fluorophenyl)-D-gluconamide.
    - Herein referred to as **2FA**

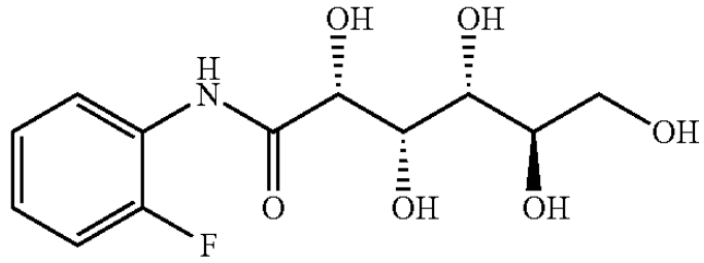

1) N-(4-chlorophenyl)-D-gluconamide.
    - Herein referred to as **4ClA**

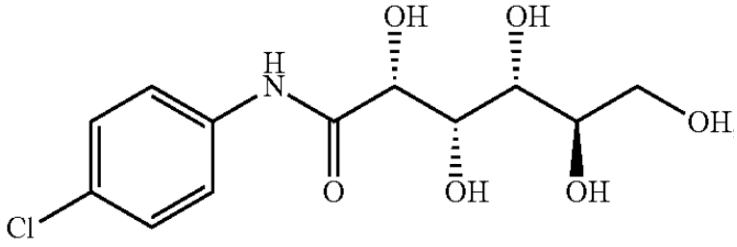

2.2.3.1 Dose-dependent Toxicity

Initial assessment of IRI toxicity was performed to assess if a dose-dependent cytotoxicity would occur. IRI concentrations were selected based on their solubility limits, resulting in exposure of BEAS-2B monolayers to 1, 2.5, 5, 10, or 15 mM 2FA or 2.5, 5, 7.5, or 10 mM 4ClA solutions in BEGM media within a 96-well plate at 37 °C 5% CO_2. Three replicates were used in each condition, and cells were treated for 30 or 60 minutes before IRI solution removal and replacement with 10% (v/v) alamarBlue™ in BEGM media. After 4 hours of alamarBlue™ incubation, absorbance was read on a spectrophotometer at 570 nm and 600 nm and Equation 1 was used to calculate percent

alamarBlue™ reduction. Data was analyzed in GraphPad Prism 8, and a $p < 0.05$ was considered to be statistically significant. A Spearman correlation test was performed to assess the correlation between IRI concentration and alamarBlue™ reduction for each IRI and duration of exposure.

2.2.3.2 Time-dependent Toxicity

For this experiment, two different cell populations were plated at a density of 36 000 cells/cm^2 in four 24-well plates and incubated at 37 °C 5% CO_2 for 24 hours. One cell population had been passaged 3 times since being received from LONZA and one population had been passaged 4 times since being received from LONZA. Following this, cells were incubated in either 15 mM 2FA in BEGM media, 10 mM 4ClA in BEGM media, 10% (v/v) DMSO in BEGM media, or BEGM media alone for 0.5, 1, 4, or 24 hours. 3 replicates from each cell population were used to generate 6 replicates total for each treatment condition. Following this, solutions were replaced with 10% (v/v) alamarBlue™ in media for 4 hours, and alamarBlue™ reduction was calculated using Equation 1 on absorbance readings from 100µL aliquots measured at 570 nm and 600 nm. Once alamarBlue™ reduction was calculated, cells from the 4- and 24-hour groups were trypsinized, counted using trypan blue and a hemocytometer, and re-plated at a cell density of 36 000 cells/cm^2. After 48 hours of 37 °C 5% CO_2 incubation, the media was replaced with 10% (v/v) alamarBlue™ and incubated for 4 hours prior to calculation of alamarBlue™ reduction, using the same method as above. In all cases, average alamarBlue™ reduction for each treatment condition was normalized to the alamarBlue™ reduction from the respective media-treated controls. Data was aggregated in Microsoft Excel and analyzed in GraphPad Prism 8, and a $p < 0.05$ was considered to be statistically significant. A non-linear regression for a straight line (slope = 0) was performed for each treatment condition to determine if alamarBlue™ reduction remained constant with increasing duration of exposure. A two-way ANOVA and Tukey's multiple comparison test was performed to assess differences between treatment conditions at each time point.

Following this analysis, an experiment was performed to assess the effects of extended 15 mM 2FA exposure in culture. 18 000 cells/cm^2 were plated in each well of a 24 well plate and incubated for 24 h at 37 °C 5% CO_2. After initial incubation, 4 wells each were assigned to undergo 24, 48, or 72 h incubations with either 15 mM 2FA in BEGM media or BEGM media alone, and culturing solutions were replaced accordingly. In all cases, media solutions were replaced every 24 h. After the required duration of exposure for each treatment condition, the media solutions were removed and replaced with 10% (v/v) alamarBlue™ in BEGM media. After 3 hours of incubation at

37 °C 5% CO_2, absorbance was read at 570 nm and 600 nm from 100 µL aliquots, and percent alamarBlue™ reduction was calculated using Equation 1. A two-way ANOVA and Sidak's multiple comparisons test was performed to assess differences in alamarBlue™ reduction between 15 mM 2FA treatment and media-treatment conditions at each time point. This analysis was performed in GraphPad Prism 8, and a $p < 0.05$ was considered to be statistically significant.

2.2.4 IRI Permeation and Ice Recrystallization Inhibition Activity

In order to determine if the IRIs can permeate BEAS-2B cells and reduce intracellular ice grain size, a visualization technique which allows for the quantification of intracellular ice must be used. This may be completed through cryofixation or through low temperature microscopy methods, each of which has their own advantages and disadvantages. For instance, cryofixation techniques allow for the delayed analysis since they may be stored for longer periods of time and may allow for higher resolution due to the lack of cryoprotectant solutions during visualization; however, this technique is more time-consuming, there is less control in freezing and warming rates, and downstream assessment is limited to those which may be performed with fixed cells. Contrastingly, low-temperature microscopy can be performed rapidly and allows for real time assessment, more controlled rates of cooling or warming, and downstream assessment in living cells; however, this comes at the expense of lower resolution. Assessment of IRI permeation and ice control, with or without the addition of DMSO, was therefore performed using cryofixation, as delayed analysis was desired. However, the ability of the IRI 2FA to function with a reduced concentration of 11 mM was also of interest; therefore, a rapid assessment of IRI concentration was performed using cryomicroscopy.

2.2.4.1 IRI Permeation and Activity in the Absence of Cryoprotectants

Our lab has previously reported on a cryofixation technique which allows for observation of ice within V79-4 hamster fibroblasts[3], and this method has also been utilized in HUVEC monolayers[157]. In this method, a low-temperature fixative is used to fix frozen cells and the cells are stained with SYTO13 before or after freezing. When visualized under fluorescent microscopy, intracellular spaces which were occupied by ice remain unstained and can be quantified. For this study, the low temperature fixative consisted of 85 parts 70% ethanol, 10 parts 38% formaldehyde, 5 parts glacial acetic acid. The ethanol in this fixative allows for protein precipitation and

aggregation and a reduction of the freezing point, while the use of formaldehyde crosslinks proteins and nucleic acids through the formation of methylene bridges [73; 90]. Acetic acid is used to increase the fixation speed and counteract excessive ethanol dehydration [90].

To assess IRI permeation and activity in the absence of other cryoprotectants, this cryofixation technique was utilized. 24 glass coverslips were plated with 50 000 cells/cm^2, using the plating method described in section 2.2.1. After 24 h incubation at 37 °C 5% CO_2, media was removed and replaced with 50 µL of 50 uM SYTO13 in PBS. After 10 min incubation at room temperature, the SYTO13 solution was replaced with 250 µL of 15 mM 2FA in PBS, 10 mM 4ClA in PBS, 10% (v/v) DMSO in PBS, or PBS alone. Cells were incubated for 30 min at room temperature before the solution was removed, and the plates were rapidly cooled in a VIAfreeze™ controlled-rate freezer (GE Healthcare) pre-cooled to -80 °C. The cells were left on the VIAfreeze™ for 30 minutes prior to being transferred on dry ice to a fume hood. 500 µL of a fixative solution composed of 85 parts 70% ethanol, 10 parts 40% formaldehyde, and 5 parts glacial acetic acid pre-cooled to -80 °C was added to each well of cell-coated coverslips on dry ice. The cell-coated coverslips were left in the fixative solution in the fume hood on dry ice for 24 hours, prior to being removed and placed on a microscope slide for observation under fluorescent microscopy (Nikon eclipse 80i). Intracellular ice grain size was quantified from two 50X images in each condition using NIS Elements AR 3.2 image analysis software (Nikon), and data was analyzed using GraphPad Prism 8. Data was log transformed, and normality was confirmed prior to use of a nested one-way ANOVA with Tukey's multiple comparison test. A p-value less than 0.05 was considered to be significant.

2.2.4.2 2FA Permeation and Activity in the Presence of DMSO

Following this assessment, the ability for the IRI 2FA to permeate BEAS-2B cells and reduce intracellular ice grain size in the presence of DMSO was assessed. For this analysis, 80 000 cells/cm^2 were added to 6 glass coverslips, which had been coated using the plating method described in section 2.2.1. Cells were cultured to confluency in a 37 °C 5% CO_2 incubator. Cells were treated for 30 minutes at room temperature with 10 % DMSO in BEGM media, 11 mM 2FA 10 % DMSO in BEGM media, or BEGM media alone. Using the same methodology described in section 2.2.4, cells were frozen on a VIAfreeze™ controlled-rate freezer (GE Healthcare) pre-cooled to -80 °C prior to cryofixation. Intracellular ice was visualized by staining of the cells with 50 uM SYTO13 in PBS and images were obtained under fluorescent microscopy (Nikon eclipse 80i). Intracellular ice grain size was quantified from two 50X images in each condition using NIS Elements AR 3.2

image analysis software (Nikon), and data was analyzed using GraphPad Prism 8. Data was log transformed, and normality was confirmed prior to use of a nested one-way ANOVA with Tukey's multiple comparison test. A p-value less than 0.05 was considered to be significant.

2.2.4.3 2FA Permeation and Activity with Reduced Concentration

Subsequent analysis utilizing cryomicroscopy was performed under reduced concentrations to ensure that a reduction from 15 mM 2FA to 11 mM 2FA retained the ability to reduce intracellular ice grain size. In this experiment, confluent cells prepared on glass coverslips, as outlined in section 2.2.1, were treated for 10 minutes with 50 μM SYTO13 in BEGM media at room temperature. Cells were then treated for 30 minutes at room temperature with 11 mM 2FA in BEGM media or 10 % DMSO in BEGM media before transfer to a cryomicroscope (Linkam FDCS196 and Nikon Eclipse 80i). Cells were frozen at a rate of -90 °C/min to -25 °C and held at -25 °C for 10 minutes. Intracellular ice was observed under fluorescent microscopy and images were captured 4 and 10 minutes after reaching -25 °C.

2.2.6 Post-thaw Viability

Following analysis of ice control by IRIs, the ability for IRIs to improve post-thaw survival under conditions which result in intracellular ice formation and growth was of interest. Considering that different methods of analyzing cell viability may result in different results and interpretations [163], two methods of determining post-thaw cell viability were assessed. The experiments performed to assess post-thaw viability are schematically represented in Figure 2.13.

First, membrane integrity was assessed immediately post-thaw, as well as 24 h post-thaw, after rapid freezing (-90 °C/min) to -25 °C and rapid thawing (+90 °C/min) to +20 °C. Considering that some literature has demonstrated that immediate membrane integrity may not be representative of prolonged survival due to delayed onset cryoinjury[23; 24], this allowed for assessment of changes to membrane integrity over time while analyzing the effect of IRI-use on post-thaw survival when freezing conditions stimulate intracellular ice formation.

This assessment was then expanded upon through the assessment of metabolic activity using alamarBlue™ 24 h post-thaw, with or without the addition of a transient warming event. This allows for evaluation of prolonged metabolic activity after freezing, and the use of a transient warming event allows for stronger assessment of ice recrystallization inhibition by IRIs since

transient warming events exacerbate recrystallization[21; 79]. The transient warming event studied in this analysis consisted of rapid freezing at a rate of -90 °C/min to -25 °C, warming at a rate of +25 °C/min to -15 °C, rapid freezing at a rate of -90 °C/min back to -25 °C, and rapid warming at a rate of +90 °C/min to +20 °C.

2.2.6.1 Post-thaw Membrane Integrity

Post-thaw membrane integrity was first assessed through the addition of 50 000 cells/cm^2 to eighteen 12 mm coverslips prepared and cultured as described in section 2.2.1. Eight coverslips were treated for 10 minutes with 50 µM SYTO13 in media. Following this, cells were treated for 30 min at room temperature with either media, 11 mM 2FA in media, 8 % DMSO 11 mM 2FA in media, or 8% DMSO in media (n=2), with each solution containing 20 µM Ethidium Bromide. Coverslips were transferred to a cryomicroscope (Linkam FDCS196 and Nikon Eclipse 80i). where they were frozen at a rate of -90 °C/min to -25 °C. After a one minute hold at -25 °C, cells were thawed at a rate of +90 °C/min to +20 °C. Fluorescent images were obtained from the center of each coverslip prior to freezing and after thawing. Images were analyzed using the Viability3 program for automated cell counting (custom software: Version 3.2, The Great Canadian Computer Company, Spruce Grove, AB, Canada) to calculate percent membrane integrity. The remaining 10 coverslips were treated for 30 min at room temperature with media (n=4), 11 mM 2FA in media (n=2), 8 % DMSO 11 mM 2FA in media (n=2), or 8% DMSO in media (n=2). All coverslips, except 2 media-treated controls, were transferred to the cryomicroscope (Linkam FDCS196 and Nikon Eclipse 80i) and were frozen at a rate of -90 °C/min to -25 °C. After a one minute hold at -25 °C, cells were thawed at a rate of +90 °C/min to +20 °C. All 10 coverslips were cultured for 24 h in an incubator set to 37 °C 5% CO_2. These cell-covered coverslips were then assessed for membrane integrity through the application of 50 uM SYTO13 and 20 uM ethidium bromide in BEGM media for 10 minutes at room temperature prior to obtaining images under fluorescent microscopy (Nikon Eclipse 80i). Images were analyzed using the Viability3 software to calculate percent membrane integrity. GraphPad Prism 8 was used to perform a one-way ANOVA with Tukey's multiple comparison test.

2.2.6.2 Post-thaw Metabolic Activity

Following assessment of post-thaw membrane integrity, cell metabolism was assessed using alamarBlue™ following cryopreservation, with or without a transient warming event. 50 000 cells/cm^2 was added to thirty-six 12 mm coverslips prepared and cultured as described in section 2.2.1. Cells were treated with 8 % DMSO in BEGM media (n=12), 8 % DMSO 11 mM 2FA in BEGM media (n=12), or BEGM media alone (n=12) for 30 min at room temperature. 6 coverslips each from the 8% DMSO and 8% DMSO 11 mM 2FA in BEGM media treatment condition were placed, one at a time, on the cryomicroscope (Linkam FDCS196 and Nikon Eclipse 80i). They were then frozen at a rate of -90 °C/min to -25 °C, held for 1 min, then warmed at a rate of +90 °C/min to +20 °C before being transferred to a new well plate containing pre-warmed media. This was repeated with 3 of the media-treated wells as negative controls, and 3 of the media treated wells were transferred to the new plate without being frozen to act as positive untreated controls. The remaining 18 wells underwent the same process but were frozen with an additional transient warming cycle in which cells were frozen at a rate of -90 °C/min to -25 °C, warmed at a rate of +25 °C/min to -15 °C, cooled at a rate of -90 °C/min to -25 °C, then warmed at a rate of +90 °C/min to +25 °C. A one minute hold occurred at each step. All cells were cultured for 24 h at 37 °C 5% CO_2, prior to the addition of 10 % alamarBlue™ in BEGM media to each well. Cells were incubated in the alamarBlue™ solution at 37 °C 5% CO_2 for 3 hours prior to aliquots being analyzed in 96-well plates as described in section 2.2.2. Data for each condition was normalized to unfrozen media-treated controls.

GraphPad Prism 8 was used to perform statistical analyses and a $p < 0.05$ was considered to be statistically significant. Differences in percent membrane integrity was compared using a one-way ANOVA. Differences in alamarBlue™ reduction between treatment and freezing conditions was assessed using a two-way ANOVA and Sidak's multiple comparison test.

2.3 Results

2.3.1 alamarBlue™ Assay Validation

The results of this experiment are shown in Figure 2.1. A significant correlation between cell concentration and alamarBlue™ reduction was found when alamarBlue™ was incubated for 2 h (r^2=0.9119 $p<0.0001$), 3 h (r^2=0.8947 $p<0.0001$),4 h (r^2=0.9172 $p<0.0001$), 5 h (r^2=0.9324

$p<0.0001$), or 6 h ($r^2=0.9256$ $p<0.0001$). No significant correlation was found after 24 h incubation ($r^2=0.3993$ $p=0.0679$).

2.3.2 Cytotoxicity of IRIs

2.3.2.1 Dose-dependent Toxicity

The impact of increasing 2FA and 4ClA concentrations on cell metabolism is demonstrated in Figure 2.2 and 2.3, respectively. No changes in metabolic activity with increasing IRI exposure was observed for 30 min or 1 h exposure times, and no significant correlation ($p>0.05$) was found between concentration of IRI and metabolic activity under any condition.

2.3.2.2 Time-dependent Toxicity

The metabolic activity of cells exposed to 15 mM 2FA, 10 mM 4ClA, and 10 % DMSO for 0.5, 1, 4, or 24 h is represented in Figure 2.4. The effect of 4 and 24 h exposure to these cryoprotectants on cell replication was assessed through re-plating, 48 h recovery, and assessment of metabolic activity. The results of this re-plate assessment are shown in Figure 2.5. The non-linear regression analysis indicated that the slope of the line from 0.5-24 h 15 mM 2FA exposure was not significantly different from zero ($p=0.2853$). In contrast, the slope of the line from 0.5-24 h exposure to 10 mM 4ClA or 10% (v/v) DMSO did significantly differ from zero ($p<0.05$). A Tukey's multiple comparison analysis indicated that metabolic activity was significantly different between 15 mM 2FA exposure and 10% (v/v) DMSO exposure at all durations of exposure. The relevant details of this multiple comparison are represented in Table 2.1.

A significant difference in metabolism between cells treated with 10% (v/v) DMSO and 15 mM 2FA for 4 h or 24 h was observed ($p<0.05$). A significant difference in cell metabolism was also observed between cells treated with 10% (v/v) DMSO and 4ClA for 24 h after 48 h recovery ($p=0.0006$). Therefore, cell metabolism 48 h after 4 h and 24 h exposure to 10% (v/v) DMSO is significantly reduced when compared to 15 mM 2FA.

The results of the prolonged 2FA exposure experiment is represented in Figure 2.6. Cell metabolism remained unchanged following 24 h, 48 h, or 72 h exposure to 15 mM 2FA. This contrasted media-treated controls which exhibited increased cell metabolism with increasing days

of culture. At each time point, cells treated with 15 mM 2FA had significantly less metabolic activity than cells treated with media alone ($p<0.001$).

2.3.3 IRI Permeation and Ice Recrystallization Inhibition Activity

2.3.3.1 IRI Permeation and Activity in the Absence of Cryoprotectants

Sample images obtained from 50X images of cryofixed cells are shown in Figure 2.7. Within these images, intracellular ice is visualized as the unstained fractions within each cell since the formation of ice nuclei excludes nucleic acid, and therefore SYTO13, from the developing lattice. Treatment with 15 mM 2FA reduced mean intracellular grain size resulting in visibly intact nuclei and nucleosomes not seen in other treatment conditions. However, treatment with 10 mM 4ClA or 10% (v/v) DMSO resulted in ice grains that were not visibly reduced in size from cryoprotectant-free controls.

The distribution of ice grain size is visualized in Figure 2.8, with the exclusion of ice grains larger than 35 μm. The median (IQR) ice grain size for 15mM 2FA, 10mM 4ClA, 10% (v/v) DMSO, or PBS, respectively, was 0.50 (0.33), 3.70 (5.03), 6.72 (6.86), and 5.41 (5.50). Data was log-transformed, and normality was confirmed using a QQ plot (Figure 2.9). Treatment with 15 mM 2FA resulted in significantly smaller intracellular ice than any other condition ($p<0.01$ in all comparisons). No difference in intracellular ice grain size was observed between 10 mM 4ClA, 10 % DMSO, or PBS treatment conditions ($p>0.05$ in all comparisons). Summary descriptive and inferential statistics are shown alongside the normal QQ plot in Figure 2.9.

2.3.3.2 2FA Permeation and Activity in the Presence of DMSO

As visualized in Figure 2.10 and 2.11, no significant differences in intracellular ice size were found between the various treatment conditions ($p=0.9586$).

2.2.4.3 2FA Permeation and Activity with Reduced Concentration

Sample images and a schematic of the freezing profile are shown in Figure 2.12. Ice grain size is visibly reduced through the addition of 11 mM 2FA, although the images were not of sufficient resolution to be quantified.

2.3.4 Post-thaw Viability

2.3.4.1 Post-thaw Membrane Integrity

As shown in Figure 2.14, regardless of the treatment condition, the majority of cells assessed for membrane integrity after -90 °C/min freezing to -25 °C and +90 °C/min warming to +25 °C became permeable to ethidium bromide immediately post-thaw. However, cells which were cultured for 24 h prior to analysis of membrane integrity were found to be mostly membrane intact. When the 24 h post-thaw images were quantified (Figure 2.15), no statistically significant difference in cell membrane integrity was observed between cells treated with 8 % DMSO alone or treated with 11 mM 2FA and 8 % DMSO ($p=0.079$). 11 mM 2FA treatment alone or media treatment alone resulted in negligible membrane integrity 24 h post-thaw, and cell lift-off can be visualized through large portions of the coverslip lacking cells although all coverslips were approximately equally confluent prior to freezing.

2.3.4.2 Post-thaw Metabolic Activity

Post-thaw cell metabolism results are shown in Figure 2.16. During plunge freeze events, with or without the addition of a transient warming event, no significant difference in alamarBlue™ reduction was found between cells treated with 8 % DMSO alone or treated with 8 % DMSO and 11 mM 2FA. The media-treated negative controls exhibited no reduction of alamarBlue™.

2.3 Discussion

The alamarBlue™ validation experiment successfully demonstrated that alamarBlue™ may be used to determine the relative number of metabolically active cells in BEAS-2B monolayers when incubations from 2-6 hours are used, since significant strong correlations were observed between cell density and alamarBlue™ reduction. However, only concentrations from 4,000 to 36,000 cells/cm^2 were assessed for this validation, which does not meet the seeding density required to generate confluent monolayers in subsequent experiments. Therefore, this validation demonstrates useful differentiation of lower cell densities which may be seen in higher levels of cellular demise during experimentation, but this experiment did not validate the ability for alamarBlue™ to differentiate cell metabolism at higher cell concentrations. However, the time-

dependent changes in alamarBlue™ reduction suggest that shorter incubations may be used when the seeding density is higher to better differentiate between conditions.

The results of the IRI toxicity experiments clearly demonstrated that one IRI, 2FA, was not cytotoxic to BEAS-2B cell monolayers. While the preliminary analysis of dose-dependent cytotoxicity did not find a relationship between increasing IRI concentration and reduced metabolism in either IRI tested, the small sample size of 3 limited the ability to provide substantive conclusions. Upon more thorough analysis using 10 mM 4ClA, 15 mM 2FA, and 10 % DMSO, it was found that 15 mM 2FA exhibited no cytotoxic effect while 10 mM 4ClA and 10% DMSO did. This was demonstrated through consistency of cell metabolism at levels comparable to media-treated controls after 0.5-24 h 15 mM 2FA exposure. Contrastingly, cells treated with 4ClA or DMSO exhibited reduced metabolism when compared to media-treated controls and a reduction in metabolic activity was observed as the concentration of 4ClA and DMSO increased. In addition, the re-plate experiments provide some indication of delayed-onset cytotoxicity by 4ClA and DMSO since cells which were membrane intact after 4 or 24 h exposure to 4ClA and DMSO had reduced metabolism when compared to media-treated controls after 48 h recovery. Considering that the doubling time of BEAS-2B cells is approximately 26 h [87], these results suggest that exposure to 4ClA and DMSO for 4 or 24 h hinders replication. This finding corroborates with previous research which demonstrated that DMSO causes molecular changes which alters cellular functions, such as replication[69; 200]. No such relationship was observed in re-plate assessments following 4 or 24 h exposure of cells to 15 mM 2FA. However, a reduction in cell metabolism when compared to media-treated controls was observed when cells were treated with 15 mM 2FA for 48 h or 72 h. Given the observed ability for cells to maintain metabolism after 24 h treatment with 15 mM 2FA and 48 h recovery during the re-plate experiment, it is possible that the reduction in metabolism observed after 48 h or 72 h exposure may not be indicative of cell death or delayed cytotoxicity. However, the long-term effect of 48 h or 72 h exposure to 15 mM 2FA or the molecular means of demise and failure to replicate in 4ClA- and DMSO-treated cells was not elucidated by this work.

The IRI permeation and ice control experiments demonstrated that 2FA is capable of reducing intracellular ice grain size when used at a concentration of 11 mM or 15 mM suggesting 2FA is able to permeate BEAS-2B cells, while 10 mM 4ClA and 10% (v/v) DMSO were ineffective at reducing intracellular ice grain size. It was additionally discovered that the use of 10% (v/v) DMSO in combination with 11 mM 2FA renders 11 mM 2FA ineffective in reducing intracellular ice grain size. While it was expected that 10% (v/v) DMSO would not inhibit intracellular ice recrystallization when compared to PBS or media, it was unexpected that no ice control would be

observed when cells were treated with 10 mM 4ClA or 11mM 2FA with 10% (v/v) DMSO. The inability for 4ClA to reduce intracellular ice grain size may simply be due to an inability of 10 mM 4ClA to permeate the cells after 30 minutes of room temperature exposure; however, it may also be caused by a lack of intracellular ice recrystallization inhibition by 4ClA in BEAS-2B cells. It is additionally unclear if the lack of reduction in intracellular ice grain size when DMSO is used with 2FA is caused by interactions of DMSO and 2FA in solution, an inability of 2FA entry into the cell when DMSO is used, or alterations of intracellular characteristics by DMSO which prevent 2FA from inhibiting ice recrystallization.

The post-thaw viability experiments demonstrated that the use of 2FA with DMSO does not improve post-thaw membrane integrity or metabolic activity of BEAS-2B cells when compared to DMSO-treated controls. This corroborates with the cryofixation data which demonstrated a lack of reduction in intracellular ice grain size by 2FA when DMSO is used. Although previous IRI research has demonstrated improved membrane integrity of red blood cells post-thaw when IRIs are used[32; 41; 157], the type of IRI used here, the cell type used, the type of permeating cryoprotectant used, and the freezing protocol differed. Therefore, this work does not contradict previous literature, even though the IRI 2FA was found to be incapable of reducing intracellular ice grain size or improving post-thaw cell survival when used with DMSO.

Interestingly, the membrane integrity experiments demonstrated that immediate post-thaw membrane integrity of BEAS-2B cells was not representative of 24 h post-thaw membrane integrity when rapid freezing results in intracellular ice nucleation. This contrasts previous findings which have concluded that immediate post-thaw membrane integrity is representative, or even an underestimation, of long term post-thaw survival due to delayed onset cryoinjury[2; 22]. The consistency of the 24 h post-thaw membrane integrity results with the 24 h post-thaw metabolic activity results suggests that the formation of intracellular ice when DMSO is used causes a transient loss in membrane integrity that is not indicative of prolonged survival. However, metabolic activity and membrane integrity were only assessed at 24 h in this case, and molecular-level injury was not assessed. Therefore, the prolonged effect of this transient loss of membrane integrity when intracellular ice forms in BEAS-2B cells is unknown.

The finding that 2FA reduces intracellular ice grain size but does not confer a survival benefit when used with DMSO raises the question as to whether 2FA can be considered a cryoprotectant. If cryoprotectants are defined as solutes which allow for heightened post-thaw recovery when compared to its absence [61; 78; 105], then 2FA would not be considered a cryoprotectant based on the findings of this chapter. However, the work performed here should

encourage us to further consider the down-stream implications of cryoinjury which does not cause immediate cellular demise in terms of loss of membrane integrity or reduction in metabolism. For instance, when the toxicity data is considered, cells which were found to be metabolically active and membrane intact failed to replicate when re-plated after prolonged treatment with 4ClA or DMSO (Figure 2.5). This substantiates the point that the quality of cells which survive is just as important as the quantity which survive. In addition, the finding that immediate post-thaw membrane integrity is not always indicative of 24 h post-thaw membrane integrity and metabolism should encourage scientists to reconsider the weight placed on immediate post-thaw cell survival. Hence, cryoprotectants may be better defined as solutes which may be used in cryopreservation practices to improve post-thaw recovery and/or quality of cryopreserved specimens. This definition may more suitably account for molecules, such as IRIs, which may be incapable of improving post-thaw cell survival under certain conditions but may be useful additives during cryopreservation in terms of improving specimen quality. Although an improvement of cell quality by the use of 2FA was not demonstrated by this work, the reduction in intracellular ice grain size may reduce intracellular damage leading to improved cell quality post-thaw. This is supported by previous work which has demonstrated that heightened intracellular ice formation increases rates of programmed cell death without causing immediate physical damage [211]. Additional research has also demonstrated that the size of intracellular ice grains is related to post-thaw survival of nematodes; hence, the reduction of intracellular ice grain size afforded by 2FA use may improve survival in larger scale specimens[169]. In addition, the extracellular ice control by 2FA has yet to be explored and the ability for 2FA to improve post-thaw cell monolayer survival when used with other cryoprotectants or in the use of tissue cryopreservation may allow 2FA to fall under the more classical definition of a cryoprotectant.

2.5 Conclusions

The research conducted in this chapter set out to characterize the role IRIs could play in lung cryopreservation through assessment of IRI toxicity, permeation, intracellular ice control, and ability to improve post-thaw survival in type II pneumocyte monolayers. It was hypothesized that IRIs would not be cytotoxic and would be capable of permeating cells and controlling intracellular ice growth resulting in improved survival of type II pneumocytes under freezing conditions which stimulated intracellular ice formation and growth, when compared to DMSO-treated controls. Although one IRI, 2FA, was found to be non-toxic for up to 24 h of exposure at 37 °C, the IRI 4ClA

was found to exhibit similar short- and long-term cytotoxicity to the commonly used cryoprotectant, DMSO. Unlike 4ClA, 2FA was found to reduce intracellular ice grain size very well during cryofixation experiments; however, this was perturbed by the addition of DMSO. It is likely that this lack of intracellular ice control in the presence of DMSO resulted in the inability of 2FA to improve post-thaw membrane integrity and cell metabolism following plunge-freeze events, with or without the addition of a transient warming event.

Ultimately, the ability for 2FA to reduce intracellular ice grain size without toxicity in the absence of DMSO warrants further analysis. It is difficult to better characterize the relationship between DMSO and 2FA within cell monolayer research, and it is unclear if 2FA may reduce ice grain size extracellularly when used with DMSO. Therefore, subsequent research assessing the inhibition of extracellular ice growth by 2FA within lung tissue will better address this relationship. It will additionally allow for further toxicity screening amongst the various cell types of the lung.

2.5 Tables and Figures

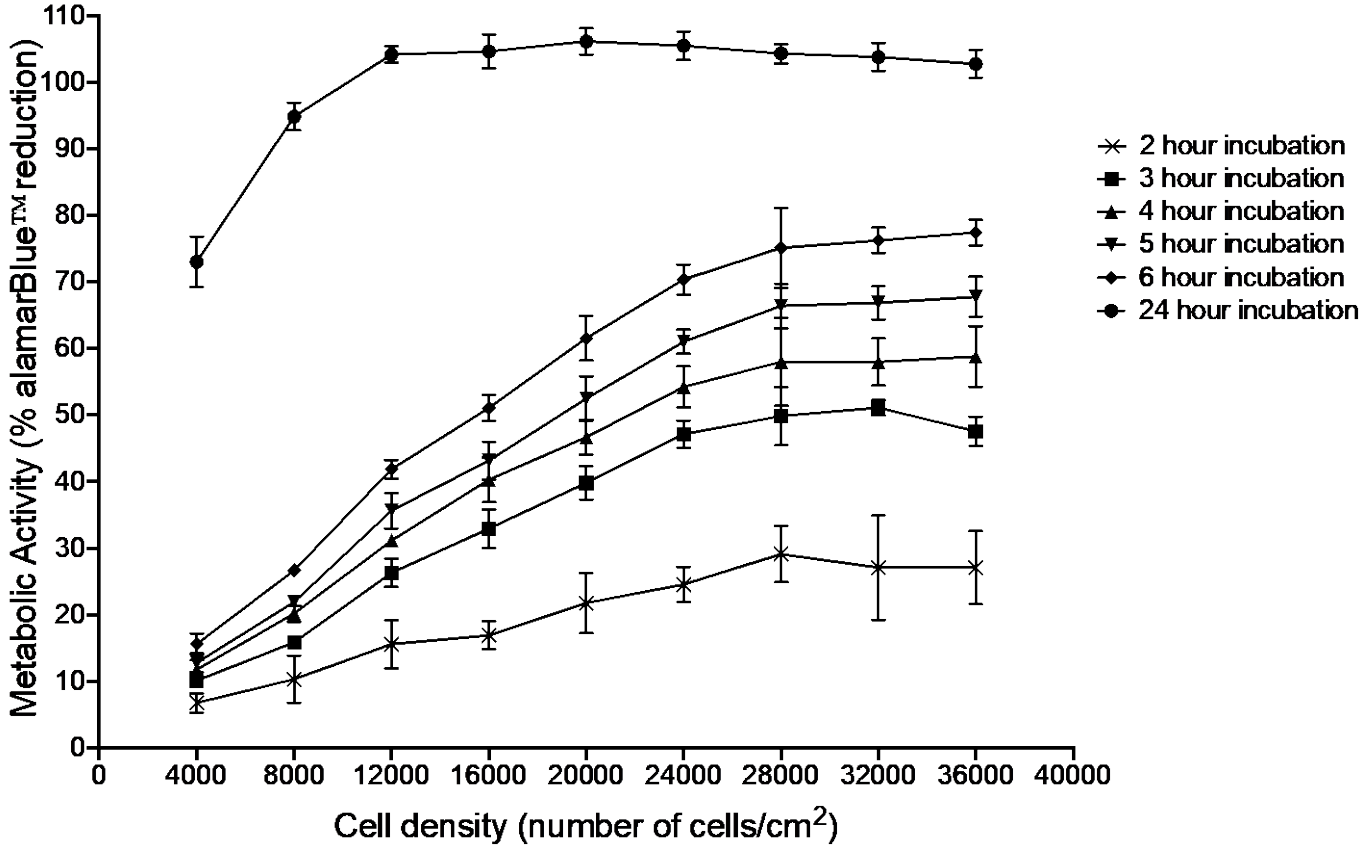

Figure 2.1 Optimization of the alamarBlue™ Assay – The Relationship Between Metabolic Activity, Cell Number, and Incubation time

BEAS-2B cells plated at various cell densities were incubated for 2, 3, 4, 5, 6, or 24 h in 10% alamarBlue™ prior to evaluation of alamarBlue™ reduction. Mean cell metabolic activity (SD) (n=4) is shown, and significant correlations between cell density and alamarBlue™ reduction was observed following 2, 3, 4, 5, 6 h incubations ($p<0.05$ in all cases).

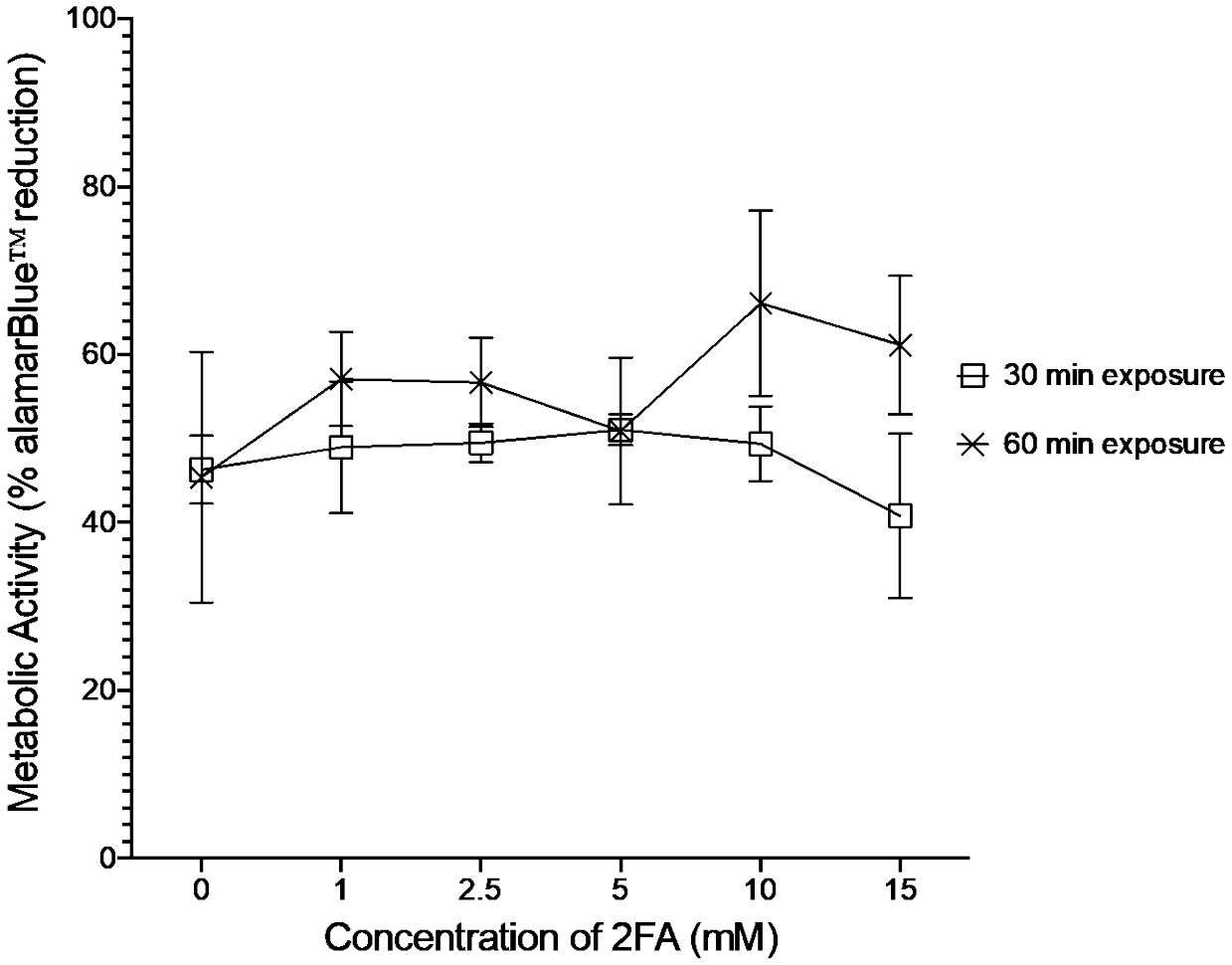

Figure 2.2 Assessment of Dose-dependent Cytotoxicity by 2FA

BEAS-2B monolayers were exposed to 0, 1, 2.5, 5, 10, or 15 mM 2FA for 30 or 60 min prior to assessment of metabolic activity. Mean (SD) cell metabolic activity (n=3) is shown. No significant relationship was found between 2FA concentration and metabolic activity when a Spearman's correlation test was performed ($p>0.990$ and $p=0.136$ for 30 min and 60 min exposure, respectively).

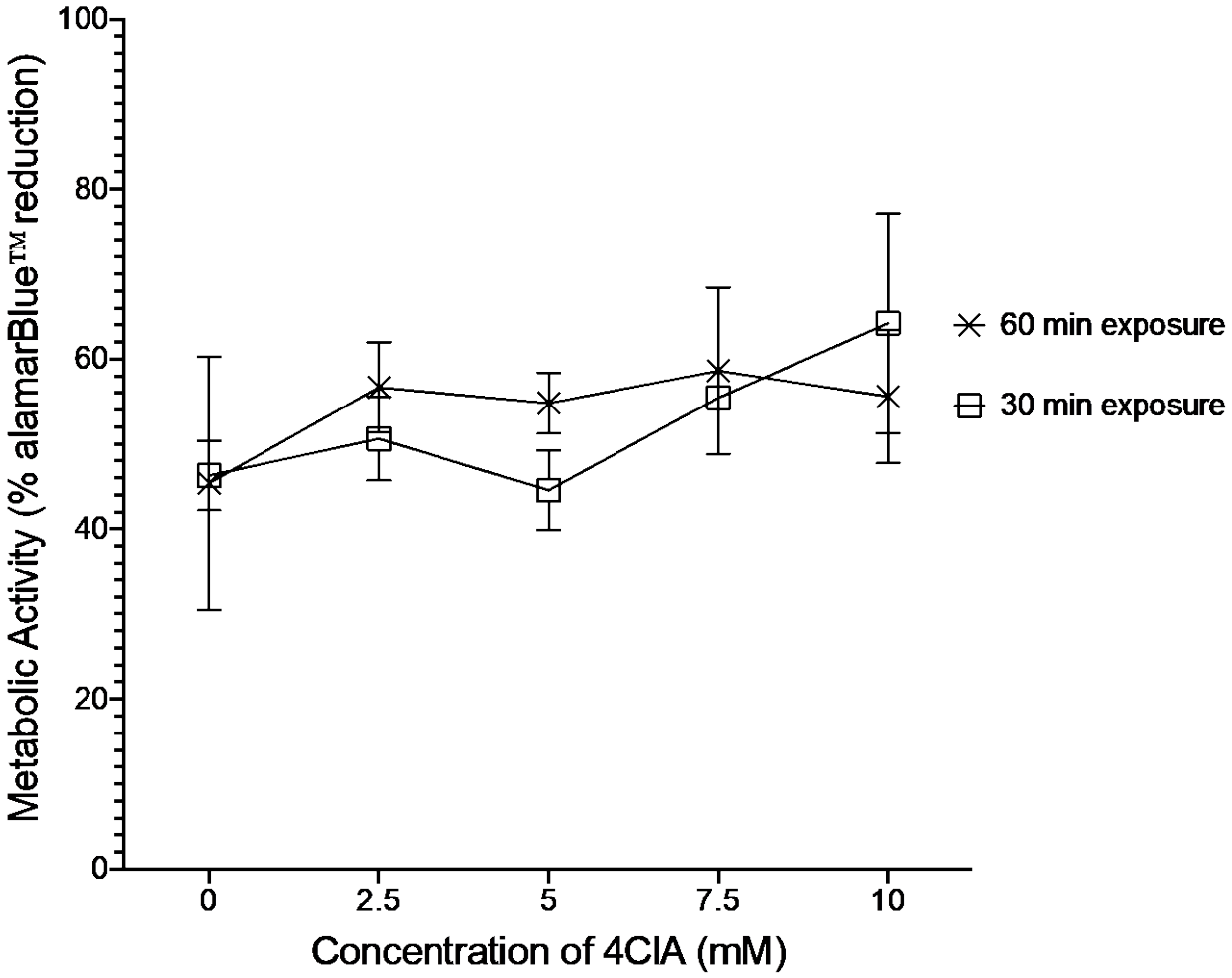

Figure 2.3 Assessment of Dose-dependent Cytotoxicity by 4ClA

BEAS-2B monolayers were exposed to 0, 2.5, 5, 7.5 or 10 mM 4ClA for 30 or 60 min prior to assessment of metabolic activity. Mean (SD) cell metabolic activity (n=3) is shown. No significant relationship was found between 4ClA concentration and metabolic activity when a Spearman's correlation test was performed (p=0.233 and p=0.450 for 30 min and 60 min exposure, respectively).

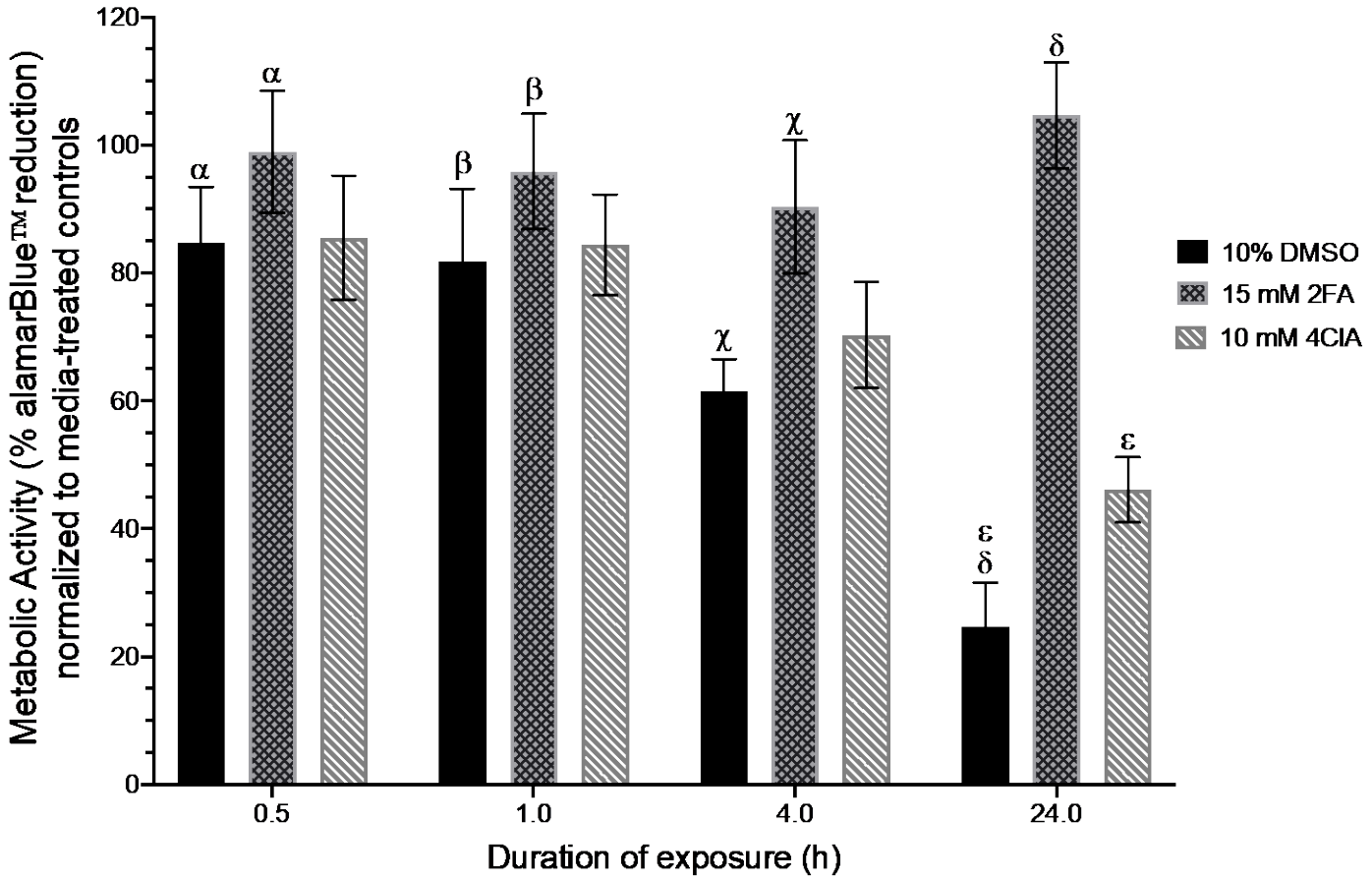

Figure 2.4 Assessment of Time-dependent Cytotoxicity of 2FA, 4ClA, and DMSO

BEAS-2B monolayers were exposed to 10% (v/v) DMSO, 15 mM 2FA, or 10 mM 4ClA for 0.5, 1, 4, or 24 h at 37 °C 5% CO_2, prior to assessment of metabolic activity. Mean cell metabolic activity (SD) of each treatment condition normalized to media-treated controls (n=6) is shown. Significant differences between conditions, as determined by a two-way ANOVA and Tukey's multiple comparison test, are indicated by matching symbols.

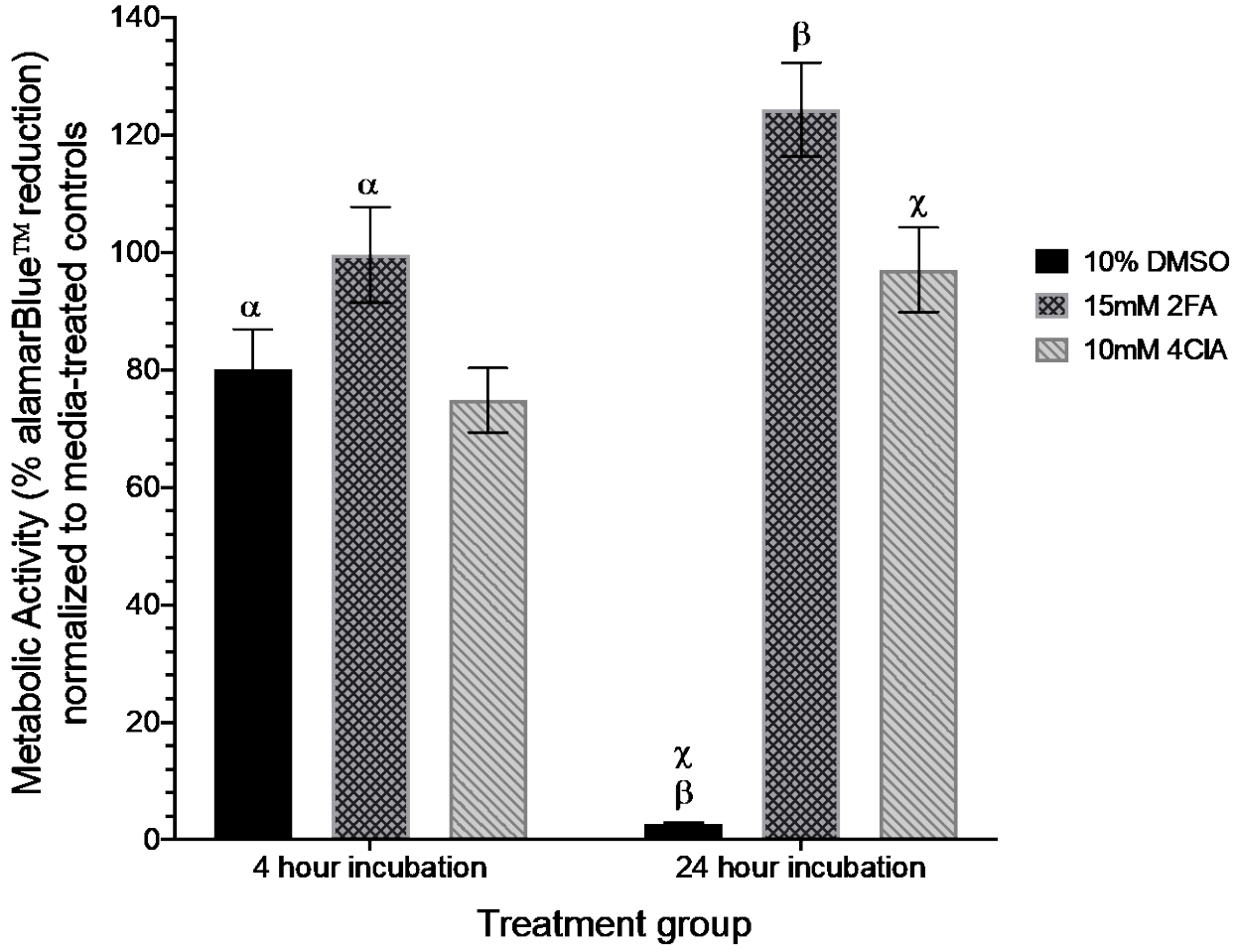

Figure 2.5 Assessment of Long-term Cytotoxicity of 2FA, 4ClA, and DMSO

BEAS-2B monolayers were exposed to 10% (v/v) DMSO, 15 mM 2FA, or 10 mM 4ClA for 4 or 24 h prior trypsinization, re-plating at the same cell density, and 48 h culture at 37 °C 5% CO_2 (n=2,6,5 for 4 h incubations in DMSO, 2FA, and 4ClA, respectively. n=2,6,2 for 24 h incubations in DMSO, 2FA, and 4ClA, respectively. Replicate variance is due to cellular demise during initial exposure). Mean cell metabolic activity (SD) of each treatment condition normalized to media-treated controls is shown. Significant differences between conditions, as determined by a two-way ANOVA and Tukey's multiple comparison test, are indicated by matching symbols.

		Tukey's multiple comparison test p-values		
	Duration of exposure	15 mM 2FA vs. 10% (v/v) DMSO	10 mM 4ClA vs. 10% (v/v) DMSO	15 mM 2FA vs 10 mM 4ClA
Short term cytotoxicity	0.5 h	**0.0153**	0.9860	**0.0234**
	1 h	**0.0164**	0.8547	**0.0619**
	4 h	**<0.0001**	0.1817	**0.0004**
	24 h	**<0.0001**	**0.0002**	**<0.0001**
Long-term cytotoxicity (Re-plate efficiency)	4 h	**0.0102**	0.6634	**<0.0001**
	24 h	**<0.0001**	**<0.0001**	**0.0006**

Table 2.1 DMSO and 4ClA have Greater Short- and Long-term Cytotoxicity than 2FA

P-values from the statistical analysis performed to compare the short- and long-term cytotoxicity of 15 mM 2FA, 10 mM 4ClA, and 10% (v/v) DMSO treatment to BEAS-2B cells. In all cases, a two-way ANOVA and Tukey's multiple comparison test was performed, and significant p-values are bolded. DMSO and 4ClA treatment resulted in significantly lower cell metabolism than treatment with 2FA following 0.5, 1, 4, and 24 h exposure. Exposure to DMSO or 4ClA for 4 or 24 h resulted in significantly less cell metabolism than exposure to 2FA after re-plating and 48 h recovery.

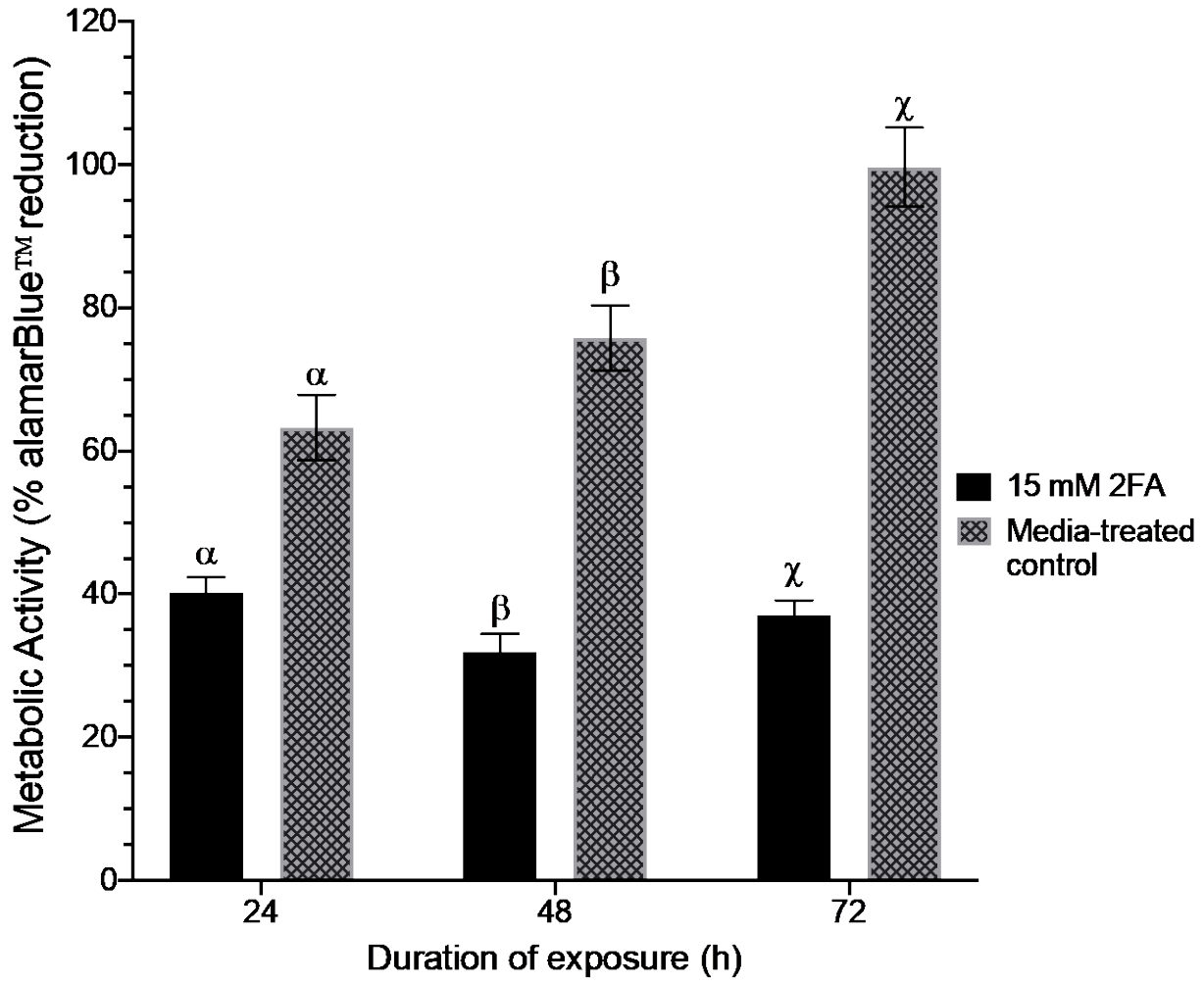

Figure 2.6 Exposure to 2FA for 24, 48, or 72 h Reduces Cellular Metabolism

BEAS-2B monolayers were exposed to 15 mM 2FA in BEGM media or media alone for 24, 48, or 72 h (n=4). Mean cell metabolic activity (SD) is shown. Significant differences between conditions, as determined by a two-way ANOVA and Tukey's multiple comparison test, are indicated by matching symbols.

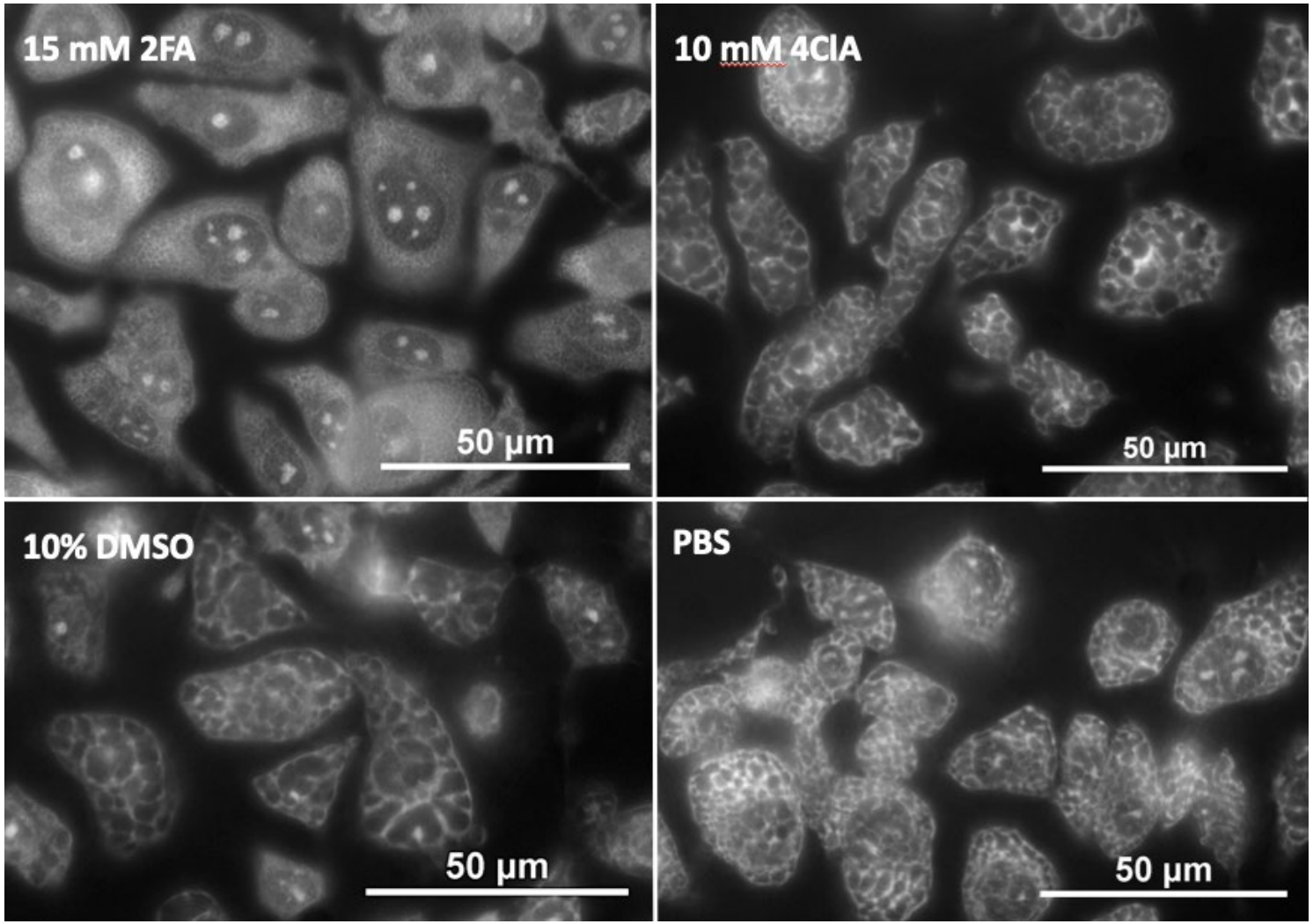

Figure 2.7 Visualization of Intracellular Ice following IRI Treatment

BEAS-2B cells were treated with 15 mM 2FA, 10 mM 4ClA, 10% (v/v) DMSO, or PBS prior to freezing to -80 °C, cryofixation, and SYTO13 staining. The unstained regions within each cell represents intracellular ice.

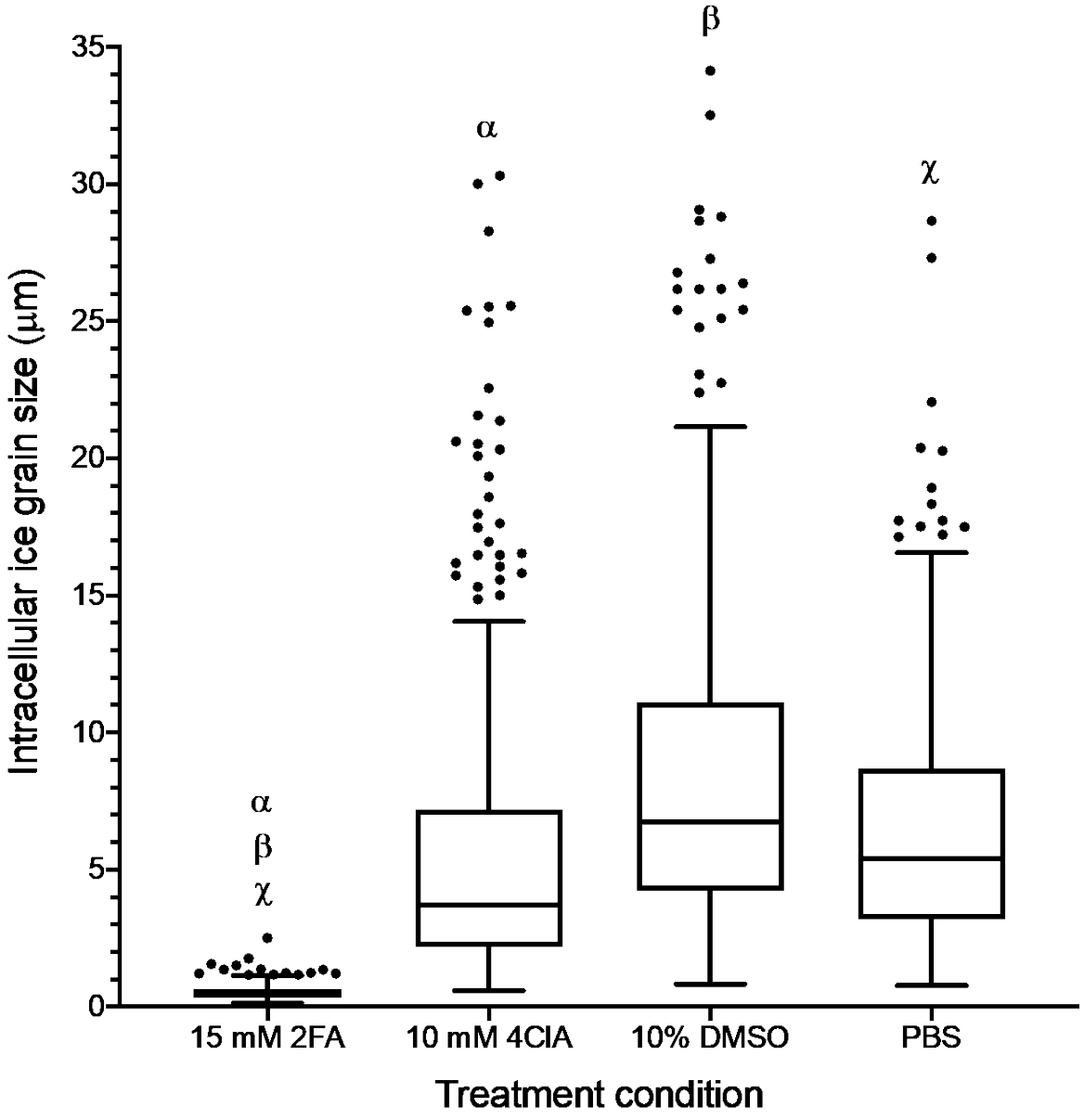

Figure 2.8 The IRI 2FA Significantly Reduces Intracellular Ice Grain Size

BEAS-2B cells were treated with 15 mM 2FA, 10 mM 4ClA, 10% (v/v) DMSO, or PBS prior to freezing to -80 °C, cryofixation, and SYTO13 staining. Distribution of intracellular ice grain size was obtained from two cryofixation images under 50X magnification, quantified using NIS Elements image analysis software. Significant differences in ice grain size between conditions, as determined by a two-way ANOVA and Tukey's multiple comparison test on log-transformed data, are indicated by matching symbols.

		15 mM 2FA	10 mM 4ClA	10% DMSO	PBS
Descriptive Statistics	Number of values	363	452	293	332
	Minimum	0.14	0.59	0.83	0.76
	25% Percentile	0.33	2.18	4.23	3.19
	Median	0.50	3.70	6.72	5.41
	75% Percentile	0.66	7.20	11.09	8.69
	Maximum	2.50	49.22	51.07	37.06
	Mean	0.54	5.57	9.04	6.72
	Std. Deviation	0.29	5.43	7.28	4.91
Tukey's multiple comparisons test p-values (on log-transformed data)	10 mM 4ClA	**0.0021**			
	10% DMSO	**0.0010**	0.3044		
	PBS	**0.0015**	0.8180	0.6661	

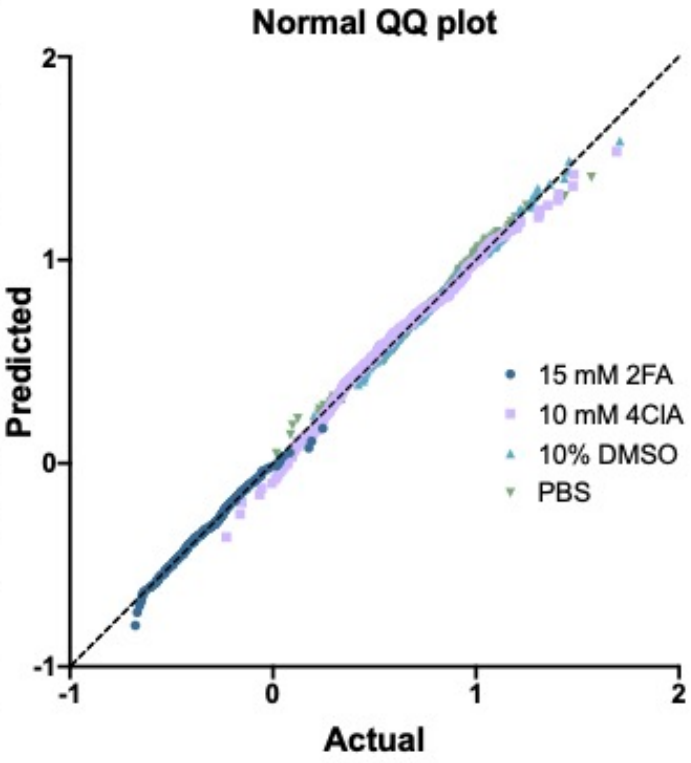

Figure 2.9 Descriptive and Inferential Statistics of Intracellular Ice grain size following IRI Treatment

Descriptive and inferential statistics of intracellular ice grain size within cryofixed BEAS-2B monolayers following 30 minute room temperature treatment with 15 mM 2FA, 10 mM 4ClA, 10% (v/v) DMSO, and PBS. The normal QQ plot demonstrating data normality following log transformation is shown.

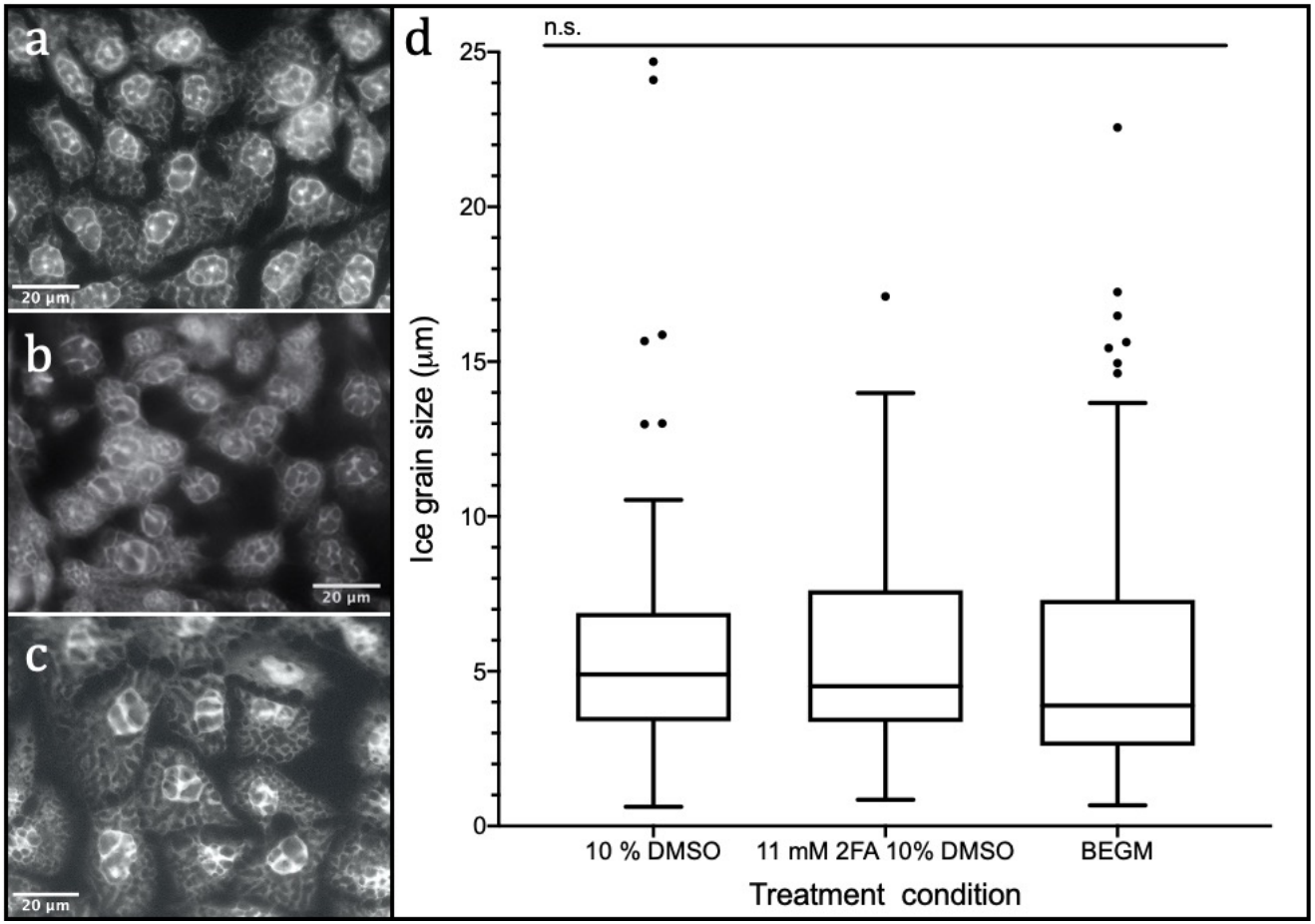

Figure 2.10 2FA Does Not Reduce Intracellular Ice Grain Size in the Presence of DMSO

Sample cryofixation images (a-c) and intracellular ice grain size distribution (d) of BEAS-2B cells after 30 min room temperature treatment with 10 % DMSO in BEGM (a), 11 mM 2FA 10% (v/v) DMSO in BEGM (b), or BEGM alone (c) prior to freezing to -80 °C, cryofixation, and SYTO13 staining. The unstained regions within each cell represents intracellular ice. Statistical significance was determined using a nested one-way ANOVA on log-transformed data.

		10% DMSO	11 mM 2FA 10% DMSO	BEGM
Descriptive Statistics	Number of values	172	191	251
	Minimum	0.62	0.41	0.67
	25% Percentile	2.30	2.39	2.51
	Median	4.63	4.17	3.99
	75% Percentile	6.79	7.63	7.60
	Maximum	24.69	29.43	28.29
	Mean	5.63	5.63	5.91
	Std. Deviation	4.11	4.38	5.18
Nested one-way ANOVA p-value		p=0.9586		

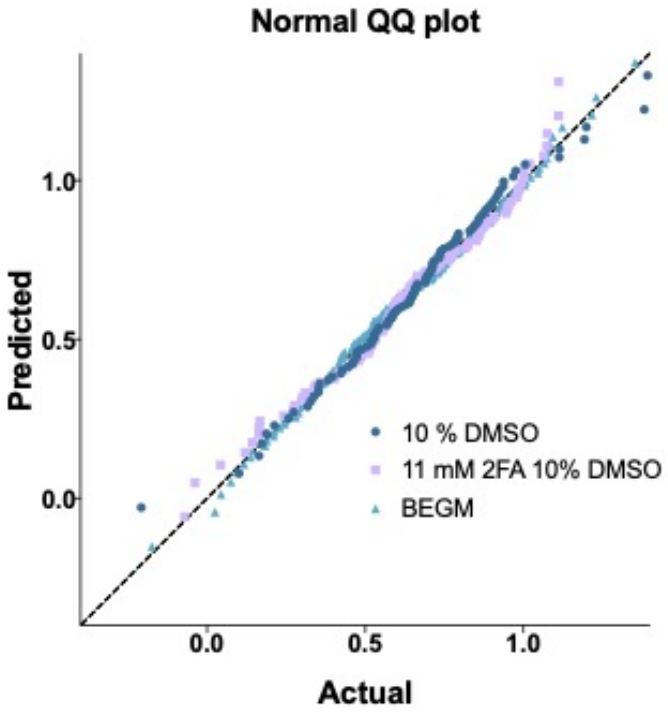

Figure 2.11 Descriptive and Inferential Statistics of Intracellular Ice grain size following IRI Treatment with DMSO

Descriptive and inferential statistics of ice grain size within cryofixed BEAS-2B monolayers following treatment with 10% (v/v) DMSO in BEGM, 11 mM 2FA 10% (v/v) DMSO in BEGM, or BEGM alone. The normal QQ plot demonstrating data normality following log transformation is shown.

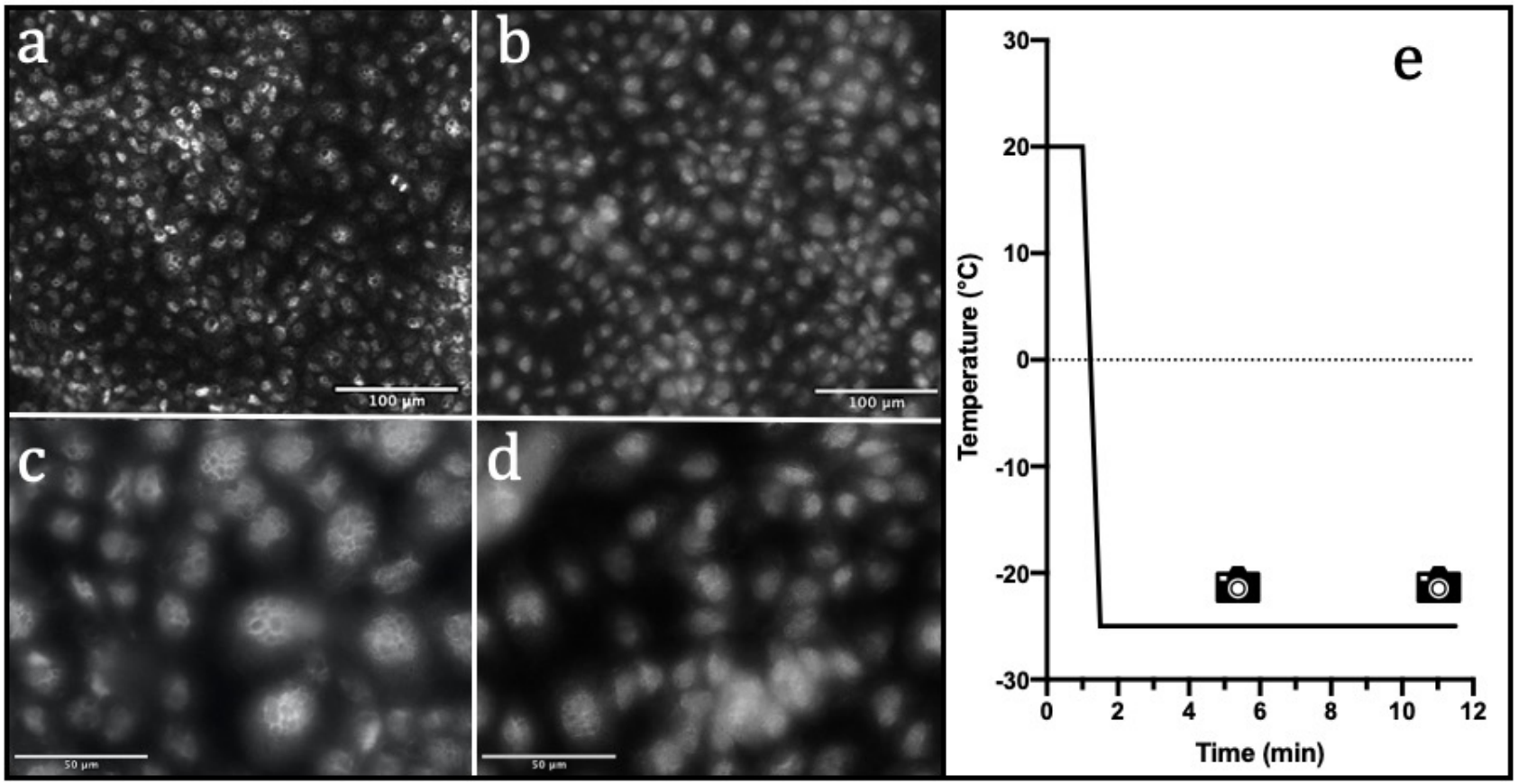

Figure 2.12 2FA Reduces Intracellular Ice Grain Size when the Concentration is Reduced to 11 mM

BEAS-2B cells were treated with 50 µM SYTO 13 with the addition of 10% (v/v) DMSO in BEGM (panels a and c) or 11 mM 2FA in BEGM media (panels b and d) prior to freezing (freezing profile shown in panel e) and cryomicroscopy. Fluorescent microscopy images were obtained 4 minutes (panels a-b), or 10 minutes (panels c-d) after reaching -25 °C. As shown in panels b and d, 11 mM 2FA treatment visually reduces intracellular ice grain size when compared to DMSO treatment (panels a and c).

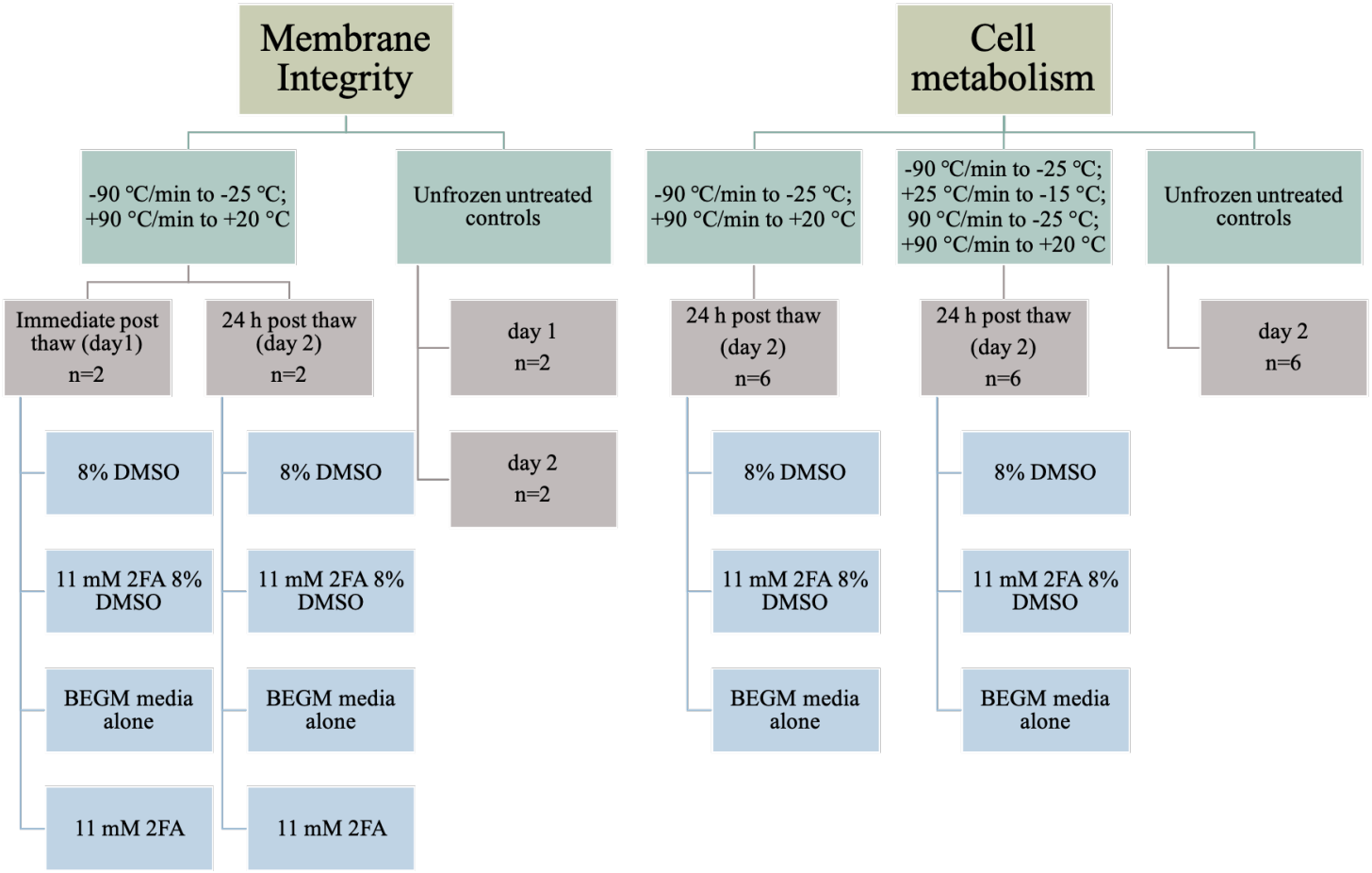

Figure 2.13 Freezing profiles and post-thaw analyses performed on BEAS-2B monolayers.

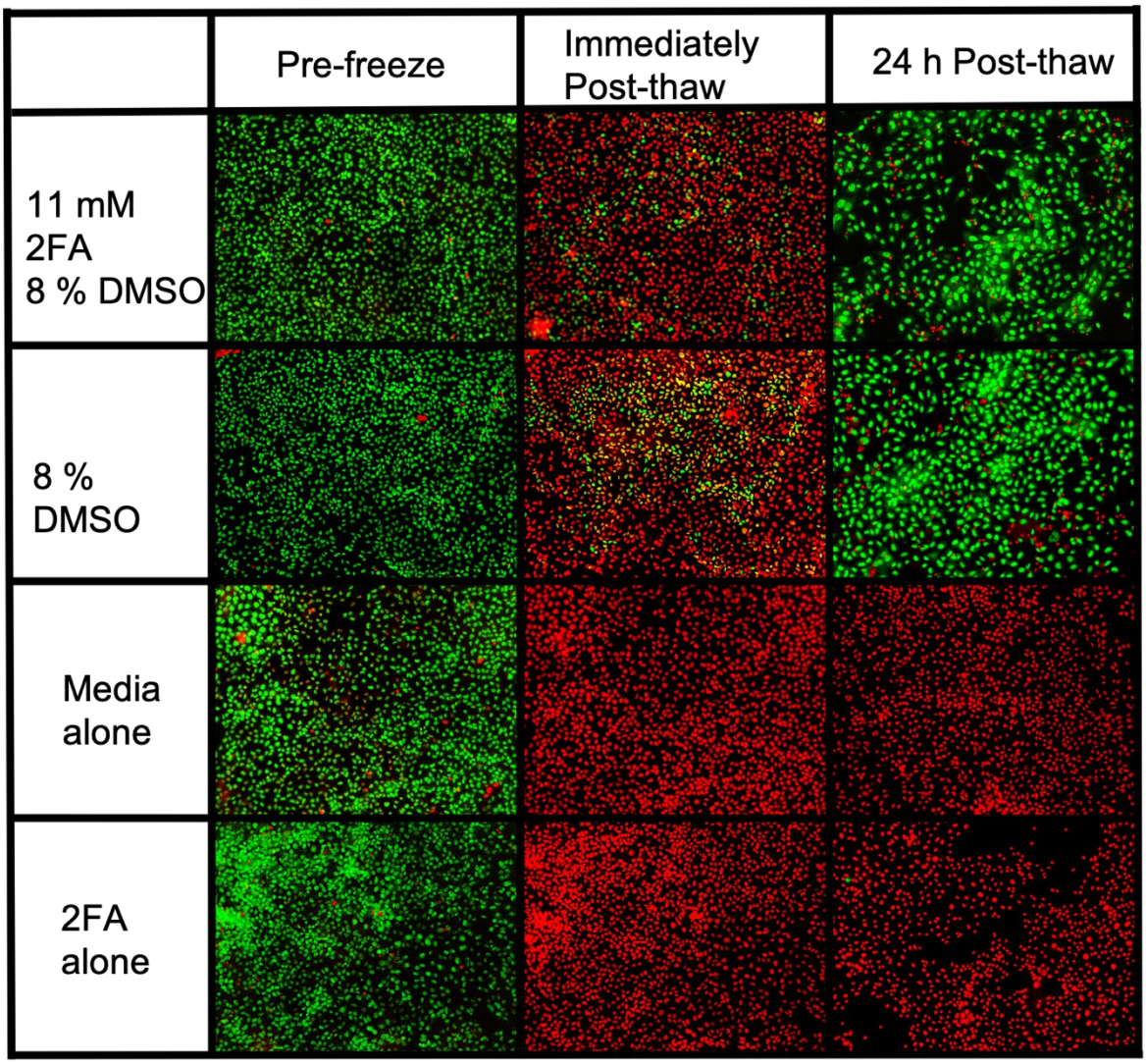

Figure 2.14 Post-thaw Loss of Membrane Integrity Following Intracellular Ice Formation is Transient in BEAS-2B cells

BEAS-2B monolayers were treated with 11 mM 2FA 8% DMSO in BEGM media, 8% DMSO in BEGM media, BEGM media alone, or 11 mM 2FA in BEGM media prior to rapid (-90 °C/min) freezing to -25 °C and rapid (+90 °C/min) thawing. Within these images, red cells are permeable to ethidium bromide, while green cells are impermeable to ethidium bromide and are therefore stained with SYTO13 only. Images obtained immediately after thawing or 24 h after thawing indicate that loss of membrane integrity following intracellular ice formation in BEAS-2B cells is transient.

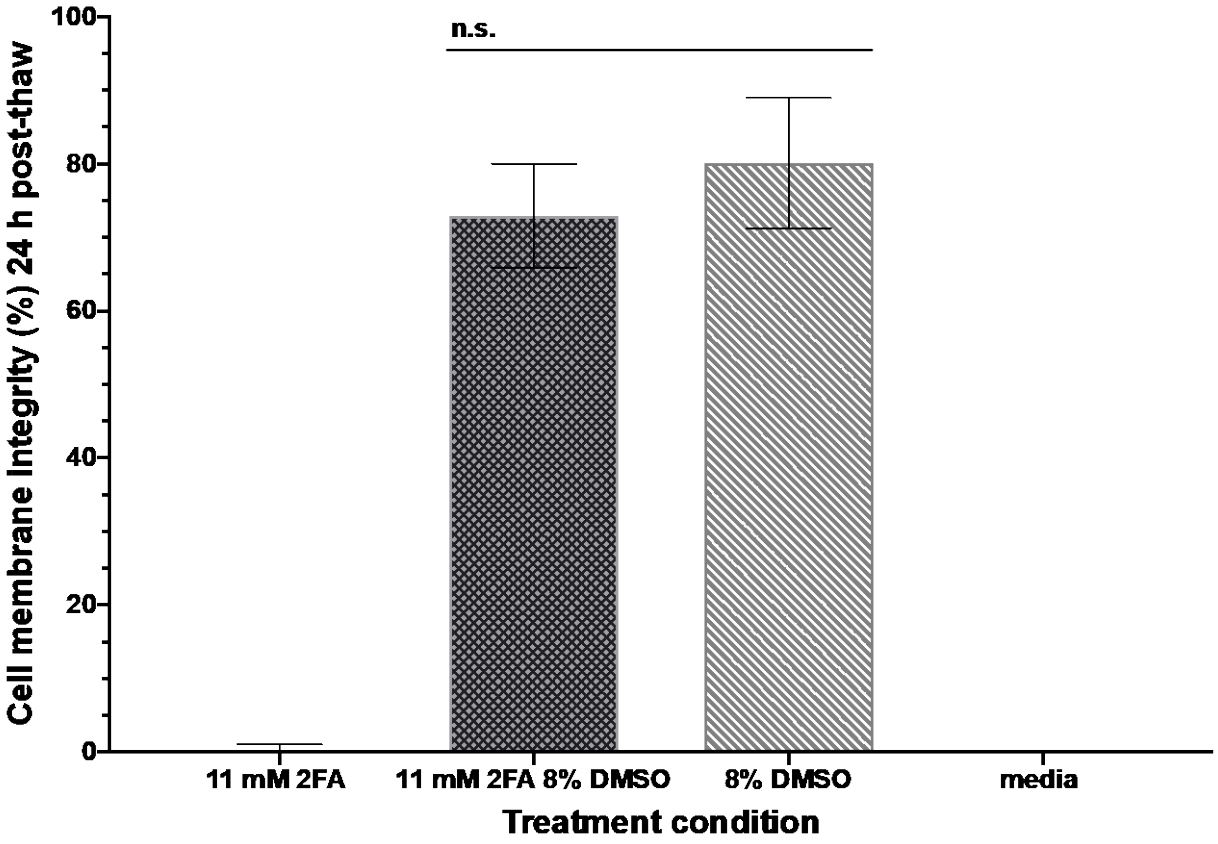

Figure 2.15 2FA Treatment Does Not Increase Post-Thaw Membrane Integrity of BEAS-2B Monolayers

BEAS-2B cells were treated with 11 mM 2FA 8% DMSO in BEGM media, 8% DMSO in BEGM media, BEGM media alone, or 11 mM 2FA in BEGM media prior to rapid (-90 °C/min) freezing to -25 °C and rapid (+90 °C/min) thawing. Membrane integrity of cells 24 h post thaw was determined from 4 images each from two coverslips, and mean percentage of membrane intact cells (SD) is shown. A nested one-way ANOVA with Tukey's multiple comparison test found no difference in post-thaw membrane integrity when 2FA was added to DMSO.

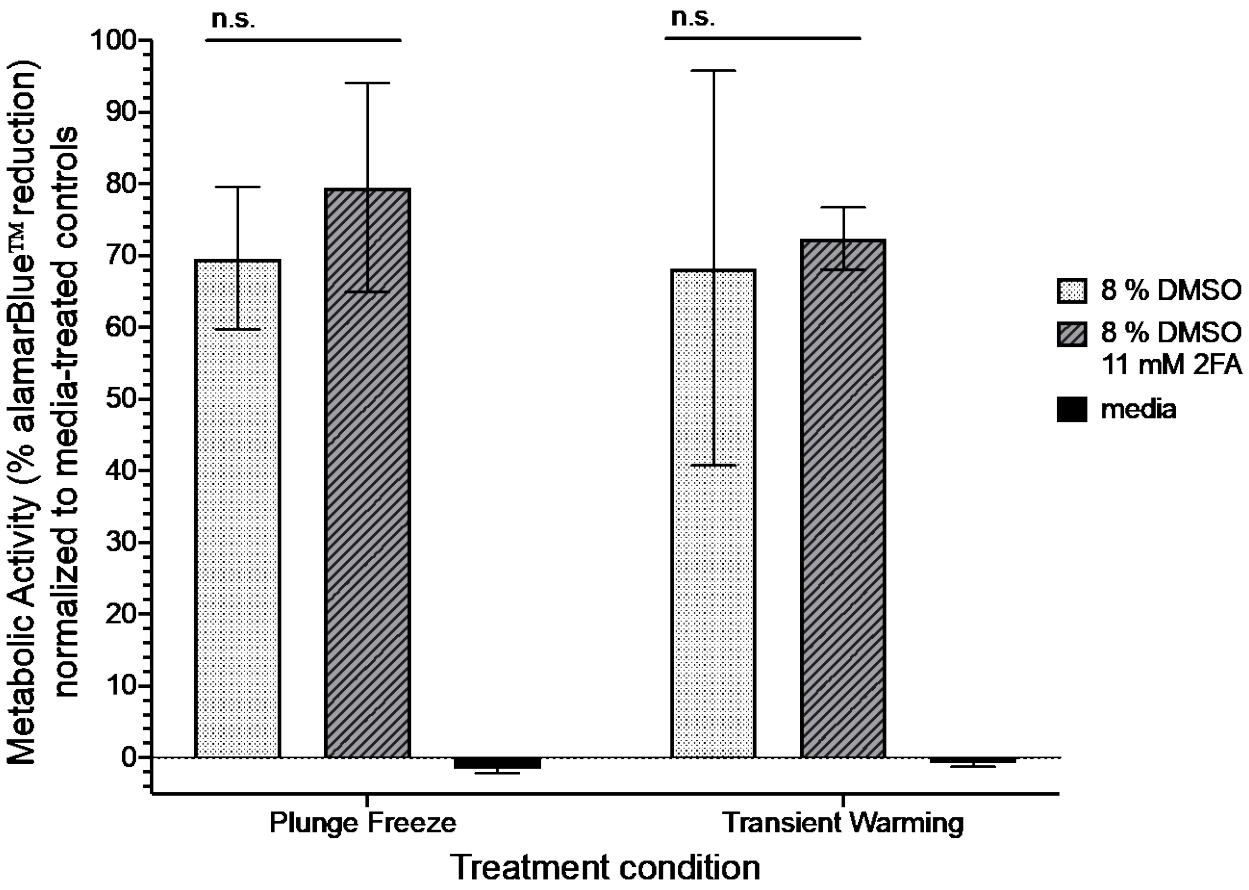

Figure 2.16 2FA Treatment Does Not Increase Post-Thaw Cell Metabolism of BEAS-2B Monolayers

BEAS-2B monolayers were treated with 11 mM 2FA 8% DMSO in BEGM media, 8% DMSO in BEGM media, BEGM media alone, or 11 mM 2FA in BEGM prior to plunge freezing and rapid thawing (-90 °C/min to -25 °C; +90 °C/min to +20 °C), with or without a transient warming event (+25 °C/min to -15 °C, -90 °C/min to -25 °C). Mean cell metabolism (SD) from 6 coverslips in each condition 24 h post-thaw is shown. A two-way ANOVA and Sidak's multiple comparison test demonstrated no difference in cell metabolism when 2FA was added to DMSO.

3. Characterizing IRI Efficacy in Rat Lung Cryopreservation

3.1 Introduction

Although lung transplant remains the only option for patients suffering from end-stage lung disease, donor lung supply is currently insufficient to meet demand. While many lungs become available for transplant, most are discarded due to failure to meet physiologic or compatibility criteria. In addition, many lungs are currently unutilized due to short preservation times, since lungs only survive for 6-8 hours on ice [17]. Successful cryopreservation of lungs would allow for extended storage to help ameliorate this problem; however, lungs remain heavily underrepresented in the whole organ cryopreservation literature.

As described in chapter 1, several features of the lung make them an ideal subject for organ cryopreservation research. When compared to other organs in which cryopreservation research has been devoted, lungs have a very low density. This, in combination with the expansive vasculature of the lung, may make lungs amenable to cryopreservation, as heat and mass transfer limitations are minimized. In addition, the use of normothermic *ex vivo* lung perfusion has been shown to increase preservation times while improving organ function[53; 144; 186]. Therefore, it may be utilized pre- and post- cryopreservation to improve lung quality and facilitate cryoprotectant delivery.

Many methods of organ cryopreservation may be pursued, from high sub-zero storage methods, such as supercooling [27; 33; 57; 127; 137; 150; 151; 190; 192; 212] and partial freezing [195; 196] to low-temperature vitrification [64; 65; 68; 108]. Regardless of the method undertaken, ice avoidance is a common theme given the destructive nature ice growth has within tissues and cells. The growth of existing ice at the expense of new ice nucleation is called ice recrystallization[79], and its occurrence is highly destructive since it can result in mechanical damage to cellular membranes, intercellular connections, and intracellular organelles. As ice recrystallizes, it may be additionally damaging due to dehydration effects. Previous research, in addition to the results of chapter 2, has demonstrated that ice recrystallization can be controlled through the use of small-molecule ice recrystallization inhibitors (**IRI**s) [32; 40; 41; 157]. Therefore, IRIs have the potential to be a useful cryoprotectant in lung cryopreservation due to their low toxicity, cell permeability, and ability to control ice growth.

However, the findings of Chapter 2 left many questions regarding IRI efficacy for lung cryopreservation unanswered. While it became clear that some IRIs reduced intracellular ice grain

size within pneumocyte monolayers, it was unclear if this finding would be applicable to the other cell types of the lung. Beyond this, the ability for IRIs to reduce extracellular ice grain size would be imperative to lung cryopreservation success; however, this could not be studied within cell monolayers. In addition, the nature of the interaction between IRIs and permeating cryoprotectants which prevented IRI function intracellularly was not elucidated through the monolayer research.

Therefore, this chapter aimed to address these unanswered questions through the study of 2FA within rat lung tissue. Given the high-cost of rat *ex vivo* lung perfusion equipment, low-cost techniques were developed to assess IRI efficacy in terms of cytotoxicity, and ability to reduce extracellular ice grain size and improve post-thaw cell membrane integrity and tissue structural integrity.

This was completed through the following aims:

1. Develop a low-cost subnormothermic rat *ex vivo* lung perfusion system and corresponding techniques which would allow for assessment of IRI cytotoxicity, ice control, and post-thaw cell membrane integrity and tissue structural integrity.
2. Assess the cytotoxicity of 11 mM 2FA in STEEN Solution™ to various cell types of the lung when perfused subnormothermically.
3. Assess the ability for 11 mM 2FA in STEEN Solution™ to reduce extracellular ice grain size, as compared to STEEN Solution™ controls, when perfused lungs are frozen at a rate of -5 °C/min to -20°C in a CryoMed™ Controlled-Rate Freezer (Thermo Scientific™), and held for 1 h at -20 °C.
4. Assess the ability for 11 mM 2FA to maintain post-thaw cell membrane integrity and tissue structural integrity when used with other cryoprotectants, following freezing at a rate of -5 °C/min to -20°C, a 1 h -20 °C hold, and thawing to 37 °C.

It was hypothesized that low-cost subnormothermic techniques for *ex vivo* rat lung perfusion could be developed which would demonstrate that 2FA is not cytotoxic, and controls extracellular ice growth resulting in improved post-thaw cell membrane integrity and tissue structural integrity when compared to DMSO-treated controls.

3.2 Materials and Methods

3.2.1 Development of Low-cost Subnormothermic *ex vivo* Lung Perfusion Techniques

3.2.1.1 Lung-heart Block Isolation

Lung-heart blocks were isolated from male Sprague-Dawley rats, as approved by the University of Alberta Research Ethics Board (AUP 3409). Rats of approximately 500 g weight were anaesthetized with 4% isoflurane. The rats were then placed on an isoflurane mask, and a SpO_2 and heart rate monitoring system for rodents (Harvard Apparatus) was used to enable monitoring of oxygen saturation and heart rate throughout the surgery. After hair was removed from the abdominal and thoracic regions and the absence of a pedal reflex was confirmed, a tracheotomy was performed with the insertion of a 16G angiocathetor. The angiocathetor was then tied in place using 3-0 silk, attached to the ventilator, and secured in place with medical tape. The lungs were ventilated with 0.8 L/min O_2 and the isoflurane was adjusted to maintain a surgical plane of anaesthesia. A midline laparotomy was then performed. The inferior vena cava (**IVC**) was identified, and heparin (0.1 mL per 100 g weight of animal) was injected through the IVC. The diaphragm was then cut distally from the midline, ensuring no contact was made with the lung tissue, to resect to either side of the thoracic cavity. A curved mosquito hemostat was placed at the midline of the diaphragm and the diaphragm was retracted to hold the abdominal organs away from the operating field. The xiphoid process was grasped with a curved mosquito hemostat, and mayo scissors were used to cut either side of the sternum at the mid-rib level extending toward the thoracic inlet. The rib cage was then retracted to allow visualization of the heart and lungs. A 21 G winged infusion set was primed with Perfadex®, and the needle was inserted into the pulmonary artery through the right ventricle. The auricles of the heart were cut, and 30 mL of Perfadex® was perfused slowly at a rate of approximately 1 mL/min to blanche the lungs and exsanguinate the animal. The ventral section of the rib cage was then removed, and the trachea was clamped with two ligature clips placed between the bifurcation and the angiocathetor, such that the lungs remained inflated. The lung-heart block was freed from the thoracic cavity by cutting through the IVC, the superior vena cava, the aortic arch, and connecting ligaments. Once the heart-lung block was removed, it was placed on gauze dampened with Perfadex®. The apex of the heart was removed with scissors, and the left ventricle and septum was resected. An 18 G winged catheter was then placed through the

right ventricle into the pulmonary artery and was tied in place using 3-0 silk. For perfusate toxicity experiments, the left pulmonary artery and left bronchus were isolated and encircled with 5-0 silk stay sutures. The lungs were then wrapped in Perfadex®-soaked gauze and placed on ice for transport. Warm ischemic time was recorded as the duration of time from exsanguination until the lungs were placed on ice.

3.2.1.2 Subnormothermic Perfusion

For each experiment, the heart-lung block was placed on the parafilm covered beaker in the syringe pump perfusion set-up pictured in Figure 3.1. The syringe pump perfusion set-up consists of a syringe pump (Figure 3.1a), a 60 mL syringe (Figure 3.1b), a length of tubing (Figure 3.1c), and a 250 mL beaker with parafilm stretched over the top with an indentation pressed in the middle for the lungs to sit on and an opening at one end for perfusate to drain into (Figure 3.1d). The syringe pump was set to perfuse the lungs at a rate of 100 mL/hr, and the 60 mL syringe was filled with perfusing solution of interest. The length of tubing was primed, and the lung perfusion was started, ensuring that no air was introduced. The rate of perfusion was increased by 100 mL/hr for every 10 mL of perfusate introduced until a rate of 900 mL/hr was achieved. The lungs were weighed again following perfusion.

3.2.3 Perfusate Toxicity and Tissue Cryofixation

Perfusate toxicity and cryofixation were performed simultaneously through the separation of the right and left lung following perfusion. In order to separate the two lungs following subnormothermic perfusion, the stay sutures encircling the left pulmonary artery and left bronchus were tied, and the left pulmonary artery and left bronchus were cut distally to this suture. Pulmonary veins and connective tissues were cut, and the left lung was removed. The right lung was then reattached to the syringe pump perfusion set-up, and was perfused with 50 mL of filtered 0.4% (w/v) trypan blue (Sigma Aldrich) at a rate of 500 mL/hr. The right lung was submerged in formalin (Sigma Aldrich) for at least 24 h. The right lung was then sectioned into approximately 0.5 cm^2 pieces which were paraffin-embedded (HistoCore PEARL Tissue Processor), sliced to 5 μm thickness using a microtome, and stained with eosin. Blue cells were considered to be dead cells, and number of dead cells was quantified from ten images of 20X magnification from each sample. These images were obtained using brightfield microscopy (Nikon Eclipse TE2000-U and Nikon

Digital Sight DS-U1) and were manually quantified using the multi-point tool in ImageJ (Version 1.52).

The left lung was transferred to a disposable plastic specimen container and was placed, uncovered, in a CryoMed™ Controlled-Rate Freezer (Thermo Scientific™). The chamber was then set to cool at a rate of -5 °C/min to -20 °C, followed by a 1 h hold at -20 °C. After this hold, the specimen container was transferred to a fume hood in a styrofoam container containing ice. Approximately 50 mL of a low-temperature fixative (85 parts 70% ethanol, 10 parts 38% formaldehyde, 5 parts glacial acetic acid) pre-cooled to -20 °C was added to the specimen container. The container was then transferred to a -20 °C freezer for at least 24 h. The left lung was paraffin-embedded (HistoCore PEARL Tissue Processor), sliced to 5 μm thickness using a microtome, and stained with hematoxylin and eosin. Ice size was manually quantified using the polygon area tool in NIS Elements AR 3.2 image analysis software (Nikon) from alveolar images obtained using brightfield microscopy (this technique is represented in Figure 3.7). Two biological replicates were performed, and two 20X images were obtained from each replicate. Over 270 ice grains were quantified in each image.

During the development phase of this technique, the internal freezing rate of the left lung was assessed through the placement of a thermocouple in the left bronchus prior to freezing. This assessment was performed after perfusion of the lungs with STEEN Solution™ alone without the addition of any cryoprotectants. Intrabronchial temperature was recorded every minute during the freezing phase and for 1 h after the chamber temperature reached -20 °C.

The following solutions were perfused prior to assessment of cytotoxicity and/or ice control:

1. 1.6 mM hydrogen peroxide in STEEN Solution™: This solution was perfused for toxicity analysis to act as a positive control for trypan blue staining. Given that hydrogen peroxide is a well-known inducer of apoptosis[181; 218], its perfusion through the lung should cause cellular demise in all cell types of the lung. Therefore, if the lung is adequately perfused with the hydrogen peroxide solution and subsequent trypan blue solution, all cells of the lung should appear blue when observed under microscopy.
2. STEEN Solution™: This solution was perfused for assessment of baseline cell death and ice grain size analysis when no cryoprotectants are used. This allows for assessment of cellular demise under this lung procurement and processing methodology and ice growth under these freezing conditions when no cryoprotectants are used.

3. 11 mM 2FA in STEEN Solution™: This solution was assessed for cytotoxicity and ice control and was compared to lungs treated with STEEN Solution™ alone. If 11 mM 2FA is not toxic to cells of the lung, then cellular demise should not be significantly different than the STEEN treated controls. If 11 mM 2FA controls extracellular ice growth, then ice grain size should be significantly reduced when compared to STEEN Solution™ alone.

The toxicity of perfusates and ice grain size during cryofixation was analyzed using GraphPad Prism 8. Normality of data sets was confirmed prior to use of a nested t-test and one-way ANOVA with Tukey's multiple comparison test for toxicity and cryofixation data, respectively. A p-value less than 0.05 was considered to be significant.

3.2.4 Post-thaw Cell Survival and Tissue Morphology

While control of ice is of the utmost importance, post-thaw cell survival and maintenance of tissue morphology provides further understanding of 2FA efficacy. In order to assess cell survival and morphology post-thaw, lungs were perfused with 10% (v/v) DMSO and 0.4% (w/v) trypan blue, with or without the addition of 11 mM 2FA, prior to freezing and thawing. Trypan blue was added to the perfusing solution in the hopes that it would enter membrane-damaged cells post-thaw without the difficulty of re-perfusing post thaw and without causing additional cell death during handling and perfusion. Perfusing trypan blue prior to freezing would also allow for the separation of the two lungs to assess differences in cell membrane integrity pre-freezing and post-thaw. However, given that trypan blue has a large molecular weight of 960.81 g/mol, it was recognized that it may act as a non-permeating cryoprotectant. Therefore, additional lungs were cryofixed following perfusion to assess the effect trypan blue has on extracellular ice grain size.

For post-thaw experiments, lungs were perfused with 10% (v/v) DMSO and 0.4% (w/v) trypan blue, with or without the addition of 11 mM 2FA, and separated in the manner described in section 3.2.2 and 3.2.3 (n=2). The right lung was immediately placed in formalin (Sigma Aldrich), and the left lung was placed in a biohazard bag with a small amount of perfusate to cover the lungs. The left lung was placed in a CryoMed™ Controlled-Rate Freezer (Thermo Scientific™), and the chamber was set to cool at a rate of -5 °C/min to -20 °C, followed by a 1 h hold at -20 °C (Figure 3.5). Left lungs were thawed in a water bath set to 37 °C for 5 minutes before placement in formalin (Sigma Aldrich). Lungs were paraffin-embedded (HistoCore PEARL Tissue Processor), sliced to 5 μm thickness using a microtome, and stained with eosin. Blue cells were considered to be dead

cells, and number of dead cells was quantified from ten images of 20X magnification from each sample. These images were obtained using brightfield microscopy and were quantified using ImageJ (Version 1.52). After confirmation of data set normality, a nested one-way ANOVA and Tukey's multiple comparison test was performed to analyze differences in cell membrane integrity between conditions. A p-value less than 0.05 was considered to be significant.

Two additional lungs were used to assess the extracellular ice grain size within lungs during freezing in the conditions described above. In this case, whole lungs were cryofixed in manner described in section 3.2.3 after being perfused with 10% (v/v) DMSO and 0.4% (w/v) trypan blue, with or without the addition of 11 mM 2FA. Ice size and loci was qualitatively described given the small sample size, and no statistics were performed.

3.3 Results

3.3.1 Surgical and Perfusion Techniques

During the pre-experimentation period, the duration of time required to complete the surgeries was reduced from approximately 1.5 h to 0.75 h. This reduction in surgical time likely occurred due to improved efficiency. While initial surgeries were performed with intubation, tracheotomies were found to be preferred since the large size of the rats afforded very limited time for intubation. Although only 20 mL of Perfadex® was used during exsanguination initially, this was increased to 30 mL to better blanche the lungs.

Initial perfusions were often unsuccessful as indicated by a lack of trypan blue staining throughout the entire lung or dark blue staining and edema. At this point in time, the lungs were being perfused with room temperature solutions immediately after being removed from ice and were perfused at a rate of 6 mL/min. Therefore, the protocol was changed to allow for pre-warming of the lungs in STEEN Solution™ heated to 37 °C, and the use of pre-warmed perfusates. In addition, the flow rate was gradually increased from 100 mL/h to 900 mL/h. This substantially reduced the occurrence of edema and the lungs perfused more evenly. A comparison of lungs perfused with trypan blue before and after these perfusion modifications is demonstrated in Figure 3.2. All experimental results reported in this chapter were performed using the modified methodology and were performed after this technique was validated.

3.3.2 Perfusate Toxicity and Tissue Cryofixation

As shown in Figure 3.3 and 3.4, the perfusion of 1.6 mM hydrogen peroxide successfully induced cell death resulting in membrane permeability to trypan blue. The number of quantified dead cells did not significantly differ from the number of hematoxylin-stained cells in a standard untreated hematoxylin and eosin (**H&E**) stained sample of rat lung tissue ($p=0.0676$). When mean data is normalized to the mean number of blue cells in the untreated H&E group, treatment with 1.6 mM hydrogen peroxide, STEEN Solution™ alone or 11 mM 2FA in STEEN Solution™ resulted in 81 ± 13 %, 10 ± 2 %, 7 ± 4 % cell death, respectively. As shown in Figure 3.4, no significant difference in cell death was observed between STEEN Solution™ alone or 11 mM 2FA in STEEN Solution™ ($p=0.9292$).

The intrabronchial freezing profile during the cryofixation protocol is shown in Figure 3.5 alongside the chamber freezing profile. The initial freezing rate was approximately -2.7 °C/min, and the lung nucleated at approximately -5 °C. Following this, the freezing rate was slower at approximately -0.6 °C/min. While this demonstrates the general freezing rates within the lung, the addition of a cryoprotectant would reduce the nucleation temperature.

Sample cryofixation images are shown in Figure 3.6, the methodology used to quantify ice in these images is demonstrated in Figure 3.7, and quantified data is summarized in Figure 3.8. Ice grains larger than 200 μm are excluded from Figure 3.8; however, treatment with STEEN Solution™ alone resulted in ice as large as 597.3 μm. The distribution of ice grain size in all cases was right skewed and was corrected to a normal distribution using a log transformation. Descriptive statistics and the normal QQ plot are shown in Figure 3.9. As shown in Figure 3.6 and 3.8, a significant reduction in the size of alveolar ice was observed as a result of treatment with 11 mM 2FA ($p = 0.0096$).

3.3.4 Post-thaw Cell Survival and Tissue Morphology

Sample images of post-thaw tissue morphology are shown in Figure 3.10, and quantification of the number of membrane-permeable cells from pre-and post-thaw samples is depicted in Figure 3.11. As shown in Figure 3.10, the perfusion of 10% (v/v) DMSO and 0.4% (w/v) trypan blue in STEEN Solution™ prior to freezing results in detachment of the bronchiole epithelium from the basement membrane. This detachment is consistent, to varying degrees, throughout the two 10% (v/v) DMSO 0.4% (w/v) trypan blue in STEEN Solution™ replicates. This appears to be mitigated by

the addition of 11 mM 2FA; however, this detachment is still present within several of the bronchioles in these samples. No other differences in post-thaw morphology between the two conditions were apparent.

Prior to freezing, no significant difference in alveoli cell membrane integrity was observed when 11 mM 2FA was added to 10% (v/v) DMSO 0.4% (w/v) trypan blue in STEEN Solution™ ($p=0.8878$). Cell permeability to trypan blue significantly increased post-thaw when lungs were perfused with 10% (v/v) DMSO 0.4% (w/v) trypan blue in STEEN Solution™ prior to freezing ($p=0.0030$). However, the addition of 11 mM 2FA resulted in significantly fewer membrane-permeable cells post-thaw when compared to the use of 10% (v/v) DMSO and 0.4% (w/v) trypan blue alone ($p=0.0034$). No significant difference in cell survival pre-freeze and post-thaw was observed when 11 mM 2FA 10% (v/v) DMSO 0.4% (w/v) trypan blue in STEEN Solution™ was perfused prior to freezing ($p=0.7638$).

Sample cryofixation images are shown in Figure 3.12. When these cryofixation images are compared to the cryofixation images from Figure 3.6, it is clear that the addition of trypan blue reduced the amount and size of ice within alveoli and bronchioles. It is visibly apparent that the addition of 11 mM 2FA reduces the amount of ice surrounding bronchiole epithelium.

3.4 Discussion

The first objective of this chapter set out to develop low-cost subnormothermic *ex vivo* rat lung perfusion techniques which could be used to assess perfusate cytotoxicity, ice control, and ability to improve post-thaw cell membrane integrity and tissue structural integrity. The surgical and perfusion techniques were optimized to reduce lung edema, and the trypan blue method was found to successfully identify loss of membrane integrity in a variety of cell types, including bronchial epithelial cells, smooth muscle cells, and pneumocytes. This method allowed for determination of perfusate toxicity, as loss of membrane integrity following induction of cellular demise by hydrogen peroxide occurred at levels comparable to the number of cells stained by hematoxylin in untreated tissue. The observed reduction in ice grain size by 2FA additionally suggests that the cryofixation technique used here discriminates ice grain size when different solutions are perfused. Lastly, the observation of gross tissue abnormalities post-thaw and the increase in trypan blue staining post-thaw suggest that this technique allows for determination of changes to post-thaw cell membrane integrity and tissue structural integrity. Although this demonstrates the usefulness of these techniques in preliminary analysis of cryoprotectant use in

lung tissue, various limitations in this methodology exist, the largest of which being the inability to assess lung function post-thaw. This becomes particularly important when interpreting research findings using these techniques, since improved post-thaw cell membrane integrity or tissue structural integrity does not assure tissue functionality. However, these methods allow for a more thorough understanding of cryoprotectant mechanisms and shortcomings when compared to *ex vivo* lung perfusion methods that allow for assessment of function, given their ability to isolate ice control and toxicity characteristics. In addition, these techniques are very inexpensive relative to the cost of normothermic *ex vivo* lung perfusion equipment available commercially. Given the infancy of lung cryopreservation research, this type of analysis is suitable for this level of development and could enable other researchers to assess cryopreservation protocols in rat lungs prior to more expensive assessment.

The second objective of this work sought to characterize the cytotoxicity of the IRI 2FA to lung cells during subnormothermic *ex vivo* perfusion. 2FA was found to be non-toxic to rat lung cells when perfused in the manner described in the methods section, as indicated by maintenance of cell membrane integrity at levels comparable to cryoprotectant-free controls. This finding is in agreement with the findings of chapter 2, which demonstrated no cytotoxicity in type II pneumocyte monolayers by 2FA for up to 24 hours of exposure. This supports the hypothesis that the IRI 2FA is not cytotoxic; however, the analysis performed here assessed only short-term cytotoxicity and may therefore not accurately represent long-term cytotoxicity. In addition, this method assessed only membrane integrity, rather than cell metabolism or function. Therefore, this method may not fully capture the extent of damage to cells by the perfusion of 2FA.

The remaining two objectives of this chapter sought to characterize the ability for the IRI 2FA to reduce alveolar ice grain size and improve post-thaw cell membrane integrity and tissue structural integrity. 2FA was found to significantly reduce alveolar ice grain size when compared to perfusion with STEEN Solution™ alone. This suggests that 2FA is capable of reducing extracellular ice grain size; however, the ability to reduce intracellular ice grain size within rat lungs could not be determined using these techniques. The addition of 2FA to DMSO was additionally found to improve post-thaw membrane integrity and tissue structural integrity, thus suggesting that the reduction in alveolar ice grain size improves post-thaw membrane integrity and tissue structural integrity. In addition, alveolar ice grain size also appeared significantly smaller in cryofixed samples perfused with trypan blue and DMSO, with or without 2FA. Therefore, it is possible that the presence of trypan blue dehydrated tissue sufficiently to reduce extracellular ice grain size between cells. Therefore, the use of non-permeating cryoprotectants similar in molecular weight to trypan

blue may improve lung cryopreservation protocols. The finding that post-thaw cell membrane integrity was comparable to pre-freeze membrane integrity when 2FA was added to DMSO and trypan blue is an interesting finding, since previous research assessing ice-allowing cryopreservation of complex tissues typically reports a significant reduction in cell membrane integrity post-thaw[62; 128]. Although these findings are promising, this study was limited by small sample sizes and the inability to assess post-thaw function. While improved alveolar cell membrane integrity is encouraging, the gross morphological damage observed in cryofixation and post-thaw samples suggests that the cryopreserved lungs would lose function. Therefore, further research assessing different perfusate compositions and freezing profiles would be valuable.

Although 2FA was found to be ineffective at reducing intracellular ice grain size or improving cell membrane integrity or metabolism when used with DMSO in Chapter 2, post-thaw membrane integrity and tissue structural integrity was improved when 2FA was used with DMSO in rat lung tissue. This suggests that the lack of 2FA efficacy when used with DMSO is solely an intracellular event. In other words, it is likely that the addition of DMSO to 2FA solutions prevents entry of 2FA into the cell or functionality of 2FA within the cell, rather than rendering the 2FA molecule ineffective in solution. These findings may help illuminate the mechanism of 2FA entry into the cell since it is well-established that DMSO increases uptake of some molecules into cells while decreasing uptake of others[95]. Increased solute uptake in the presence of DMSO occurs due to increased permeability of cell membranes through a reduction in membrane thickness and through the formation of water pores[95; 148; 222]. Therefore, it is possible that 2FA does not enter cells through the same means as other molecules in which DMSO serves to improve cellular uptake. This, in addition to the reported ability of DMSO to alter protein secondary structure[11; 200], such as that found in transmembrane proteins, suggests that 2FA does not enter cells through a passive transport mechanism. In addition, DMSO has been found to increase the fraction of content released from a vesicle during exocytosis[126]. Therefore, if cells are ridding themselves of 2FA by means of exocytosis, this may be accelerated by the presence of DMSO. This work expands upon existing IRI publications, as no other IRI publications have demonstrated prevention of IRI function in the presence of DMSO. Considering that one of the large hindrances in expanding IRI research has been the lack of mechanistic understanding, the work described here is a valuable contribution to the IRI literature as it begins to elucidate mechanism of 2FA entry into the cell and provides further avenues of IRI research.

Ultimately, to the author's knowledge, this research is the first to study lung cryopreservation in an ice-allowing manner. The findings of this work provide support for the use

of various cryoprotectants during lung cryopreservation including permeating cryoprotectants, non-permeating cryoprotectants, and ice recrystallization inhibitors. The mechanism of 2FA remains unclear; however, it is now known that 2FA is likely not cytotoxic to lung cells, given the maintenance of cell membrane integrity, reduces alveolar ice grain size when used alone, and improves alveolar cell membrane integrity and tissue structural integrity when used with DMSO. It can be postulated that 2FA enters through a non-passive membrane transport mechanism, given the known effects of DMSO on cellular membranes and proteins. Further research to better elucidate the mechanism of improved cell membrane integrity in rat lungs by 2FA would be valuable, as would further development of the cryosolutions and freezing profiles to reduce gross morphological damage due to ice.

3.5 Conclusions

The research for this chapter was conducted to characterize the efficacy of 2FA for lung cryopreservation, in terms of cytotoxicity and ability to reduce extracellular ice grain size leading to improved post-thaw cell membrane integrity and tissue structural integrity. This work additionally served to expand upon the findings of chapter 2, by further describing the relationship between 2FA and DMSO. It was hypothesized that low-cost subnormothermic techniques for ex vivo rat lung perfusion could be developed which would demonstrate that 2FA is not cytotoxic, and controls extracellular ice growth resulting in improved post-thaw cell membrane integrity and tissue structural integrity when compared to DMSO-treated controls.

This hypothesis was supported by the experimental findings, as it was concluded that 2FA reduced alveolar ice grain size when compared to cryoprotectant-free controls and improved post-thaw membrane integrity and tissue structural integrity when compared to DMSO-treated controls, without apparent lung cell toxicity.

The research conducted in this chapter contributes to the fields of cryobiology and organ preservation as it is the first work to demonstrate the ability for IRIs to reduce extracellular ice grain size in tissue, and the results expand upon current IRI knowledge by beginning to elucidate the mechanism of IRI entry into cells. In addition, this work provides some of the first research studying whole lung cryopreservation, and the techniques described here for low-cost subnormothermic *ex vivo* rat lung perfusion may be used by other researchers to further research lung cryopreservation protocols. Although there are various limitations to the experimental design, the findings described here provide a promising outlook for lung cryopreservation and IRI use.

3.5 Figures

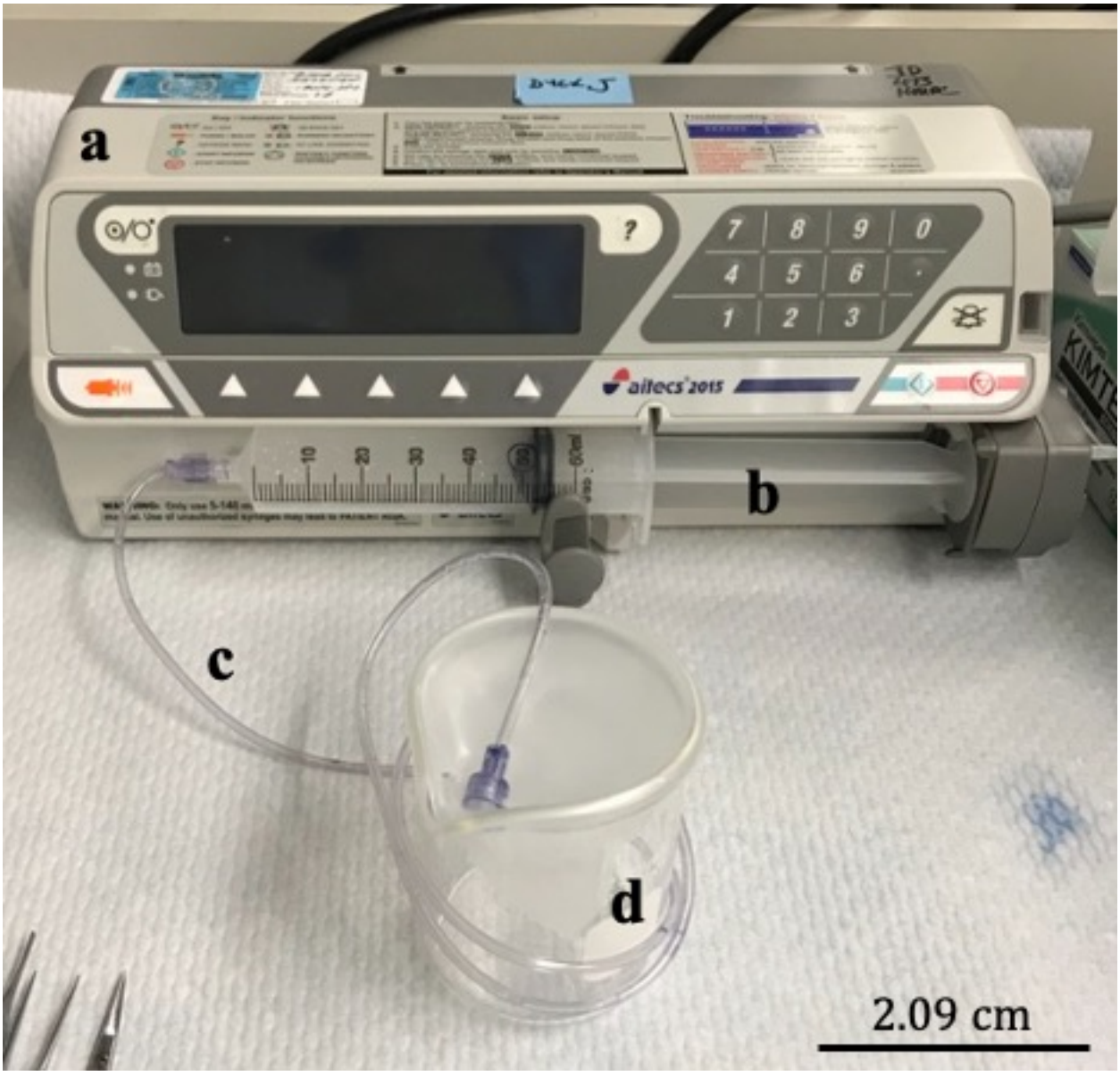

Figure 3.1 The Subnormothermic *ex vivo* Lung Perfusion Set-up

A 60 mL syringe (b) is placed within a syringe pump (a). This is connected by a length of tubing (c) to the 18 G angiocathetor cannulating the pulmonary artery of a heart-lung block. The lungs sit atop a 250 mL beaker which has been covered with parafilm (d) that has been pressed to create an indent and cut to create a drainage route for perfusate.

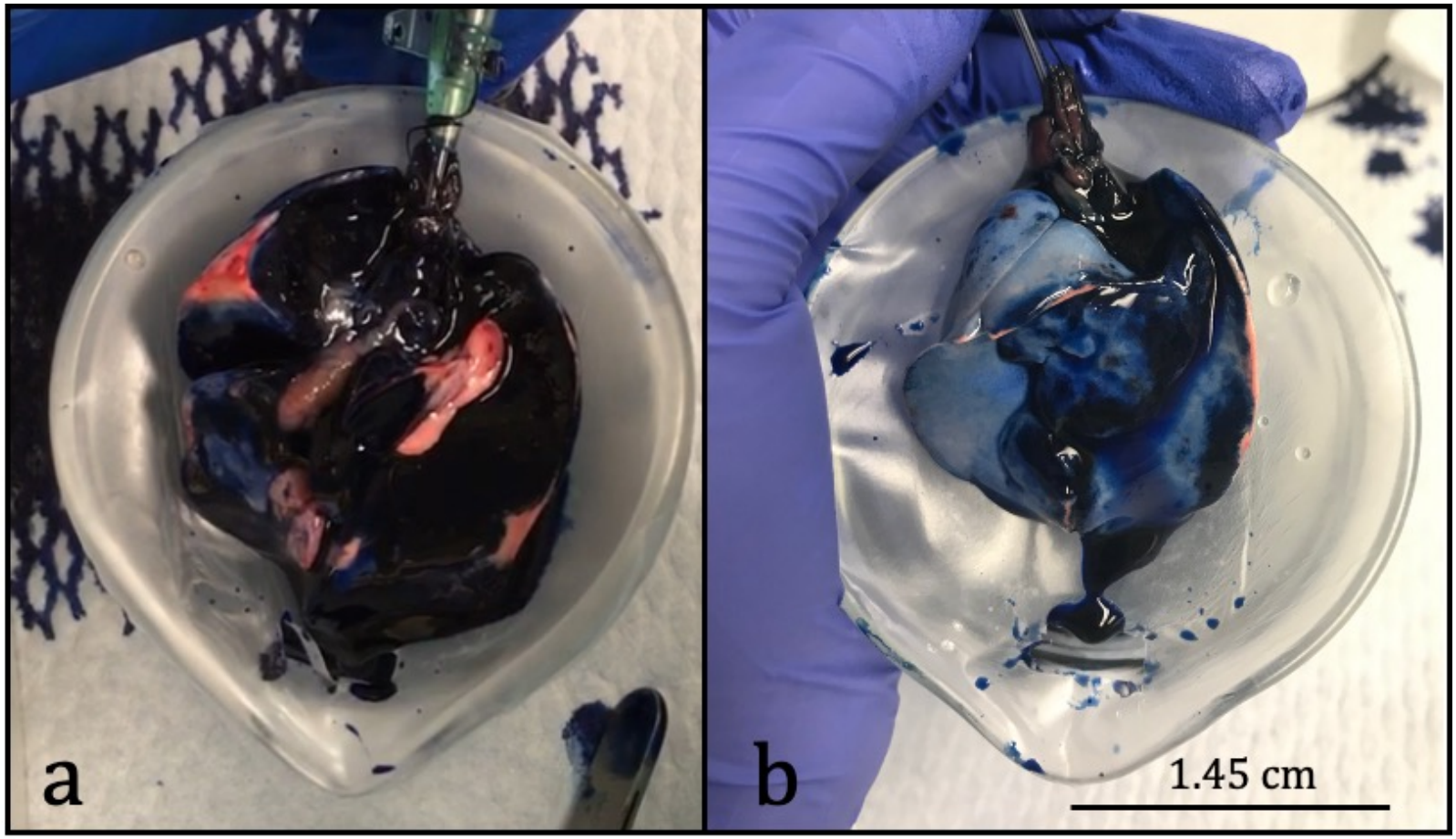

Figure 3.2 Modifications to the Perfusion Protocol Reduce Lung Edema

A comparison of lungs perfused with trypan blue before (a) and after (b) modification to the perfusion protocol, including a gradual flow rate increase and the use of pre-warmed perfusates. Panel (a) lungs exhibited dark blue staining and lung enlargement, thus indicating severe edema. Lungs in Panel (b) are paler in color without enlargement, therefore indicating significantly less edema.

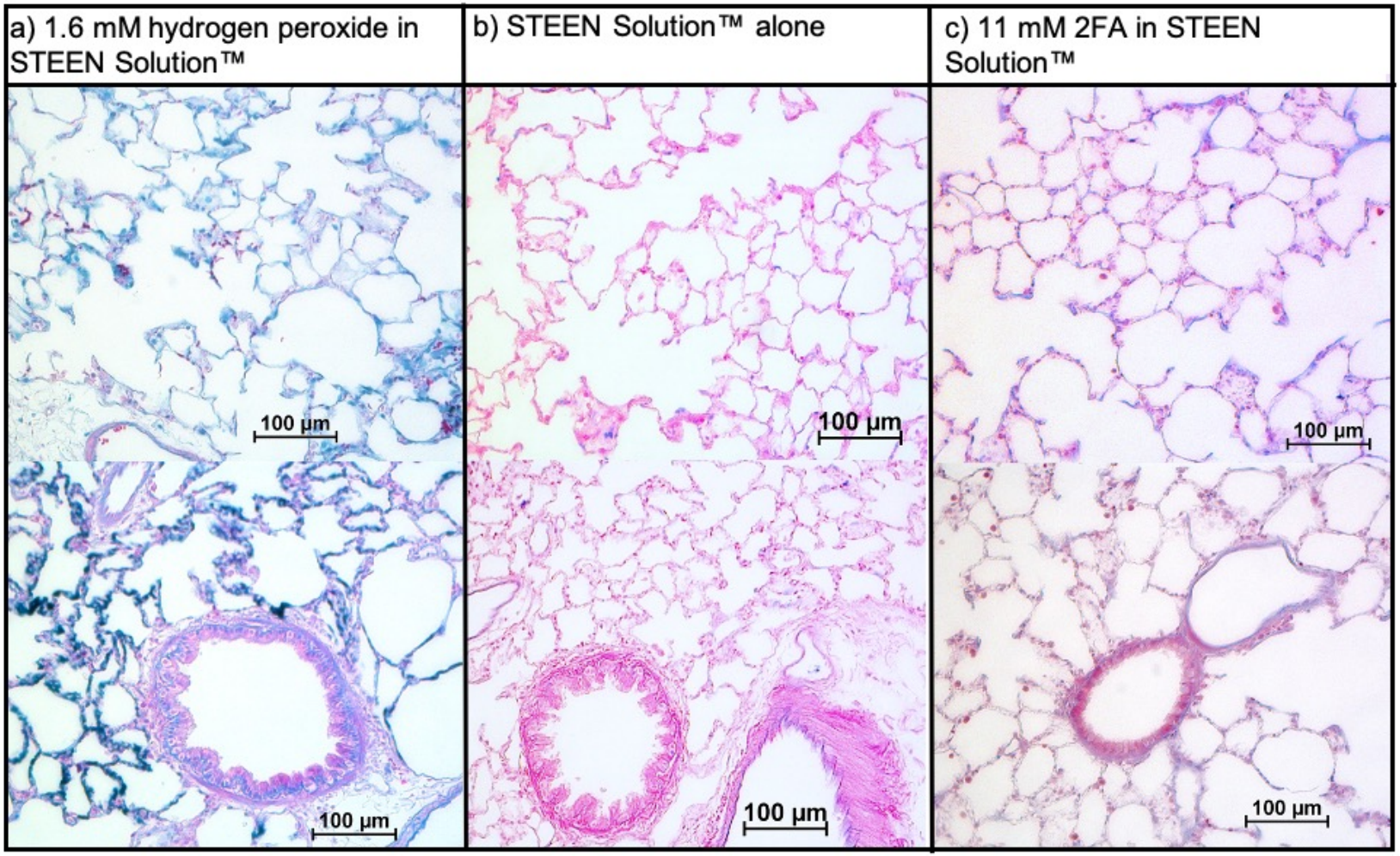

Figure 3.3 Images of the Trypan Blue Perfusion Method for Assessing Cell Membrane Integrity in Lung Tissue

Representative images of rat lung tissue perfused with 1.6 mM hydrogen peroxide in STEEN solution™, STEEN Solution™ alone, or 11 mM 2FA in STEEN Solution™ prior to perfusion with 0.4 % trypan blue. Images of alveoli are represented in the top images while bronchioles and associated vessels are shown in lower images. In all cases, tissue was formalin fixed, paraffin-embedded, sliced, and eosin stained.

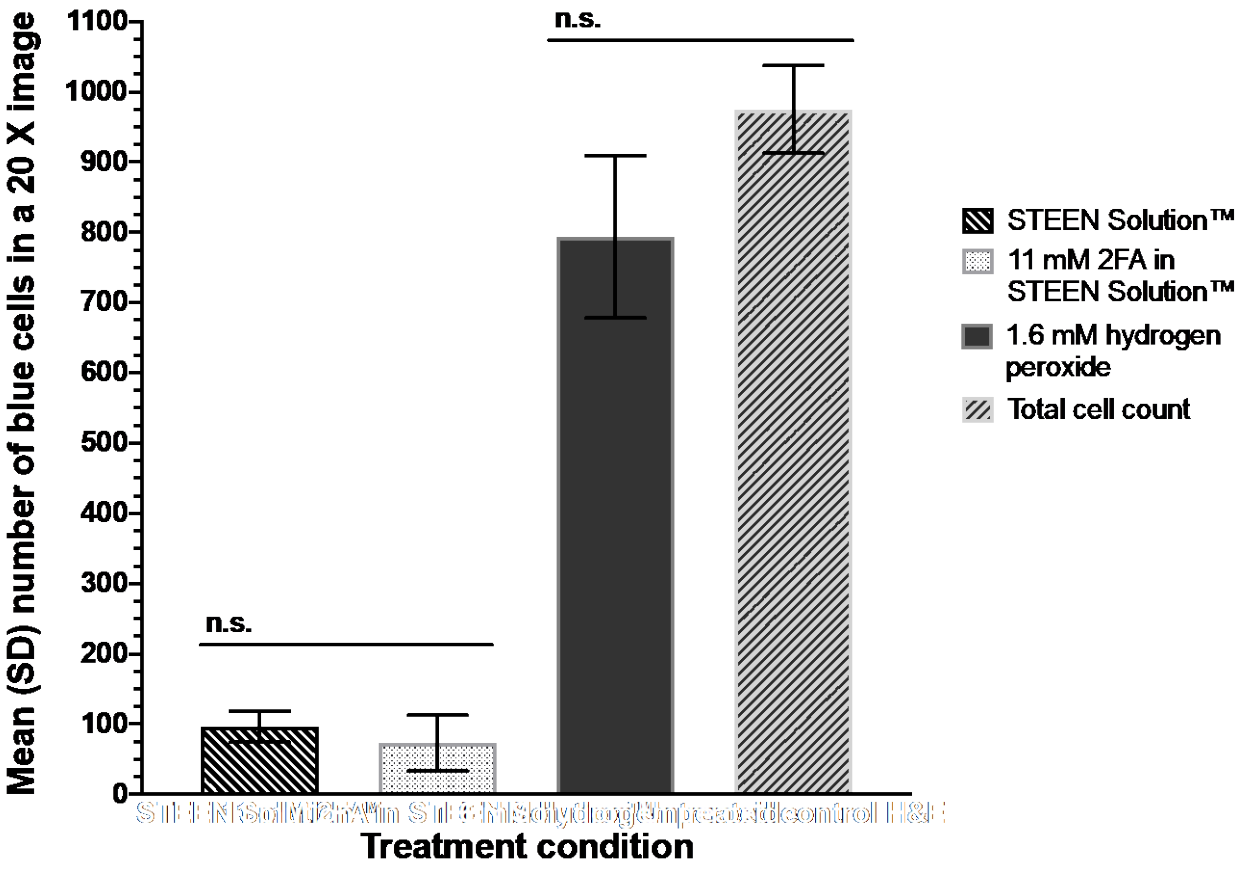

Figure 3.4 2FA is Not Cytotoxic to Lung Cells and Trypan Blue can be Perfused to Visualize Loss in Cell Membrane Integrity

Mean (SD) number of blue cells in a 20X image of lung tissue, as obtained from 10 images each from two biological replicates. Tissues perfused with STEEN Solution™, 11 mM 2FA in STEEN Solution™, or 1.6 mM hydrogen peroxide were then perfused with 0.4% (w/v) trypan blue prior to formalin-fixation, paraffin-embedding, slicing, and staining with eosin. To assess the effectiveness of the trypan blue method, control lung tissue which was not perfused was formalin-fixed, paraffin-embedded, sliced, and stained with hematoxylin and eosin (H&E) to allow for total cell counts within a 20X image. A nested one-way ANOVA and Tukey's multiple comparison test demonstrated that the addition of 2FA did not increase the number of membrane permeable cells. This analysis also found no significant difference in the number of blue cells in tissue treated with trypan blue and hydrogen peroxide and untreated tissue stained with H&E, thus indicating the effectiveness of this technique for quantification of membrane-permeable cells.

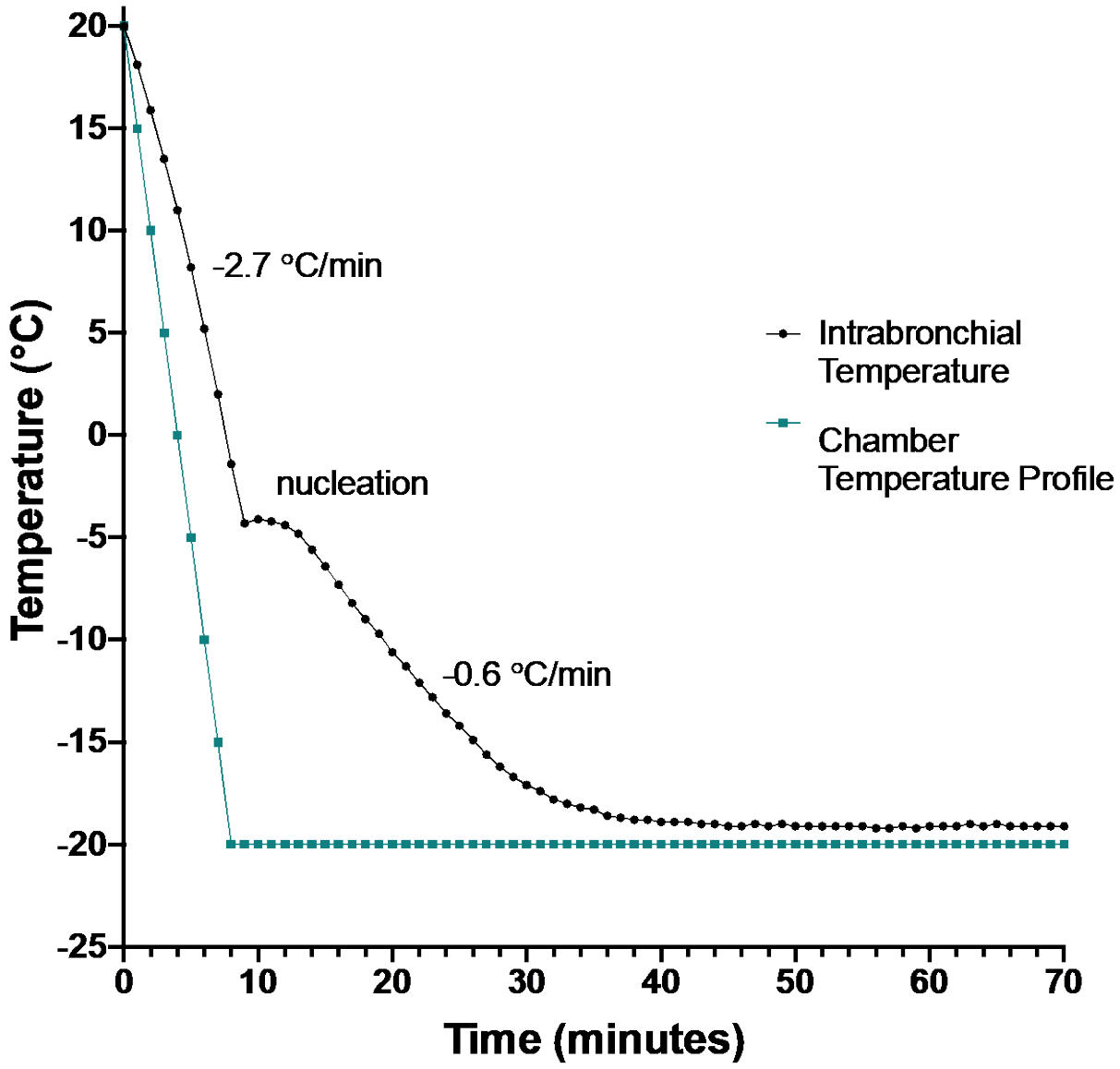

Figure 3.5 Intrabronchial Freezing Rate and Chamber Temperature Profile

A thermocouple was placed in the bronchial of a left rat lung prior to freezing at a chamber rate of -5 °C/min to -20 °C and a 1 h hold at -20 °C in a CryoMed™ Controlled-Rate Freezer (Thermo Scientific™). In this assessment, the lungs were perfused with STEEN Solution™ alone. Both the intrabronchial temperature and the chamber freezing profile are shown.

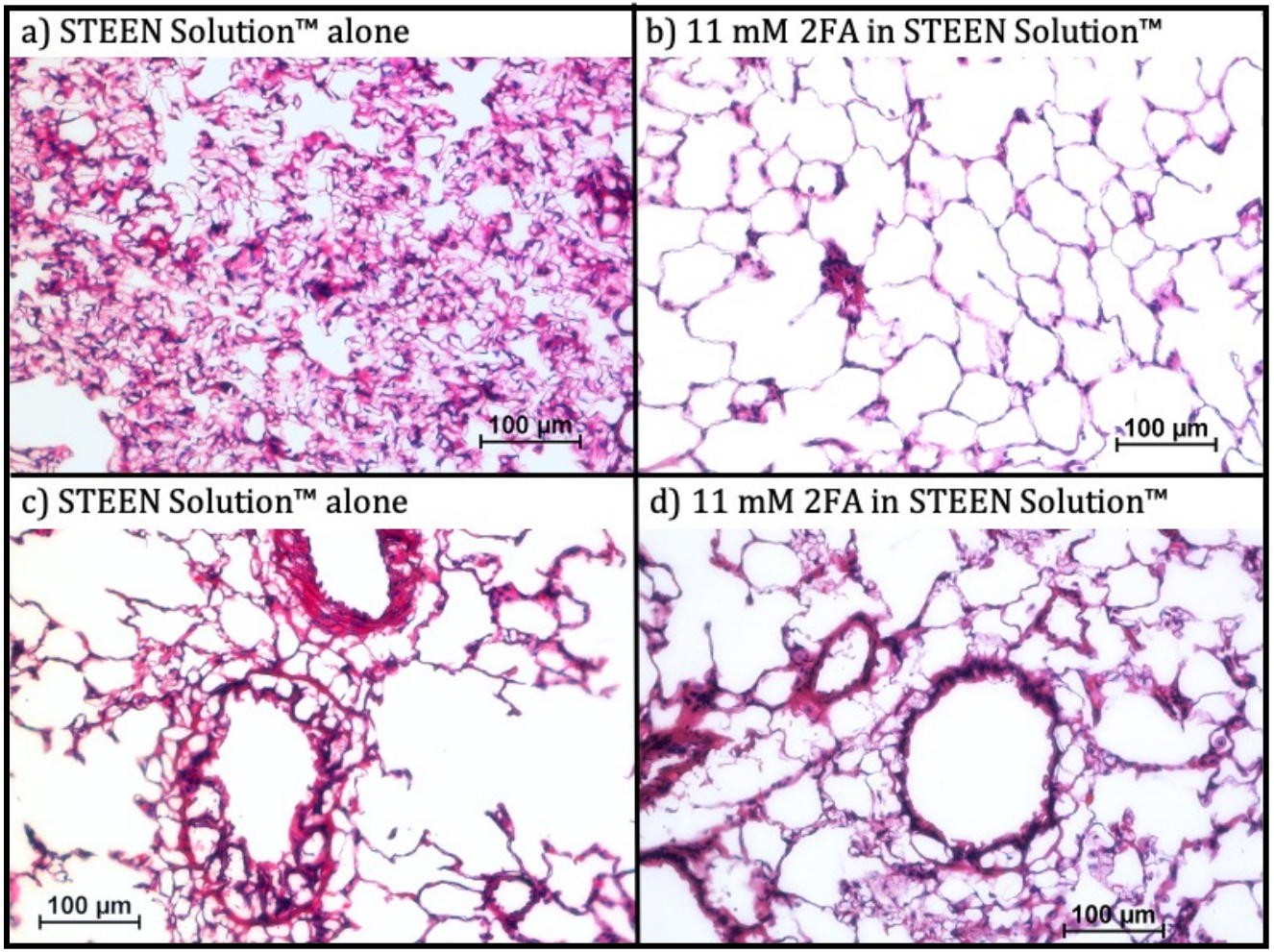

Figure 3.6 Cryofixed Rat Lungs Perfused with STEEN Solution™, With or Without 2FA

Sample images of cryofixed tissue after perfusion with STEEN Solution™ alone (panels a and c) or 11 mM 2FA in STEEN Solution™ (panels b and d). Alveoli are depicted in panels a and b, while bronchioles and associated vessels are depicted in panels c and d.

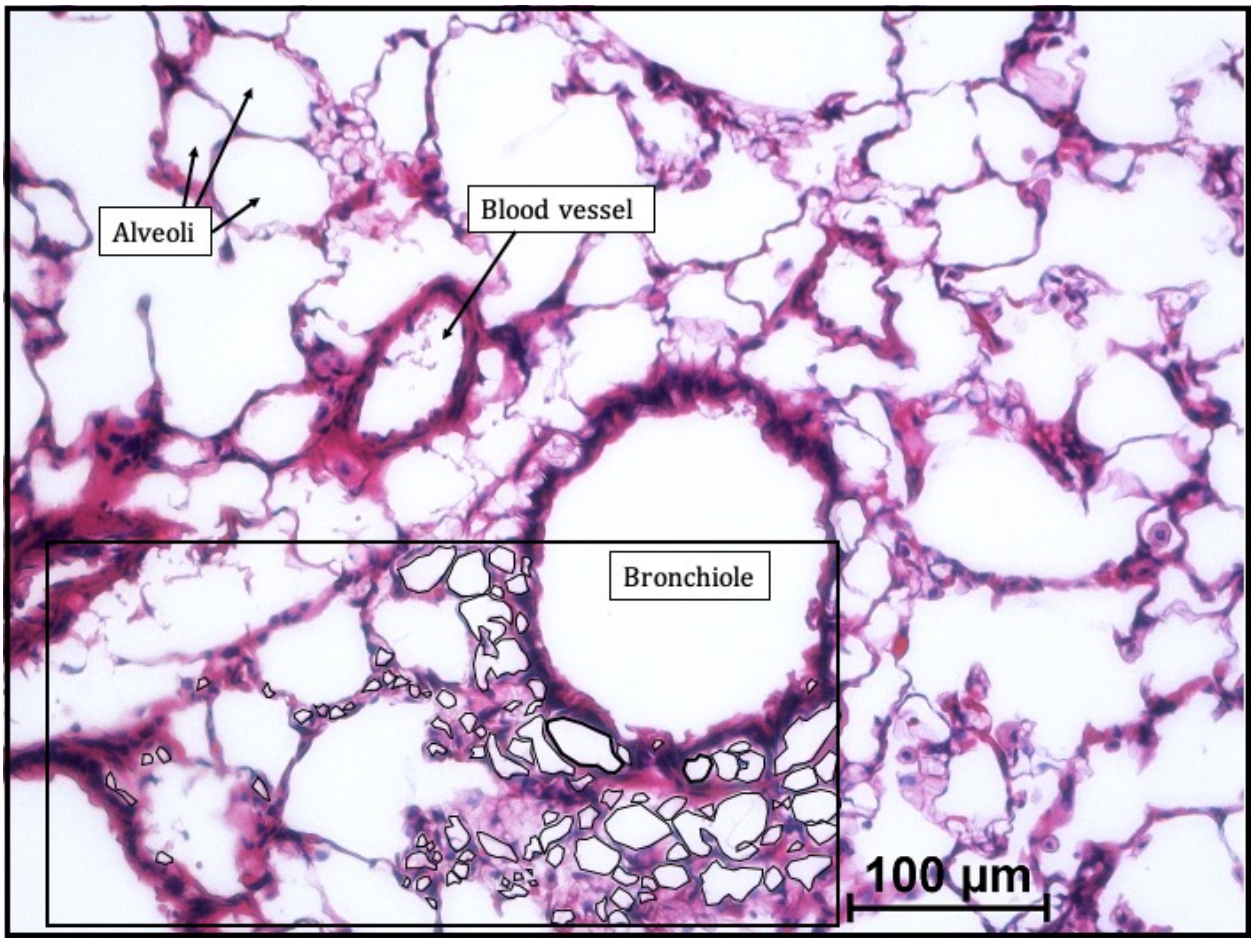

Figure 3.7 Methodology for Quantification of Ice Grain Size within Lung Tissue

Cryofixation images were quantified from alveolar images obtained using brightfield microscopy using the polygon area tool in NIS Elements AR 3.2 image analysis software (Nikon). The black rectangle within this image has ice grains traced in black as a representation of how they were quantified with the polygon area tool. Other open spaces of the lungs, including bronchioles, blood vessels, and alveoli are labelled. These regions may contain ice, but ice in these regions cannot be quantified by this method.

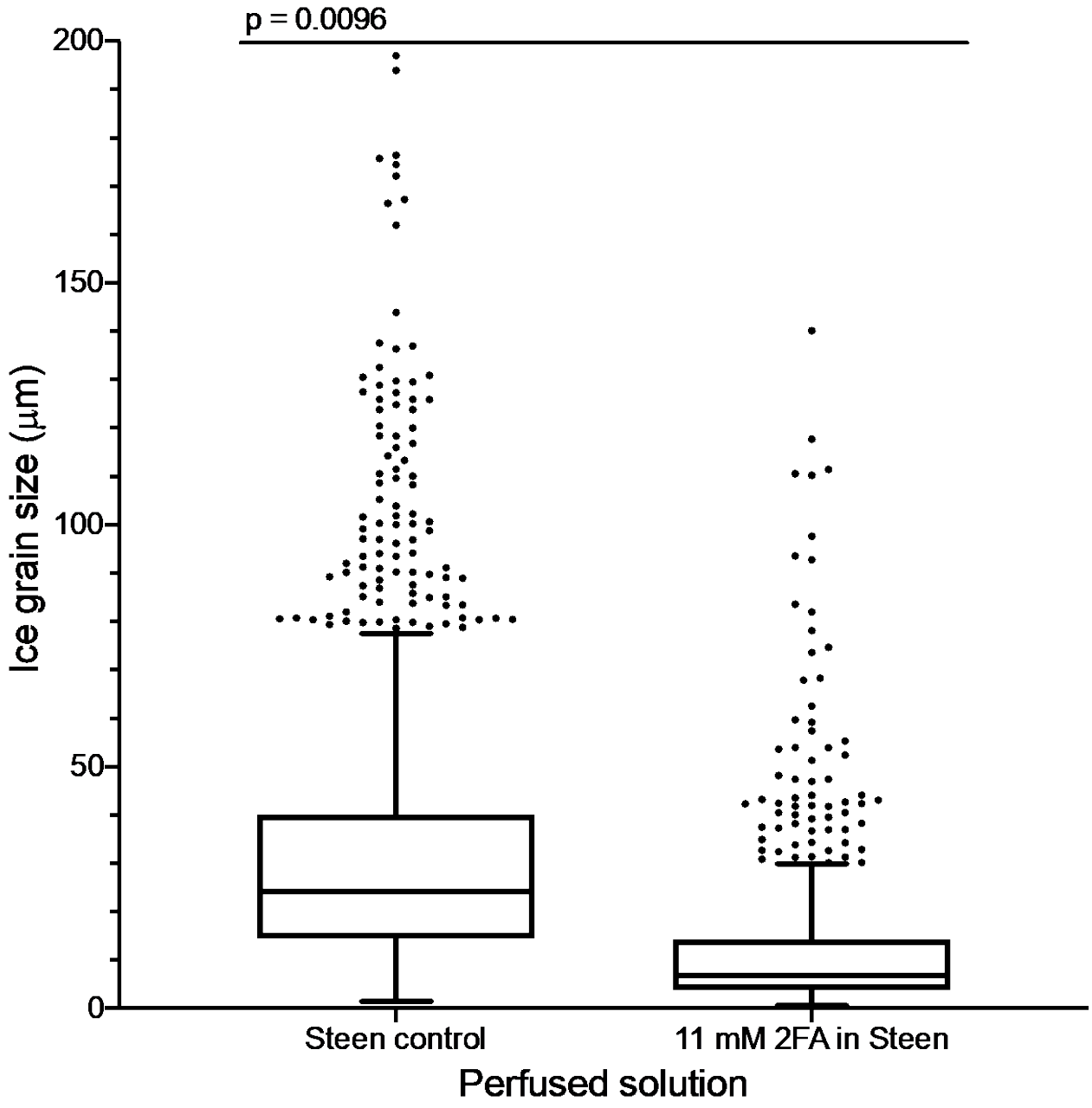

Figure 3.8 Perfusion with 2FA Significantly Reduces Alveolar Ice Grain Size

Ice grain size distribution in cryofixed lung tissue following perfusion with STEEN Solution™ alone or 11 mM 2FA in STEEN Solution™. Ice grains larger than 200 μM are excluded from this graph. Two biological replicates were performed and two 20X images were quantified from each image. A nested t-test on log-transformed data demonstrated a significant reduction in extracellular ice grain size when 2FA is used.

		STEEN Solution™	11 mM 2FA in STEEN Solution™
Descriptive Statistics	Number of values	3131	1149
	Minimum	0.66	0.55
	25th Percentile	10.65	3.31
	Median	21.49	6.37
	75th Percentile	40.92	13.35
	Maximum	597.90	142.10
	Mean	32.32	11.76
	Std. Deviation	36.56	15.81
Nested t-test (log-transformed data)		p = 0.0096	

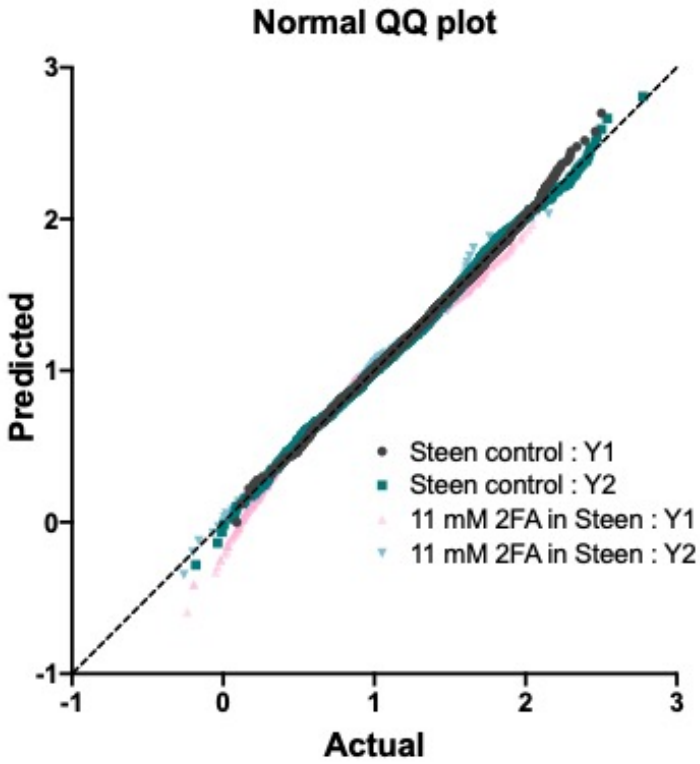

Figure 3.9 Alveolar Ice Grain Size Descriptive and Inferential Statistics

Descriptive and inferential statistics of ice grain size in cryofixed lung tissue after perfusion with STEEN Solution™ alone or 11 mM 2FA in STEEN Solution™. The normal QQ plot of log transformed data is shown to demonstrate the normality of transformed data.

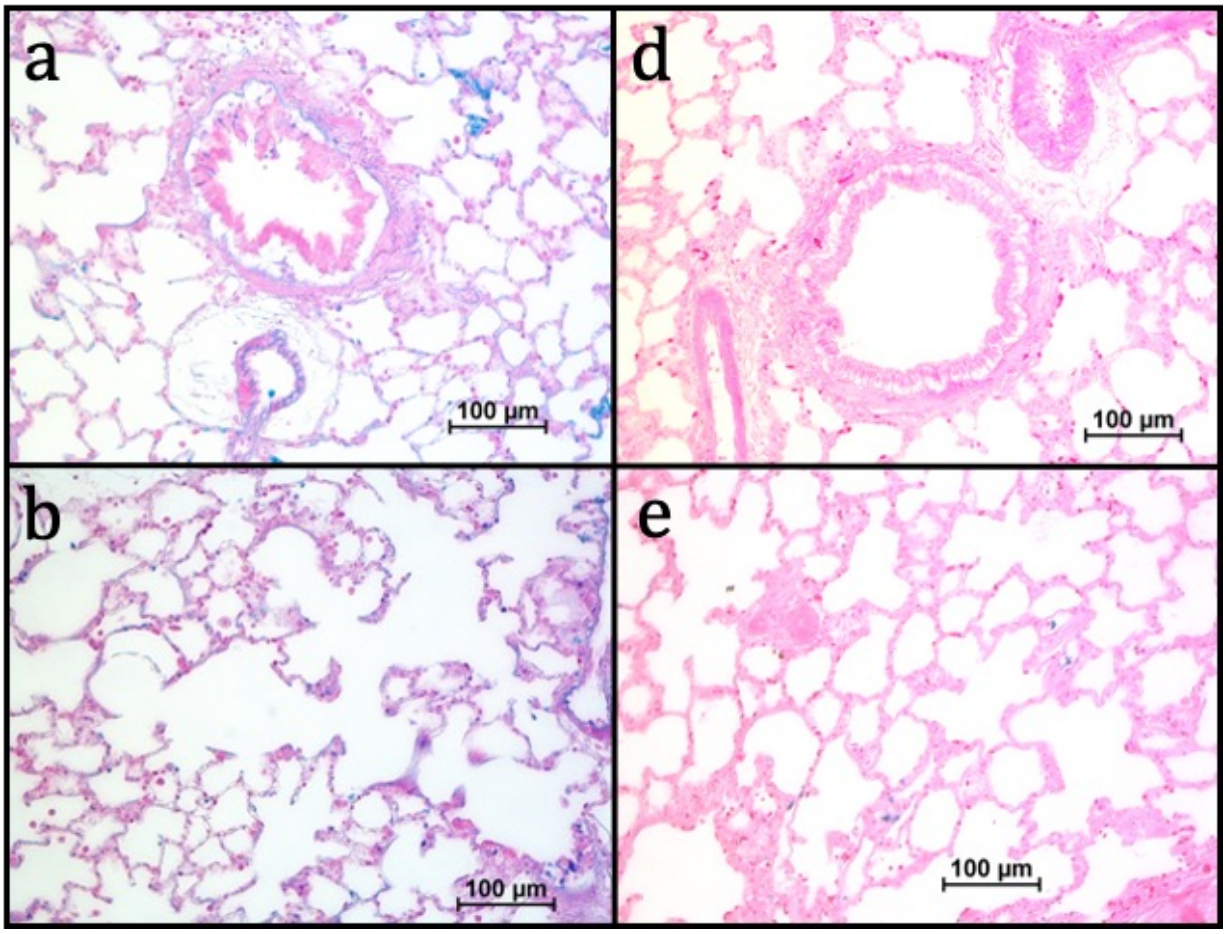

Figure 3.10 Post-thaw Images of Rat Lungs

Sample 20X post-thaw images of lung tissue perfused with 10% (v/v) DMSO 0.4% (w/v) trypan blue in STEEN Solution™ (panels a-b) or 11 mM 2FA 10% (v/v) DMSO 0.4% (w/v) trypan blue in STEEN Solution™ (panels d-e). Samples were frozen at a chamber rate of -5 °C/min to -20 °C, held for 1 h at -20 °C, prior to thawing in a 37 °C waterbath for 5 min. Tissue was formalin-fixed, paraffin-embedded, sliced, and stained with eosin.

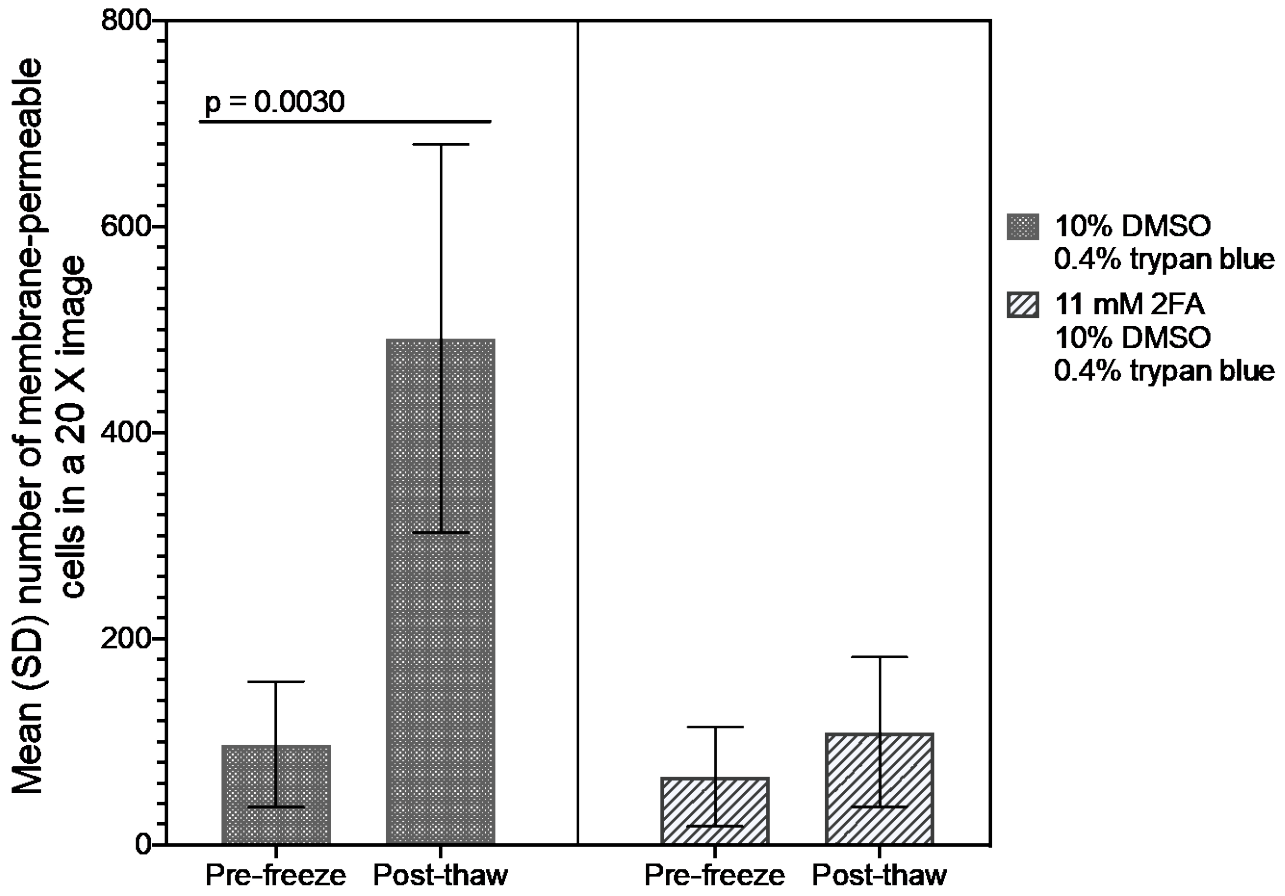

Figure 3.11 Perfusion of 2FA Prior to Freezing Increases Post-Thaw Cell Membrane Integrity

Mean (SD) number of membrane permeable cells in a 20X image of lung tissue pre-freeze or post-thaw, as obtained from 10 images each from two biological replicates. Tissues perfused with 10% (v/v) DMSO 0.4% (w/v) trypan blue in STEEN Solution™, with or without 11 mM 2FA, were frozen at a chamber rate of -5 °C/min to -20 °C, held for 1 h at -20 °C, prior to thawing in a 37 °C waterbath for 5 min. Tissue was formalin-fixed, paraffin-embedded, sliced, and stained with eosin. A nested one-way ANOVA and Tukey's multiple comparison test demonstrated a significant increase in membrane permeability post-thaw when 10% (v/v) DMSO 0.4% trypan blue was perfused prior to freezing. The use of 11 mM 2FA 10% (v/v) DMSO and 0.4% trypan blue was found to maintain post-thaw membrane integrity at rates comparable to pre-freeze membrane integrity. Therefore, the addition of 2FA improves post-thaw cell membrane integrity when compared to DMSO-treated controls.

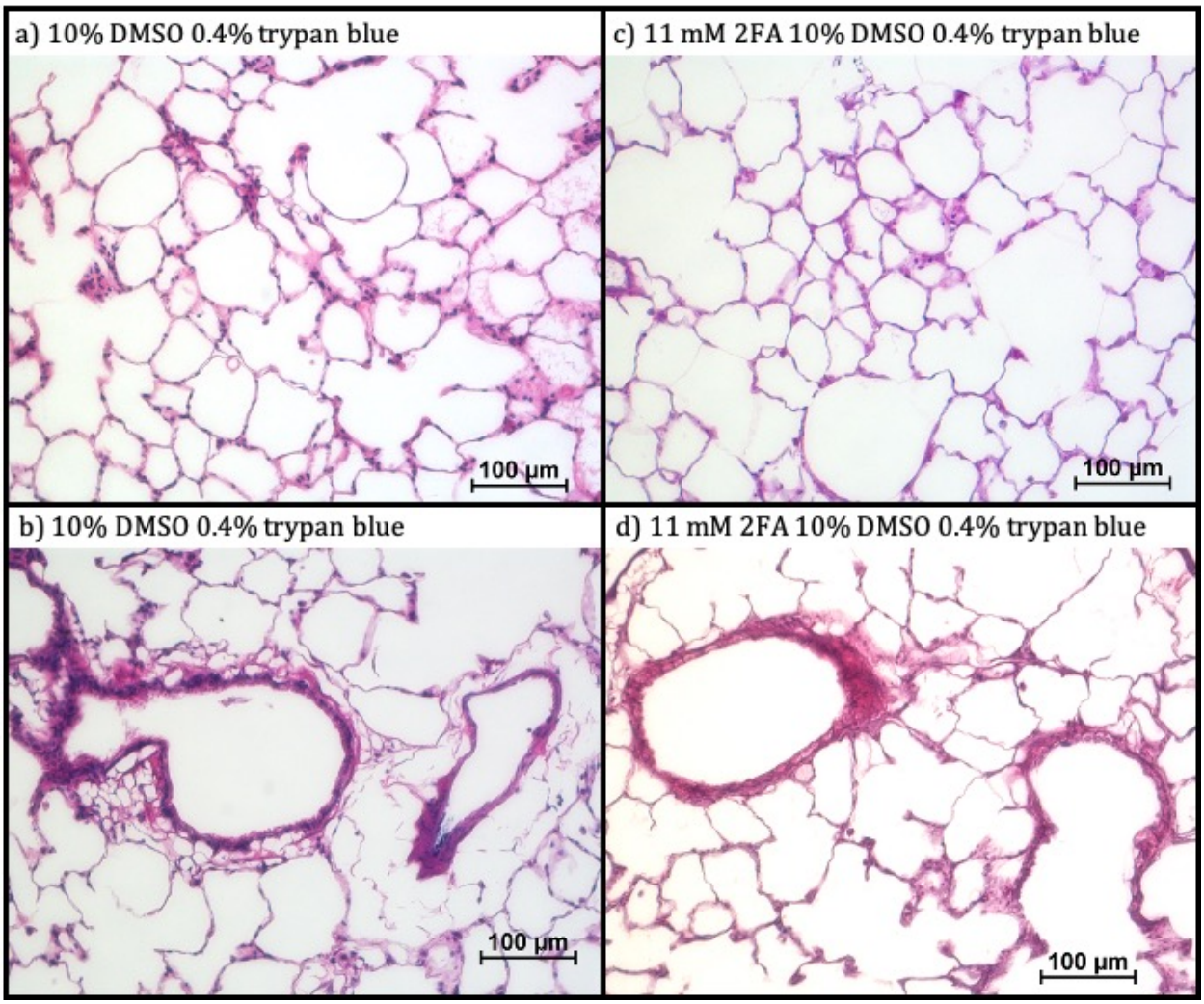

Figure 3.12 Cryofixed Rat Lungs Perfused with DMSO and Trypan Blue in STEEN Solution™, With or Without 2FA

20X cryofixation images of lung tissue perfused with 10% (v/v) DMSO 0.4% (w/v) trypan blue in STEEN Solution™, with or without 11 mM 2FA, frozen at a chamber rate of -5 °C/min to -20 °C and held for 1 h at -20 °C prior to cryofixation. Samples were paraffin-embedded, sliced, and stained with eosin.

4. Conclusions and Significance

Over the past few decades, organ preservation research has almost exclusively studied ice avoidance strategies[27; 33; 57; 64; 65; 67; 82; 107; 127; 137; 150; 151; 190; 192; 216]. This is due to the current inability to control ice growth and location during initial nucleation, prolonged storage, or thawing[22; 72; 79; 120; 194]. IRIs offer a novel direction of research due to their documented ability to reduce intracellular ice grain size[157] and improve post-thaw cell survival[32]. However, their ability to function in the presence of DMSO or to reduce intra- and extra-cellular ice grain size in any organ model was unknown. Lungs were selected as the model of interest given the heightened transplant demand, the current underrepresentation of lungs in the whole organ cryopreservation literature, and the unique qualities of the lung which may make them amenable to cryopreservation (Table 1.1). Therefore, the research performed for this thesis aimed to assess the utility of IRIs as novel cryoprotectants for lung cryopreservation.

4.1 Review of Results

It was hypothesized that IRIs would not be cytotoxic and would be capable of controlling intra- and extra-cellular ice growth resulting in improved cellular survival following cryopreservation of type II pneumocyte monolayers and rat lung tissue, when compared to DMSO-treated controls. Objective 1 set out to determine the cytotoxicity of IRIs and the ability for IRIs to reduce intracellular ice grain size resulting in improved post-thaw survival over DMSO-treated controls, in the immortalized type 2 pneumocyte cell line BEAS-2B. Objective 2 progressed to tissue and aimed to determine the cytotoxicity of IRIs to lung cells during *ex vivo* subnormothermic perfusion of rat lungs, as well as the ability of IRIs to reduce extracellular ice grain size and improve cell survival and structural morphology of rat lungs after -20°C cryopreservation.

In assessment of the first objective, one IRI, 2FA, was observed to successfully reduce intracellular ice grain size without cytotoxicity when used alone in pneumocyte monolayer cryopreservation; however, this effect was perturbed by the addition of DMSO. This appeared to result in an inability for 2FA addition to improve post-thaw cell survival during rapid (-90°C/min) freezing, with or without the addition of a transient warming event. However, it was unclear whether the lack of intracellular ice control and inability to improve post-thaw survival when 2FA was used with DMSO was due to solution or cell characteristics. While it was possible that DMSO

rendered 2FA non-functional due to chemical or physical interactions, it was also possible that DMSO simply prevented entry of 2FA into the cell.

In the assessment of the second objective, 2FA did not appear to be cytotoxic in rat lungs and reduced extracellular ice grain size resulting in improved alveolar cell membrane integrity and tissue structural integrity post-thaw. This suggested that the relationship between DMSO and 2FA observed in assessment of the first objective may not be due to a chemical or physical interaction. It can be speculated that DMSO alters the cell membrane in such a way as to prevent 2FA entry and/or the presence of DMSO increases the rate of 2FA removal from the cell[11; 95; 126; 148; 200]. This expands upon existing IRI literature[20; 31; 32; 40; 41; 42; 157], as these findings begin to elucidate mechanism of 2FA entry into the cell and provides further avenues of IRI research.

Ultimately, 2FA appears to be a useful cryoprotectant in terms of its ability to reduce intra- and extra-cellular ice grain size and improve post-thaw cell membrane integrity and tissue structural integrity in whole rat lung cryopreservation, without apparent cytotoxicity.

4.2 Future Directions

This work illuminates several directions of future study regarding IRIs and lung cryopreservation. While this work better characterised the function of one IRI, 2FA, the reasons for which 2FA does not reduce intracellular ice grain size when used with DMSO, or the mechanism by which IRIs prevent ice growth in any capacity remain unknown. Therefore, future research could assess the mechanism by which 2FA enters cells and interacts with ice and water. The interactions between 2FA, DMSO, and cellular constituents could be studied using raman spectroscopy[113; 221], and mass spectrometry could be used to verify that no physical or chemical interactions occur between DMSO and 2FA[36]. Considering that a variety of IRIs exist[26], future research could additionally assess the efficacy of these various IRIs for cell, tissue, and organ cryopreservation research. In a lung cryopreservation direction, the protocols developed here may be improved upon through a more thorough analysis utilizing various cryoprotectants, cooling rates, and storage temperatures. For example, the apparent dehydrative effect of trypan blue encourages the use of a non-permeating cryoprotectant, such as sucrose, to be used in combination with a permeating cryoprotectant, such as DMSO, and IRIs. Furthermore, more expensive assessments could be performed utilizing normothermic ex vivo lung perfusion equipment which allows for assessment of lung function pre- and post-cryopreservation.

4.3 Significance to Cryopreservation of Complex Systems

Prior to this work, IRI use had been limited to the study of red blood cells, HUVEC monolayers, and hematopoietic stem cells, and no publications had attempted to elucidate the mechanism of IRI function or entry into the cell[31; 32; 41; 157]. This work expands upon previous research by demonstrating the ability for IRIs to reduce intra- and extra-cellular ice grain size in BEAS-2B monolayers and rat lung tissue, respectively. In addition, this work begins to address the mechanism of IRI entry into cells and the relationship between IRIs and DMSO. The finding that 2FA fails to reduce intracellular ice grain size but maintains the ability to reduce extracellular ice grain size when used with DMSO suggests that DMSO and 2FA do not undergo a chemical or physical interaction in solution. Rather, this suggests that the presence of DMSO prevents 2FA function within the cell or DMSO prevents entry of 2FA into the cell. Therefore, the findings of this work contribute to the basic cryobiology literature by addressing the use of IRIs in lung cells and in whole lungs while providing a prefatory contribution to the mechanistic understanding of IRIs.

An unintended, but significant, finding of this work was the discovery that the loss of membrane integrity following intracellular ice formation in BEAS-2B cells is transient. Although other research has demonstrated that the formation of intracellular ice can have a protective effect in cell monolayer cryopreservation[2], no other work has documented a loss and subsequent return of membrane integrity which parallels metabolic activity. This suggests that intracellular ice formation is not as inherently lethal as it is often described in the literature[131; 132; 142; 211], although the downstream effects of this transient loss in membrane integrity are unknown. This finding, in addition to the observed reduction in intracellular ice grain size when 2FA is used alone, suggests that immediate membrane integrity assessments are insufficient to address post-thaw viability, and the quality of cells or tissue following cryopreservation should be considered as greatly as survival.

Perhaps the greatest contribution of this work to the scientific literature is the development of a low-cost subnormothermic *ex vivo* rat lung perfusion technique for the purposes of cryopreservation research, and the discovery that post-thaw lung cell membrane integrity can be maintained at pre-freeze levels through IRI use. While organ cryopreservation is an exciting and re-emerging field, lungs have been severely underrepresented in the organ cryopreservation literature (Table 1.1). The development of these techniques facilitates early assessment of cryoprotectant functionality and may be used by other researchers prior to more expensive assessment. The findings of this work provide support for further lung cryopreservation research, and additionally

demonstrate the efficacy of the IRI 2FA in improving post-thaw cell membrane integrity in the cryopreservation of a complex tissue. Although there are various limitations to the experimental design, namely the small sample size and inability to assess function, the findings described here provide a promising outlook for whole lung cryopreservation and IRI use in tissue and organ cryopreservation research.

4.4 Conclusions

Although there are many potential research directions in the pursuit of extending organ preservation, successful cryopreservation has the potential to drastically increase organ preservation times or even allow for organ banking. However, the cryopreservation of any organ system is a daunting endeavor given the complexity of cryopreservation challenges which exist at the cell, tissue, and whole organ level. Although livers and kidneys are the most commonly studied organ systems for whole organ cryopreservation research (Table 1.1), the lungs offer unique challenges due to their delicate nature and complexity. However, there are various advantages to studying the cryopreservation of lungs including the ability to reduce ischemic time through maintenance in an inflated state, and the low density and ability to rapidly perfuse thereby reducing the heat and mass transfer limitations common in organ cryopreservation. This work set out to study the efficacy of IRIs for lung cryopreservation and successfully demonstrated the ability for the IRI 2FA to reduce intra- and extra-cellular ice grain size and improve post-thaw cell membrane integrity and tissue structural integrity in whole rat lung cryopreservation, without cytotoxicity. In addition, this work demonstrated the potential for whole lung cryopreservation and generated low-cost techniques which may enable future researchers to study whole lung cryopreservation protocols. Although clinical organ cryopreservation is not yet within grasp, research such as this provides a promising outlook on organ cryopreservation and generates an abundance of future research directions which may one day influence clinical practice.

References

[1] N.S. Aboelnazar, S. Himmat, S. Hatami, C.W. White, M.S. Burhani, P. Dromparis, N. Matsumura, G. Tian, J.R.B. Dyck, M. Mengel, D.H. Freed, and J. Nagendran, Negative pressure ventilation decreases inflammation and lung edema during normothermic ex-vivo lung perfusion. Journal of Heart and Lung Transplantation 37 (2018) 520-530.

[2] J.P. Acker, Innocuous intracellular ice formation: mechanisms and implications, Laboratory Medicine and Pathology, University of Alberta, 2000, pp. 196.

[3] J.P. Acker, and I.M. Croteau, Pre- and post-thaw assessment of intracellular ice formation. Journal of Microscopy 215 (2004) 131-138.

[4] J.P. Acker, Biopreservation of cells and engineered tissues. Advances in Biochemical Engineering/Biotechnology 103 (2006) 157-187.

[5] O. Ahmad, A.E. Shafii, D.M. Mannino, R. Choate, and M.A. Baz, Impact of donor lung pathogenic bacteria on patient outcomes in the immediate post-transplant period. Transplant Infectious Disease 20 (2018) 1-8.

[6] C. Aigner, A. Slama, K. Hötzenecker, A. Scheed, B. Urbanek, W. Schmid, F.J. Nierscher, G. Lang, and W. Klepetko, Clinical ex vivo lung perfusion - Pushing the limits. American Journal of Transplantation 12 (2012) 1839-1847.

[7] N. Aizarani, A. Saviano, Sagar, L. Mailly, S. Durand, P. Pessaux, T.F. Baumert, and D. Grun, A human liver cell atlas reveals heterogeneity and epithelial progenitors. Nature 572 (2019) 199-204.

[8] A. Ali, C. Summers, S. Keshavjee, and M. Cypel, Normothermic Ex Vivo Lung Perfusion: A Review of the Toronto Protocol. University of Toronto Medical Journal 94 (2017) 26-31.

[9] G. Amir, B. Rubinsky, S.Y. Basheer, L. Horowitz, L. Jonathan, M.S. Feinberg, A.K. Smolinsky, and J. Lavee, Improved viability and reduced apoptosis in sub-zero 21-hour preservation of transplanted rat hearts using anti-freeze proteins. Journal of Heart and Lung Transplantation 24 (2005) 1915-1929.

[10] A. Andreasson, D.M. Karamanou, J.D. Perry, A. Perry, F. Özalp, T. Butt, K.E. Morley, H.R. Walden, S.C. Clark, M. Prabhu, P.A. Corris, K. Gould, A.J. Fisher, and J.H. Dark, The effect of ex vivo lung perfusion on microbial load in human donor lungs. Journal of Heart and Lung Transplantation 33 (2014) 910-916.

[11] T. Arakawa, Y. Kita, and S.N. Timasheff, Protein precipitation and denaturation by dimethyl sulfoxide. Biophysical Chemistry 131 (2007) 62-70.

[12] A. Arav, B. Rubinsky, G. Fletcher, and E. Seren, Cryogenic protection of oocytes with antifreeze proteins. Molecular Reproduction and Development 36 (1993) 488-493.

[13] W.J. Armitage, and B.K. Juss, The influence of cooling rate on survival of frozen cells differs in monolayers and in suspensions. Cryo-Letters 17 (1996) 213-218.

[14] W.J. Armitage, S.C. Hall, and C. Routledge, Recovery of endothelial function after vitrification of cornea at -110°C. Investigative Ophthalmology and Visual Science 43 (2002) 2160-2164.

[15] V.S. Avlonitis, A. Krause, L. Luzzi, H. Powell, J.A. Phillips, P.A. Corris, F.K. Gould, and J.H. Dark, Bacterial colonization of the donor lower airways is a predictor of poor outcome in lung transplantation. European Journal of Cardio-thoracic Surgery 24 (2003) 601-607.

[16] J.E. Baatz, D.A. Newton, E.C. Riemer, C.E. Denlinger, E.E. Jones, R.R. Drake, and D.D. Spyropoulos, Cryopreservation of viable human lung tissue for versatile post-thaw analyses and culture. In Vivo 28 (2014) 411-423.

[17] A. Bagul, and S.A. Hosgood, Organ retrieval and preservation. Surgery (Oxford) 29 (2011) 306-311.

[18] Y. Bai, N. Krishnamoorthy, K.R. Patel, I. Rosas, M.J. Sanderson, and X. Ai, Cryopreserved human precision-cut lung slices as a bioassay for live tissue banking a viability study of bronchodilation with bitter-taste receptor agonists. American Journal of Respiratory Cell and Molecular Biology 54 (2016) 656-663.

[19] A.K. Balcerzak, K. McClymont, R.N. Ben, M. Bayer-Giraldi, I. Weikusat, C. Isert, S. Kipfstuhl Alfred-Wegener, M. Bar Dolev, J. Liu, Y. Qin, Y. Celik, R. Drori, J. Wettlaufer, P.L. Davies, and I. Braslavsky, The importance of hydrophobic moieties in ice recrystallization inhibitors. Cryobiology 3 (2013) 3232-3236.

[20] A.K. Balcerzak, C.J. Capicciotti, J.G. Briard, and R.N. Ben, Designing ice recrystallization inhibitors: from antifreeze (glyco)proteins to small molecules. RSC Advances 4 (2014) 42682-42696.

[21] H. Bank, Visualization of freezing damage. II. Structural alterations during warming. Cryobiology 10 (1973) 157-170.

[22] J.G. Baust, D. Gao, and J.M. Baust, Cryopreservation: An emerging paradigm change. Organogensis 5 (2009) 90-96.

[23] J.M. Baust, Molecular Mechanisms of Cellular Demise Associated with Cryopreservation Failure. Cell Preservation Technology 1 (2003) 17-31.

[24] J.M. Baust, M.J. Vogel, K.K. Snyder, R.G. Van Buskirk, and J.G. Baust, Activation of Mitochondrial-Associated Apoptosis Contributes to Cryopreservation Failure. Cell Preservation Technology 5 (2007) 155-163.

[25] F.O. Belzer, and J.H. Southard, Principles of solid organ preservation by cold storage. Transplantation 45 (1988) 673-676.

[26] R.N. Ben, C.J. Capicciotti, and J.G. Briard, Small Molecule Ice Recrystallization Inhibitors And Methods Of Use Thereof, The University of Ottawa, United States, 2018.

[27] T.A. Berendsen, B.G. Bruinsma, C.F. Puts, N. Saeidi, O.B. Usta, B.E. Uygun, M.L. Izamis, M. Toner, M.L. Yarmush, and K. Uygun, Supercooling enables long-term transplantation survival following 4 days of liver preservation. Nature Medicine 20 (2014) 790-793.

[28] M. Boffini, D. Ricci, R. Bonato, V. Fanelli, M. Attisani, M. Ribezzoa, P. Solidoro, L. Del Sorbo, V.M. Ranierib, and M. Rinaldi, Incidence and severity of primary graft dysfunction after lung transplantation using rejected grafts reconditioned with ex vivo lung perfusion. European Journal of Cardio-thoracic Surgery 46 (2014) 789-793.

[29] P.N. Bonde, N.D. Patel, M.C. Borja, S.H. Allan, C.J. Barreiro, J.A. Williams, N.A. Thakur, J.B. Orens, and J.V. Conte, Impact of donor lung organisms on post-lung transplant pneumonia. Journal of Heart and Lung Transplantation 50 (2006) 1065-1070.

[30] R.G. Boutilier, Mechanisms of cell survival in hypoxia and hypothermia. The Journal of experimental biology 204 (2001) 3171-3181.

[31] J.G. Briard, S. Jahan, P. Chandran, D. Allan, N. Pineault, and R.N. Ben, Small-Molecule Ice Recrystallization Inhibitors Improve the PostThaw Function of Hematopoietic Stem and Progenitor Cells. ACS OMEGA 1 (2016) 1010-1018.

[32] J.G. Briard, J.S. Poisson, T.R. Turner, C.J. Capicciotti, J.P. Acker, and R.N. Ben, Small molecule ice recrystallization inhibitors mitigate red blood cell lysis during freezing, transient warming and thawing. Scientific Reports 6 (2016) 1-10.

[33] B.G. Bruinsma, T.A. Berendsen, M.L. Izamis, H. Yeh, M.L. Yarmush, and K. Uygun, Supercooling preservation and transplantation of the rat liver. Nature Protocols 10 (2015) 484-494.

[34] M.T. Buchko, S. Himmat, C.J. Stewart, S. Hatami, P. Dromparis, B. Adam, D.H. Freed, and J. Nagendran, Continuous Hemodialysis Does Not Improve Graft Function During Ex Vivo Lung Perfusion Over 24 Hours. Transplantation proceedings 51 (2019) 2022-2028.

[35] E.C. Burdette, S. Wiggins, R. Brown, and A.M. Karow, Microwave thawing of frozen kidneys: A theoretically based experimentally effective design. Cryobiology 17 (1980) 393-402.

[36] E. Calvo, E. Camafeita, J.F. Diaz, and J. Antonio Lopez, Mass Spectrometry for Studying the Interaction between Small Molecules and Proteins. Current Proteomics 5 (2008).

[37] B.K. Campbell, J. Hernandez-Medrano, V. Onions, C. Pincott-Allen, J. Fisher, A.S. McNeilly, R. Webb, and H.M. Picton, Restoration of ovarian function and natural fertility following the cryopreservation and autotransplantation of whole adult sheep ovaries. Human Reproduction 29 (2014) 1749-1763.

[38] Canadian Institute for Health Information, Treatment of End-Stage Organ Failure in Canada, Canadian Organ Replacement Register, 2009 to 2018: End-Stage Kidney Disease and Kidney Transplants — Data Tables. , CIHI, Ottawa, ON, 2019.

[39] Canadian Institute for Health Information, Treatment of End-Stage Organ Failure in Canada, Canadian Organ Replacement Register, 2009 to 2018: Extra-Renal Transplants — Data Tables., CIHI, Ottawa, ON, 2019.

[40] C.J. Capicciotti, M. Leclère, F.A. Perras, D.L. Bryce, H. Paulin, J. Harden, Y. Liu, and R.N. Ben, Potent inhibition of ice recrystallization by low molecular weight carbohydrate-based surfactants and hydrogelators. Chemical Science 3 (2012) 1408-1416.

[41] C.J. Capicciotti, J.D.R. Kurach, T.R. Turner, R.S. Mancini, J.P. Acker, and R.N. Ben, Small molecule ice recrystallization inhibitors enable freezing of human red blood cells with reduced glycerol concentrations. Scientific Reports 29 (2015) 277.

[42] C.J. Capicciotti, R.S. Mancini, T.R. Turner, T. Koyama, M. Alteen, M. Doshi, T. Inada, J.P. Acker, and R.N. Ben, O-Aryl-Glycoside Ice Recrystallization Inhibitors as Novel Cryoprotectants: A Structure−Function Study. ACS OMEGA 1 (2016) 656-662.

[43] R. Carnevale, G. Biondi-Zoccai, M. Peruzzi, E. De Falco, I. Chimenti, F. Venuta, M. Anile, D. Diso, E. Cavarretta, A.G.M. Marullo, P. Sartini, P. Pignatelli, F. Violi, and G. Frati, New Insights into the Steen Solution Properties: Breakthrough in Antioxidant Effects via NOX2 Downregulation. Oxidative Medicine and Cellular Longevity 2014 (2014) 1-10.

[44] D.T. Carrell, A.L. Wilcox, and R.L. Urry, Effect of fluctuations in temperature encountered during handling and shipment of human
cryopreserved semen. Andrologia 28 (1996) 315-319.

[45] V. Castranova, J. Rabovsky, J.H. Tucker, and P.R. Miles, The alveolar type II epithelial cell: A multifunctional pneumocyte. Toxicology and Applied Pharmacology 93 (1988) 472-483.

[46] R.S. Chang, K. Wright, and R.M. Effros, Role of albumin in prevention of edema in perfused rabbit lungs. Journal of Applied Physiology 50 (1981) 1065-1070.

[47] J.Z. Clark, L. Chen, C. Chou, H. Jun Jung, J. Wook Lee, and M.A. Knepper, Representation and relative abundance of cell-type selective markers in whole-kidney RNA-Seq data. Kidney International 95 (2019) 787-796.

[48] P. Coelho, L. Dobrila, and P. Rubinstein, Effect of transient warming events on cell viability of placental cord blood. Cytotherapy 3 (2000) 55-60.

[49] J.D. Crapo, B.E. Barry, P. Gehr, M. Bachofen, and E. Weibel, Cell number and cell characteristics of the normal human lung. American Thoracic Society Journals 126 (1982) 332-337.

[50] M. Cypel, J.C. Yeung, S. Hirayama, M. Rubacha, S. Fischer, M. Anraku, M. Sato, S. Harwood, A. Pierre, T.K. Waddell, M. de Perrot, M. Liu, and S. Keshavjee, Technique for Prolonged Normothermic Ex Vivo Lung Perfusion. Journal of Heart and Lung Transplantation 27 (2008) 1319-1325.

[51] M. Cypel, M. Liu, M. Rubacha, J.C. Yeung, S. Hirayama, M. Anraku, M. Sato, J. Medin, B.L. Davidson, M. De Perrot, T.K. Waddell, A.S. Slutsky, and S. Keshavjee, Functional repair of human donor lungs by IL-10 gene therapy. Science Translational Medicine 1 (2009) 1-9.

[52] M. Cypel, M. Rubacha, J. Yeung, S. Hirayama, K. Torbicki, M. Madonik, S. Fischer, D. Hwang, A. Pierre, T.K. Waddell, M. De Perrot, M. Liu, and S. Keshavjee, Normothermic Ex Vivo perfusion prevents lung injury compared to extended cold preservation for transplantation. American Journal of Transplantation 9 (2009) 2264-2269.

[53] M. Cypel, J.C. Yeung, M. Liu, M. Anraku, F. Chen, W. Karolak, M. Sato, J. Laratta, S. Azad, M. Madonik, C.-W. Chow, C. Chaparro, M. Hutcheon, L.G. Singer, A.S. Slutsky, K. Yasufuku, M. de Perrot, A.F. Pierre, T.K. Waddell, and S. Keshavjee, Normothermic Ex Vivo Lung Perfusion in Clinical Lung Transplantation. New England Journal of Medicine 364 (2011) 1431-1440.

[54] M. Cypel, J.C. Yeung, T. Machuca, M. Chen, L.G. Singer, K. Yasufuku, M. de Perrot, A. Pierre, T.K. Waddell, and S. Keshavjee, Experience with the first 50 ex vivo lung perfusions in clinical transplantation. The Journal of Thoracic and Cardiovascular Surgery 144 (2012) 1200-1206.

[55] M. Cypel, C. Aigner, E. Sage, T. Machuca, A. Slama, M. Stern, W. Klepetko, A. Chapelier, and S. Keshavjee, Three Center Experience with Clinical Normothermic Ex Vivo Lung Perfusion. The Journal of Heart and Lung Transplantation 32 (2013) S16.

[56] J.H. Dark, D. Karamanou, S. Clark, P. Mahesh, B. Watson, P.A. Corris, and A.J. Fisher, 323 Successful Transplantation of Unusable Donor Lungs Using Ex-Vivo Lung Perfusion: The Newcastle Experience. The Journal of Heart and Lung Transplantation 31 (2012) 115.

[57] R.J. de Vries, S.N. Tessier, P.D. Banik, S. Nagpal, C.S.E. J., S. Ozer, E.O.A. Hafiz, T.M. van Gulik, M.L. Yarmush, J.F. Markmann, M. Toner, H. Yeh, and K. Uygun, Supercooling extends preservation time of human livers. Nature Biotechnology 37 (2019) 1131-1136.

[58] A.L. DeVries, Antifreeze glycopeptides and peptides: Interactions with ice and water. Methods in Enzymology 127 (1986) 293-303.

[59] R.H. Dietzman, A.E. Rebelo, E.F. Graham, B.G. Crabo, and R.C. Lillehei, Long-term functional success following freezing of canine kidneys. Surgery 74 (1973) 181-189.

[60] M. Dolev, I. Braslavsky, and P. Davies, Ice-binding proteins and their function. Annual Review of Biochemistry 85 (2016) 515-542.

[61] G.D. Elliott, S. Wang, and B.J. Fuller, Cryoprotectants: A review of the actions and applications of cryoprotective solutes that modulate cell recovery from ultra-low temperatures. Cryobiology 76 (2017) 74-91.

[62] G. Erdag, A. Eroglu, J.R. Morgan, and M. Toner, Cryopreservation of fetal skin is improved by extracellular trehalose. Cryobiology 44 (2002) 218-228.

[63] G. Fahy, and A.M. Karow, Ultrastructure-function correlative studies for cardiac cryopreservation. V. Absence of a correlation between electrolyte toxicity and cryoinjury in the slowly frozen, cryoprotected rat heart. Cryobiology 14 (1977) 418-427.

[64] G. Fahy, Consequences and control of ice formation in the renal inner medulla. Cryobiology 67 (2013) 409-410.

[65] G. Fahy, Elimination of most damage after perfusing rabbit kidneys with M22 solutions. Cryobiology 73 (2016) 407.

[66] G.M. Fahy, The relevance of cryoprotectant "toxicity" to cryobiology. Cryobiology 23 (1986) 1-13.

[67] G.M. Fahy, B. Wowk, J. Wu, J. Phan, C. Rasch, A. Chang, and E. Zendejas, Cryopreservation of organs by vitrification: Perspectives and recent advances. Cryobiology 48 (2004) 157-178.

[68] G.M. Fahy, B. Wowk, R. Pagotan, A. Chang, J. Phan, B. Thomson, and L. Phan, Physical and biological aspects of renal vitrification. Organogenesis 5 (2009) 167-175.

[69] M. Falk, I. Falková, O. Kopečná, A. Bačíková, E. Pagáčová, D. Šimek, M. Golan, S. Kozubek, M. Pekarová, S.E. Follett, B. Klejdus, K.W. Elliott, K. Varga, O. Teplá, and I. Kratochvílová, Chromatin architecture changes and DNA replication fork collapse are critical features in cryopreserved cells that are differentially controlled by cryoprotectants. Scientific Reports 8 (2018) 1-18.

[70] J. Farrant, Mechanism of cell damage during freezing and thawing and its prevention. Nature 205 (1965) 1284-1287.

[71] J. Farrant, Water transport and cell survival in cryobiological procedures. Philosophical transactions of the Royal Society of London. Series B, Biological sciences 278 (1977) 191-205.

[72] E.B. Finger, and J.C. Bischof, Cryopreservation by vitrification. Current Opinion in Organ Transplantation 23 (2018) 353-360.

[73] C.H. Fox, F.B. Johnson, J. Whiting, and P.P. Roller, Formaldehyde fixation. The Journal of histochemistry and cytochemistry (1985) 845.

[74] T.J. Franks, T.V. Colby, W.D. Travis, R.M. Tuder, H.Y. Reynolds, A.R. Brody, W.V. Cardoso, R.G. Crystal, C.J. Drake, J. Engelhardt, M. Frid, E. Herzog, R. Mason, S.H. Phan, S.H. Randell, M.C. Rose, T. Stevens, J. Serge, M.E. Sunday, J.A. Voynow, B.M. Weinstein, J. Whitsett, and M.C. Williams, Resident Cellular Components of the Human Lung: Current Knowledge and Goals for Research on Cell Phenotyping and Function. Proceedings of the American Thoracic Society 5 (2008) 763-766.

[75] S. Fujikawa, Freeze-fracture and etching studies on membrane damage on human erythrocytes caused by formation of intracellular ice. Cryobiology 17 (1980) 351-362.

[76] T. Fujita, Y. Takami, K. Ezoe, T. Saito, K. Sato, N. Takeda, Y. Yamamoto, K. Homma, K. Jimbow, and N. Sato, Successful preservation of human skin by vitrification. Journal of Burn Care and Rehabilitation 21 (2000) 304-309.

[77] B.J. Fuller, B.W. Grout, and R.J. Woods, Biochemical and ultrastructural examination of cryopreserved hepatocytes in rat. Cryobiology 19 (1982) 493-502.

[78] B.J. Fuller, Cryoprotectants: The essential antifreezes to protect life in the frozen state. Cryo-Letters 25 (2004) 375-388.

[79] B.J. Fuller, N. Lane, and E. Benson, Life in the Frozen State. (2004).

[80] M. Galasso, J. Feld, Y. Watanabe, M. Pipkin, C. Summers, A. Ali, R. Qaqish, M. Chen, R.V.P. Ribeiro, K. Ramadan, L. Pires, V.S. Bagnato, C. Kurachi, V. Cherepanov, G. Moonen, A. Gazzalle, T.K. Waddell, M. Liu, S. Keshavjee, B.C. Wilson, A. Humar, and M. Cypel, Inactivating hepatitis C virus in donor lungs using light therapies during normothermic ex vivo lung perfusion. Nature communications 10 (2019) 1-12.

[81] J.S. Gammie, D.R. Stukus, S.M. Pham, B.G. Hattler, M.F. McGrath, K.R. McCurry, B.P. Griffith, and R.J. Keenan, Effect of ischemic time on survival in clinical lung transplantation. Annals of Thoracic Surgery 68 (1999) 2015-2019.

[82] Z. Gao, B. Namsrai, H. Ring, V. Ravikumar, A. Sharma, Y. Guo, M. Garwood, E. Tolkacheva, E. Finger, and J. Bischof, Iron Oxide Nanoparticles And Vs55 Perfusion In Rat Hearts. Cryobiology 91 (2019) 160.

[83] A. Germann, Y.J. Oh, T. Schmidt, U. Schön, H. Zimmermann, and H. von Briesen, Temperature fluctuations during deep temperature cryopreservation reduce PBMC recovery, viability and T-cell function. Cryobiology 67 (2013) 193-200.

[84] D.F. Gilbert, and O. Friedrich, Cell viability assays: methods and protocols, Humana Press, New York, NY, 2017.

[85] H. Gilgenkrantz, and A. Collin de l'Hortet, Understanding liver regeneration: From mechanisms to regenerative medicine. The American Journal of Pathology 188 (2018) 1316-1327.

[86] D.O. Halwani, K.G.M. Brockbank, J.G. Duman, and L.H. Campbell, Recombinant Dendroides canadensis antifreeze proteins as potential ingredients in cryopreservation solutions. Cryobiology 68 (2014) 411-418.

[87] H. Haniu, N. Saito, Y. Matsuda, T. Tsukahara, K. Maruyama, Y. Usui, K. Aoki, S. Takanashi, S. Kobayashi, H. Nomura, M. Okamoto, M. Shimizu, and H. Kato, Culture medium type affects endocytosis of multi-walled carbon nanotubes in BEAS-2B cells and subsequent biological response. Toxicology in Vitro 27 (2013) 1679-1685.

[88] Y. Hirano, Y. Nishimiya, S. Matsumoto, M. Matsushita, S. Todo, A. Miura, Y. Komatsu, and S. Tsuda, Hypothermic preservation effect on mammalian cells of type III antifreeze proteins from notched-fin eelpout. Cryobiology 57 (2008) 46-51.

[89] S.W. Hong, V. Sepilian, H.M. Chung, and T.J. Kim, Cryopreserved human blastocysts after vitrification result in excellent implantation and clinical pregnancy rates. Fertility and Sterility 92 (2009) 2062-2064.

[90] D. Hopwood, Fixatives and fixation: a review. The Histochemical Journal 1 (1969) 323-360.

[91] J. Hornung, T. Müller, and G. Fuhr, Cryopreservation of anchorage-dependent mammalian cells fixed to structured glass and silicon substrates. Cryobiology 33 (1996) 260-270.

[92] W.E. Huckabee, Relationships of pyruvate and lactate during anaerobic metabolism. I. Effects of infusion of pyruvate or glucose and of hyperventilation. The Journal of clinical investigation 37 (1958) 244-254.

[93] A. Ideta, Y. Aoyagi, K. Tsuchiya, Y. Nakamura, K. Hayama, A. Shirasawa, K. Sakaguchi, N. Tominaga, Y. Nishimiya, and S. Tsuda, Prolonging hypothermic storage (4 C) of bovine embryos with fish antifreeze protein. The Journal of reproduction and development 61 (2015) 1-6.

[94] H. Ishiguro, and B. Rubinsky, Influence of fish antifreeze proteins on the freezing of cell suspensions with cryoprotectant penetrating cells. International Journal of Heat and Mass Transfer 41 (1998) 1907-1915.

[95] S.W. Jacob, and R. Herschler, Pharmacology of DMSO. Cryobiology 23 (1986) 14-27.

[96] I.A. Jacobson, D.E. Pegg, H. Starklint, J. Chemnitz, C. Hunt, P. Barfort, and M.P. Diaper, Effect of cooling and warming rate on glycerolized rabbit kidneys. Cryobiology 21 (1984) 637-653.

[97] Z. Jia, Q. Chen, and H. Qin, Ischemia-induced apoptosis of intestinal epithelial cells correlates with altered integrin distribution and disassembly of F-actin triggered by calcium overload. Journal of Biomedicine and Biotechnology 2012 (2012) 1-10.

[98] J.W. Jo, B.C. Jee, J.R. Lee, and C.S. Suh, Effect of antifreeze protein supplementation in vitrification medium on mouse oocyte developmental competence. Fertility and Sterility 96 (2011) 1239-1245.

[99] N.H.P.M. Jutte, P. Heyse, H.G. Jansen, G.J. Bruining, and G.H. Zeilmaker, Vitrification of mouse islets of Langerhans: Comparison with a more conventional freezing method. Cryobiology 24 (1987) 292-302.

[100] T. Kakishita, T. Oto, S. Hori, K. Miyoshi, S. Otani, S. Yamamoto, N. Waki, O. Yoshida, M. Okazaki, M. Yamane, S. Toyooka, Y. Sano, and S. Miyoshi, Suppression of Inflammatory Cytokines During Ex Vivo Lung Perfusion With an Adsorbent Membrane. Annals of Thoracic Surgery 89 (2010) 1773-1781.

[101] T. Kamijima, M. Sakashita, A. Miura, Y. Nishimiya, and S. Tsuda, Antifreeze Protein Prolongs the Life-Time of Insulinoma Cells during Hypothermic Preservation. PLoS ONE 8 (2013) 1-6.

[102] J.O. Karlsson, E.G. Cravalho, I.H. Borel Rinkes, R.G. Tompkins, M.L. Yarmush, and M. Toner, Nucleation and growth of ice crystals inside cultured hepatocytes during freezing in the presence of dimethyl sulfoxide. Biophysical Journal 65 (1993) 2524-2536.

[103] J.O.M. Karlsson, E.G. Cravalho, and M. Toner, A model of diffusion-limited ice growth inside biological cells during freezing. Journal of Applied Physics 75 (1994) 4442-4455.

[104] J.O.M. Karlsson, and M. Toner, Long-term storage of tissues by cryopreservation: Critical issues. Biomaterials 17 (1996) 243-256.

[105] A.M. Karow, Cryoprotectants - a new class of drugs. The Journal of pharmacy and pharmacology 21 (1969) 209-223.

[106] M. Kasai, K. Niwa, and A. Iritani, Survival of mouse embryos frozen and thawed rapidly. Reproduction 59 (1980) 51-56.

[107] H. Kato, S. Tomita, S. Yamaguchi, H. Ohtake, and G. Watanabe, Subzero 24-hr nonfreezing rat heart preservation: A novel preservation method in a variable magnetic field. Transplantation 94 (2012) 473-477.

[108] B. Kheirabadi, and G. Fahy, Permanent life support by kidneys perfused with a vitrifiable (7.5 molar) cryoprotectant solution. Transplantation 70 (2000) 51-57.

[109] M. Koval, Sharing signals: connecting lung epithelial cells with gap junction channels. American Journal of Physiology-Lung Cellular and Molecular Physiology 27 (2002) 875-893.

[110] S.A. Kraft, S. Fujishima, G.P. McGuire, J.S. Thompson, T.A. Raffin, and R.G. Pearl, Effect of blood and albumin on pulmonary hypertension and edema in perfused rabbit lungs. Journal of Applied Physiology 78 (1985) 499-504.

[111] T. Kristián, and B.K. Siesjö, Calcium in ischemic cell death. Stroke 29 (1970) 705-718.

[112] S. Kubota, E.F. Graham, B.G. Crabo, R.C. Lillehei, and R.H. Dietzman, The effect of freeze rate, duration of phase transition and warming rate on survival of frozen canine kidneys. Cryobiology 13 (1976) 455-462.

[113] Y. Kumamoto, Y. Harada, T. Takamatsu, and H. Tanaka, Label-free Molecular Imaging and Analysis by Raman Spectroscopy. Acta Histochem Cytochem 51 (2018) 101-110.

[114] M. Kuwayama, G. Vajta, S. Ieda, and O. Kato, Comparison of open and closed methods for vitrification of human embryos and the elimination of potential contamination. Reproductive BioMedicine Online 11 (2005) 608-614.

[115] M. Kuwayama, G. Vajta, O. Kato, and S.P. Leibo, Highly efficient vitrification method for cryopreservation of human oocytes. Reproductive biomedicine online 11 (2005) 300-308.

[116] T. Laumonier, A.J. Walpen, C.F. Maurus, P.J. Mohacsi, K.M. Matozan, E.Y. Korchagina, N.V. Bovin, B. Vanhove, J.D. Seebach, and R. Rieben, Dextran sulfate acts as an endothelial cell protectant and inhibits human complement and natural killer cell-mediated cytotoxicity against porcine cells. Transplantation 76 (2003) 838-843.

[117] J.L. Lautner, D.H. Freed, J. Nagendran, and J.P. Acker, Current techniques and the future of lung preservation. Cryobiology In Press (2020).

[118] L. Lautner, N. William, and J.P. Acker, High subzero cryofixation: A technique for observing ice within tissues. Cryobiology In Press (2020).

[119] S. Lindstedt, A. Eyjolfsson, B. Koul, P. Wierup, L. Pierre, R. Gustafsson, and R. Ingemansson, How to Recondition Ex Vivo Initially Rejected Donor Lungs for Clinical Transplantation: Clinical Experience from Lund University Hospital. Journal of Transplantation 2011 (2011) 358-364.

[120] D. Liu, and F. Pan, Advances in cryopreservation of organs. Journal of Huazhong University of Science and Technology 36 (2016) 153-161.

[121] J. Lovelock, The denaturation of lipid-protein complexes as a cause of damage by freezing. Proceedings of the Royal Society of London. Series B - Biological Sciences 147 (1957) 427-433.

[122] J.G.Y. Luc, S.J. Bozso, D.H. Freed, and J. Nagendran, Successful Repair of Donation After Circulatory Death Lungs With Large Pulmonary Embolus Using the Lung Organ Care System for Ex Vivo Thrombolysis and Subsequent Clinical Transplantation. Transplantation 99 (2015) 1-2.

[123] J.G.Y. Luc, N.S. Aboelnazar, S. Himmat, S. Hatami, A. Haromy, N. Matsumura, V. Vasanthan, C.W. White, M. Mengel, D.H. Freed, and J. Nagendran, A Leukocyte Filter Does Not Provide Further Benefit During Ex Vivo Lung Perfusion. ASAIO Journal 63 (2017) 672-678.

[124] T.N. Machuca, M. Cypel, and S. Keshavjee, Advances in lung preservation. Surgical Clinics of North America 93 (2013) 1373-1394.

[125] T.N. Machuca, M.K. Hsin, H.C. Ott, M. Chen, D.M. Hwang, M. Cypel, T.K. Waddell, and S. Keshavjee, Injury-Specific Ex Vivo Treatment of the Donor Lung: Pulmonary Thrombolysis Followed by Successful Lung Transplantation. American Journal of Respiratory and Critical Care Medicine 188 (2013) 878-880.

[126] S. Majdi, N. Najafinobar, J. Dunevall, J. Lovric, and A.G. Ewing, DMSO Chemically Alters Cell Membranes to Slow Exocytosis and Increase the Fraction of Partial Transmitter Released. ChemBioChem 18 (2017) 1898-1902.

[127] G.S. Makin, and J.M. Howard, Dimethyl Sulfoxide and Supercooling for Storage of Canine Kidneys. Archives of Surgery 91 (1965) 564-567.

[128] L.S. Marques, A.A.N. Fossati, R.B. Rodrigues, H.T. Da Rosa, A.P. Izaguirry, J.B. Ramalho, J.C.F. Moreira, F.W. Santos, T. Zhang, and D.P. Streit, Slow freezing versus vitrification for the cryopreservation of zebrafish (Danio rerio) ovarian tissue. Nature Scientific Reports 9 (2019).

[129] S. Masuodi, J. Blackwell, P. Stewart, and T.M. Egan, Cytokine Levels in Steen Solution Perfusate Increase During Ex-Vivo Lung Perfusion (EVLP) of Lungs from Conventional Donors (Conv) and Uncontrolled Donation After Circulatory Determination of Death Donors (uDCDDs). The Journal of Heart and Lung Transplantation 36 (2017) 311-312.

[130] P. Mazur, Kinetics of Water Loss from Cells at Subzero Temperatures and the Likelihood of Intracellular Freezing. The Journal of General Physiology 47 (1963) 347-369.

[131] P. Mazur, S.P. Leibo, and E.H.Y. Chu, A two-factor hypothesis of freezing injury. Experimental Cell Research 71 (1972) 345-355.

[132] P. Mazur, Freezing of living cells: mechanisms and implications. The American journal of physiology 16 (1984) 125-142.

[133] P. Mazur, W.F. Rall, and S.P. Leibo, Kinetics of water loss and the likelihood of intracellular freezing in mouse ova - Influence of the method of calculating the temperature dependence of water permeability. Cell Biophysics 6 (1984) 197-213.

[134] J.H. Mehaffey, E.J. Charles, A.K. Sharma, M. Salmon, D. Money, S. Schubert, M.H. Stoler, C.G. Tribble, V.E. Laubach, M.E. Roeser, and I.L. Kron, Ex Vivo Lung Perfusion Rehabilitates Sepsis-Induced Lung Injury. The Annals of Thoracic Surgery 103 (2017) 1723-1729.

[135] F. Migishima, R. Suzuki-Migishima, S.-Y. Song, T. Kuramochi, S. Azuma, M. Nishijima, and M. Yokoyama, Successful Cryopreservation of Mouse Ovaries by Vitrification. Biology of Reproduction 68 (2003) 881-887.

[136] P.N. Mohite, A. Sabashnikov, D. Garcia Saez, B. Pates, M. Zeriouh, F. De Robertis, and A.R. Simon, Utilization of the Organ Care System Lung for the assessment of lungs from a donor after cardiac death (DCD) before bilateral transplantation. Perfusion 30 (2015) 427-430.

[137] K. Monzen, T. Hosoda, D. Hayashi, Y. Imai, Y. Okawa, T. Kohro, H. Uozaki, T. Nishiyama, M. Fukayama, and R. Nagai, The use of a supercooling refrigerator improves the preservation of organ grafts. Biochemical and Biophysical Research Communications 337 (2005) 534-539.

[138] E.B. Moore, E. De La Llave, K. Welke, D.A. Scherlis, and V. Molinero, Freezing, melting and structure of ice in a hydrophilic nanopore. Physical Chemistry Chemical Physics 12 (2010) 4124-4134.

[139] F. Moradiellos, J. Naranjo, M. Cordoba, C. Salas, D. Gomez, J. Campo-Canaveral, D. Crowley, M. Valle, and A. Varela de Ugarte, Clinical lung transplantation after ex vivo evaluation of uncontrolled non-heart-beating donors lungs: Initial experience. Journal of Heart and Lung Transplantationmm 30 (2011) 38.

[140] C. Morris, and J. McGrath, Intracellular ice nucleation and gas bubble formation in spirogyra. Cryo letters 2 (1981) 341-352.

[141] T. Mukaida, C. Oka, T. Goto, and K. Takahashi, Artificial shrinkage of blastocoeles using either a micro-needle or a laser pulse prior to the cooling steps of vitrification improves survival rate and pregnancy outcome of vitrified human blastocysts. Human Reproduction 21 (2006) 3246-3252.

[142] K. Muldrew, and L.E. McGann, The osmotic rupture hypothesis of intracellular freezing injury. Biophysical Journal 66 (1994) 532-541.

[143] K. Muldrew, K. Novak, H. Yang, R. Zernicke, N.S. Schachar, and L.E. McGann, Cryobiology of articular cartilage: Ice morphology and recovery of chondrocytes. Cryobiology 40 (2000) 102-109.

[144] D. Nakajima, M. Cypel, R. Bonato, T.N. Machuca, I. Iskender, K. Hashimoto, V. Linacre, M. Chen, R. Coutinho, S. Azad, T. Martinu, T.K. Waddell, D.M. Hwang, S. Husain, M. Liu, and S. Keshavjee, Ex Vivo Perfusion Treatment of Infection in Human Donor Lungs. American Journal of Transplantation 16 (2016) 1229-1237.

[145] D. Nakajima, M. Liu, A. Ohsumi, R. Kalaf, I. Iskender, M. Hsin, T. Kanou, M. Chen, B. Baer, R. Coutinho, L. Maahs, P. Behrens, S. Azad, T. Martinu, T.K. Waddell, J.F. Lewis, M. Post, R.A.W. Veldhuizen, M. Cypel, and S. Keshavjee, Lung Lavage and Surfactant Replacement During Ex Vivo Lung Perfusion for Treatment of Gastric Acid Aspiration–Induced Donor Lung Injury. Journal of Heart and Lung Transplantation 36 (2017) 577-585.

[146] NHS Blood and Tranplant, Annual Report on Cardiothoracic Organ Transplantation 2017/2018, 2018.

[147] K. Nishijima, M. Tanaka, Y. Sakai, C. Koshimoto, M. Morimoto, T. Watanabe, J. Fan, and S. Kitajima, Effects of type III antifreeze protein on sperm and embryo cryopreservation in rabbit. Cryobiology 69 (2014) 22-25.

[148] R. Notman, M. Noro, B. O'Malley, and J. Anwar, Molecular Basis for Dimethylsulfoxide (DMSO) Action on Lipid Membranes. Journal of the American Chemical Society 128 (2006) 13982-13983.

[149] F.G.J. Offerjins, and H.F.T. Welle, The effect of freezing, of supercooling and of DMSO on the function of mitochondria and on the contractility of the rat heart. Cryobiology 11 (1974) 152-159.

[150] T. Okamoto, T. Nakamura, J. Zhang, A. Aoyama, F. Chen, T. Fujinaga, T. Shoji, H. Hamakawa, H. Sakai, T. Manabe, H. Wada, H. Date, and T. Bando, Successful sub-zero non-freezing preservation of rat lungs at -2 degrees C utilizing a new supercooling technology. Journal of Heart and Lung Transplantation 27 (2008) 1150-1157.

[151] T. Okamoto, X. Tang, C. Farver, and K. McCurry, Supercooling Preservation at -2°C Protects Rat Lung Grafts from Ischemia-Reperfusion Injury Via Elevated Expression of Heat ShockProtein 70. The Journal of Heart and Lung Transplantation 30 (2011) 136.

[152] F. Pagano, C. Nocella, S. Sciarretta, L. Fianchini, C. Siciliano, G. Mangino, M. Ibrahim, E. De Falco, R. Carnevale, I. Chimenti, and G. Frati, Cytoprotective and Antioxidant Effects of Steen Solution on Human Lung Spheroids and Human Endothelial Cells. American Journal of Transplantation 17 (2017) 1885-1894.

[153] D.E. Pegg, L. Wang, and D. Vaughan, Cryopreservation of articular cartilage. Part 3: The liquidus tracking method. Cryobiology 52 (2006) 360-368.

[154] N. Pertaya, C.B. Marshall, Y. Celik, P.L. Davies, and I. Braslavsky, Direct visualization of spruce budworm antifreeze protein interacting with ice crystals: Basal plane affinity confers hyperactivity. Biophysical Journal 95 (2008) 333-341.

[155] P. Pinton, D. Ferrari, E. Rapizzi, F. Di Virgilio, T. Pozzan, and R. Rizzuto, The Ca2+ concentration of the endoplasmic reticulum is a key determinant of ceramide-induced apoptosis: Significance for the molecular mechanism of Bcl-2 action. EMBO Journal 20 (2001) 2690-2701.

[156] P. Pinton, C. Giorgi, R. Siviero, E. Zecchini, and R. Rizzuto, Calcium and apoptosis: ER-mitochondria Ca2+ transfer in the control of apoptosis. Oncogene 27 (2008) 6407-6418.

[157] J.S. Poisson, J.P. Acker, J.G. Briard, J.E. Meyer, and R.N. Ben, Modulating Intracellular Ice Growth with Cell-Permeating Small-Molecule Ice Recrystallization Inhibitors. Langmuir 35 (2018) 7452-7458.

[158] C. Polge, A.U. Smith, and A.S. Parkes, Revival of spermatozoa after vitrification and dehydration at low temperatures. Nature 164 (1949) 666.

[159] K. Pollock, D. Sumstad, D. Kadidlo, D.H. McKenna, and A. Hubel, Clinical mesenchymal stromal cell products undergo functional changes in response to freezing. Cytotherapy 17 (2015) 38-45.

[160] M.J. Powell-Palm, J. Aruda, and B. Rubinsky, Thermodynamic Theory and Experimental Validation of a Multiphase Isochoric Freezing Process. Journal of Biomechanical Engineering 141 (2019) 081011.

[161] M.J. Powell-Palm, Y. Zhang, J. Aruda, and B. Rubinsky, Isochoric conditions enable high subfreezing temperature pancreatic islet preservation without osmotic cryoprotective agents. Cryobiology 86 (2019).

[162] J.A. Preciado, and B. Rubinsky, Isochoric preservation: A novel characterization method. Cryobiology 60 (2010) 23-29.

[163] K.A. Puttonen, S. Lehtonen, P. Lampela, P.T. Mannisto, and A. Raasmaja, Different viabilities and toxicity types after 6-OHDA and Ara-C exposure evaluated by four assays in five cell lines. Toxicology in Vitro 22 (2008) 182-189.

[164] S. Qadeer, M.A. Khan, M.S. Ansari, B.A. Rakha, R. Ejaz, R. Iqbal, M. Younis, N. Ullah, A.L. DeVries, and S. Akhter, Efficiency of antifreeze glycoproteins for cryopreservation of Nili-Ravi (Bubalus bubalis) buffalo bull sperm. Animal Reproduction Science 157 (2015) 56-62.

[165] A.B. Quintana, C.D. Coda Zabetta, N.O. Baumgartner, M.E. Biancardi, V. Bessone, J.V. Rodriguez, M.E. Mamprin, G. Furno, E.E. Guibert, and V. Sujatovich, Morphological and biochemical analysis of human cardiac valve allografts after an increment of the cryostorage temperature. Cryobiology 59 (2009) 96-101.

[166] K. Raghavendran, J. Nemzek, L.M. Napolitano, and P.R. Knight, Aspiration-induced lung injury. Critical Care Medicine 39 (2011) 818-826.

[167] U. Rauen, and H. de Groot, Mammalian cell injury induced by hypothermia - The emerging role for reactive oxygen species. Biological Chemistry 383 (2002) 477-488.

[168] J.A. Raymond, P. Wilson, and A.L. DeVries, Inhibition of growth of nonbasal planes in ice by fish antifreezes. Proceedings of the National Academy of Sciences of the United States of America 86 (1989) 881-885.

[169] M.R. Raymond, and D.A. Wharton, The ability to survive intracellular freezing in nematodes is related to the pattern and distribution of ice formed. Journal of Experimental Biology 219 (2016) 2060-2065.

[170] L. Rienzi, S. Romano, L. Albricci, R. Maggiulli, A. Capalbo, E. Baroni, S. Colamaria, F. Sapienza, and F. Ubaldi, Embryo development of fresh 'versus' vitrified metaphase II oocytes after ICSI: A prospective randomized sibling-oocyte study. Human Reproduction 25 (2010) 66-73.

[171] S.R. Rosner, S. Ram-Mohan, J.R. Paez-Cortez, T.L. Lavoie, M.L. Dowell, L. Yuan, X. Ai, A. Fine, W.C. Aird, J. Solway, J.J. Fredberg, and R. Krishnan, Airway contractility in the precision-cut lung slice after cryopreservation. American Journal of Respiratory Cell and Molecular Biology 50 (2014) 876-881.

[172] M. Roth, M. Solèr, M. Hornung, L.R. Emmons, P. Stulz, and A.P. Perruchoud, Cell cultures from cryopreserved human lung tissue. Tissue and Cell 24 (1992) 455-459.

[173] B. Rubinsky, and A.L. DeVries, Effect of ice crystal habit on the viability of glycerol-protected red blood cells. Cryobiology 26 (1989) 580.

[174] B. Rubinsky, P.A. Perez, and M.E. Carlson, The Thermodynamic principles of isochoric cryopreservation. Cryobiology 50 (2005) 121-138.

[175] L. Rubinsky, N. Raichman, J. Lavee, H. Frenk, E. Ben-Jacob, and P.E. Bickler, Antifreeze protein suppresses spontaneous neural activity and protects neurons from hypothermia/re-warming injury. Neuroscience Research 67 (2010) 256-259.

[176] I. Ruiz, J. Gavaldà, V. Monforte, O. Len, A. Román, C. Bravo, A. Ferrer, L. Tenorio, F. Román, J. Maestre, I. Molina, F. Morell, and A. Pahissa, Donor-to-host transmission of bacterial and fungal infections in lung transplantation. American Journal of Transplantation 6 (2006) 178-182.

[177] A.T. Sage, J.D. Besant, L. Mahmoudian, M. Poudineh, X. Bai, R. Zamel, M. Hsin, E.H. Sargent, M. Cypel, M. Liu, S. Keshavjee, S.O. Kelley, S.M. Studer, R.D. Levy, K. McNeil, J.B. Orens, J.D. Meester, J.M. Smits, G.G. Persijn, A. Haverich, J.D. Christie, L.B. Edwards, P. Aurora, F. Dobbels, R. Kirk, A.O. Rahmel, D.O. Taylor, A.Y. Kucheryavaya, M.I. Hertz, J.D. Christie, J.S. Sager, S.E. Kimmel, V.N. Ahya, C. Gaughan, N.P. Blumenthal, R.M. Kotloff, J.C. Lee, J.D. Christie, B.F. Meyers, M.d.l. Morena, S.C. Sweet, E.P. Trulock, T.J. Guthrie, E.N. Mendeloff, C. Huddleston, J.D. Cooper, G.A. Patterson, E.P. Trulock, J.D. Christie, L.B. Edwards, M.M. Boucek, P. Aurora, D.O. Taylor, F. Dobbels, A.O. Rahmel, B.M. Keck, M.I. Hertz, M. Anraku, M.J. Cameron, T.K. Waddell, M. Liu, T. Arenovich, M. Sato, M. Cypel, A.F. Pierre, M.d. Perrot, D.J. Kelvin, S. Keshavjee, Y. Suzuki, E. Cantu, J.D. Christie, M.d. Perrot, M. Liu, T.K. Waddell, S. Keshavjee, J.C. Lee, J.D. Christie, S. Keshavjee, J.D. Christie, M. Carby, R. Bag, P. Corris, M. Hertz, D. Weill, G. Thabut, H. Mal, J. Cerrina, P. Dartevelle, C. Dromer, J.F. Velly, M. Stern, P. Loirat, G. Leseche, M. Bertocchi, J.F. Mornex, A. Haloun, P. Despins, C. Pison, D. Blin, M. Reynaud-Gaubert, et al., Unilateral lung transplantation for pulmonary fibrosis. Toronto Lung Transplant Group. The New England journal of medicine 314 (1986) 1140-1145.

[178] E. Sage, S. Mussot, G. Trebbia, P. Puyo, M. Stern, P. Dartevelle, A. Chapelier, M. Fischler, P. Bonnette, D. Mitilian, P. Puyo, N. Salley, E. Sage, A. Chapelier, S. De Miranda, D. Grenet, A. Hamid, C. Picard, A. Roux, M. Stern, J. Bresson, V. Dumans-Nizard, J.L. Dumoulin, S. Ghiglione, S. Jacqmin, M. Le Guen, L. Ley, N. Liu, J.Y. Marandon, M. Michel-Cherqui, O. Pruszkowski, B. Rives, B. Szekely, B. Vandenbunder, N. Verroust, M. Fischler, J. Devaquet, F. Parquin, A.G. Si Larbi, G. Trebbia, and C. Cerf, Lung transplantation from initially rejected donors after ex vivo lung reconditioning: The French experience. European Journal of Cardio-thoracic Surgery 46 (2014) 794-799.

[179] M. Schmidt, E. Zogheib, H. Rozé, X. Repesse, G. Lebreton, C.E. Luyt, J.L. Trouillet, N. Bréchot, A. Nieszkowska, H. Dupont, A. Ouattara, P. Leprince, J. Chastre, and A. Combes, The PRESERVE mortality risk score and analysis of long-term outcomes after extracorporeal membrane oxygenation for severe acute respiratory distress syndrome. Intensive Care Medicine 39 (2013) 1704-1713.

[180] A. Sharma, B. Namsrai, H. Ring, Z. Han, E. Finger, C. Lee, and J. Bischof, Vitrification and nanowarming of livers. Cryobiology 91 (2019) 160.

[181] M. Singh, H. Sharma, and N. Singh, Hydrogen peroxide induces apoptosis in HeLa cells through mitochondrial pathway. Mitochondrion 7 (2007) 367-373.

[182] D.A. Skelly, G.T. Squiers, M.A. McLellan, M.T. Bolisetty, P. Robson, N.A. Rosenthal, and A.R. Pinto, Single-cell transcriptional profiling reveals cellular diversity and intercommunication in the mouse heart. Cell Reports 22 (2018) 600-610.

[183] A.U. Smith, and C. Polge, Survival of spermatozoa at low temperatures. Nature (1950).

[184] G.I. Snell, M. Rabinov, A. Griffiths, T. Williams, A. Ugoni, R. Salamonsson, and D. Esmore, Pulmonary allograft ischemic time: an important predictor of survival after lung transplantation. The Journal of heart and lung transplantation 15 (1996) 160-168.

[185] Y.C. Song, B.S. Khirabadi, F. Lightfoot, K.G.M. Brockbank, and M.J. Taylor, Vitreous cryopreservation maintains the function of vascular grafts. Nature Biotechnology (2000).

[186] S. Steen, T. Sjöberg, L. Pierre, Q. Liao, L. Eriksson, and L. Algotsson, Transplantation of lungs from a non-heart-beating donor. Lancet 357 (2001) 825-829.

[187] S. Steen, Q. Liao, P.N. Wierup, R. Bolys, L. Pierre, and T. Sjöberg, Transplantation of lungs from non-heart-beating donors after functional assessment ex vivo. Annals of Thoracic Surgery 76 (2003) 244-252.

[188] S. Steen, R. Ingemansson, L. Eriksson, L. Pierre, L. Algotsson, P. Wierup, Q. Liao, A. Eyjolfsson, R. Gustafsson, and T. Sjöberg, First Human Transplantation of a Nonacceptable Donor Lung After Reconditioning Ex Vivo. Annals of Thoracic Surgery 83 (2007) 2191-2195.

[189] J.P. Stone, W.R. Critchley, T. Major, G. Rajan, I. Risnes, H. Scott, Q. Liao, B. Wohlfart, T. Sjöberg, N. Yonan, S. Steen, and J.E. Fildes, Altered immunogenicity of donor lungs via removal of passenger leukocytes using ex vivo lung perfusion. American Journal of Transplantation 16 (2016) 33-43.

[190] T. Sultana, J.I. Lee, J.H. Park, and S. Lee, Supercooling Storage for the Transplantable Sources From the Rat and the Rabbit: A Preliminary Report. Transplantation Proceedings 50 (2018) 1178-1182.

[191] T. Takahashi, A. Hirsh, E.F. Erbe, J.B. Bross, R.L. Steere, and R.J. Williams, Vitrification of human monocytes. Cryobiology (1986).

[192] T. Takahashi, A. Kakita, Y. Takahashi, K. Yokoyama, I. Sakamoto, and S. Yamashina, Preservation of rat livers by supercooling under high pressure. Transplantation Proceedings 33 (2001) 916-919.

[193] M.J. Taylor, H.L. Bank, and M.J. Benton, Selective destruction of leucocytes by freezing as a potential means of modulating tissue immunogenicity: Membrane integrity of lymphocytes and macrophages. Cryobiology 24 (1987) 91-102.

[194] M.J. Taylor, B.P. Weegman, S.C. Baicu, and S.E. Giwa, New Approaches to Cryopreservation of Cells, Tissues, and Organs. Transfusion Medicine and Hemotherapy 46 (2019) 197-215.

[195] S. Tessier, S. Cronin, C. Pendexter, R. De Vries, S. Kimura, S. Ozer, H. Yeh, K. Uygun, M. Toner, P. Banik, and S. Nagpal, Partial Freezing: A New Integrated Approach To Organ Banking. Cryobiology 91 (2019) 178.

[196] S.N. Tessier, S.E.J. Cronin, C.A. Pendexter, S. Ozer, R.J. de Vries, S. Nagpal, P.D. Banik, K. Uygun, and M. Toner, Partial freezing: A nature-inspired strategy for organ banking. Cryobiology 81 (2018) 220.

[197] H.E. Tomalty, E.F. Hamilton, A. Hamilton, O. Kukal, T. Allen, and V.K. Walker, Kidney preservation at subzero temperatures using a novel storage solution and insect ice-binding proteins. Cryo-Letters (2017).

[198] A.R. Tonelli, J. Zein, J. Adams, and J.P.A. Ioannidis, Effects of interventions on survival in acute respiratory distress syndrome: an umbrella review of 159 published randomized trials and 29 meta-analyses. Intensive care medicine 40 (2014) 769-787.

[199] J.F. Trant, R.A. Biggs, C.J. Capicciotti, and R.N. Ben, Developing highly active small molecule ice recrystallization inhibitors based upon C-linked antifreeze glycoprotein analogues. RSC Advances 3 (2013) 26005-26009.

[200] S. Tuncer, R. Gurbanov, I. Sheraj, E. Solel, O. Esenturk, and S. Banerjee, Low dose dimethyl sulfoxide driven gross molecular changes have the potential to interfere with various cellular processes. Scientific Reports 8 (2018).

[201] U.S. Department of Health and Human Services, Kaplan-Meier Graft Survival Rates For Transplants Performed : 2008 - 2015, 2019.

[202] F. Valenza, L. Rosso, S. Gatti, S. Coppola, S. Froio, J. Colombo, R. Dossi, M. Pizzocri, V. Salice, M. Nosotti, P. Reggiani, D. Tosi, A. Palleschi, M. Pappalettera, S. Ferrero, A. Perazzoli, D. Costantini, M. Scalamogna, G. Rossi, C. Colombo, L. Santambrogio, and L. Gattinoni,

Extracorporeal lung perfusion and ventilation to improve donor lung function and increase the number of organs available for transplantation. Transplantation Proceedings 44 (2012) 1826-1829.

[203] D. Van Raemdonck, F. Rega, S. Rex, and A. Neyrinck, Machine perfusion of thoracic organs. Journal of Thoracic Disease 10 (2018) S910-S923.

[204] H. Vu, L. Campbell, J. Duman, and K. Brockbank, Increased survivorship in cryopreservation assays with insect and plant antifreeze glycolipids. Cryobiology (2016).

[205] L. Wan, M.J. Powell-Palm, M.G. Clemens, and B. Rubinsky, Time-dependent Effects of Pressure during Preservation of Rat Hearts in an Isochoric System at Subfreezing Temperatures. Cryo Letters 40 (2019) 64-70.

[206] L. Wang, D.E. Pegg, J. Lorrison, D. Vaughan, and P. Rooney, Further work on the cryopreservation of articular cartilage with particular reference to the liquidus tracking (LT) method. . Cryobiology 55 (2007) 138-147.

[207] S.Q. Wang, and Z.Q. Zhou, Alpha-stat calibration of indo-1 fluorescence and measurement of intracellular free calcium in rat ventricular cells at different temperatures. Life Sciences 65 (1999) 871-877.

[208] T. Wang, C.P. Connery, P.R. Batty, G.L. Hicks, J.A. DeWeese, and J.R. Layne, Freezing preservation of adult mammalian heart at high subzero temperatures. Cryobiology 28 (1991) 171-176.

[209] G. Warnecke, J. Moradiellos, I. Tudorache, C. Kuhn, M. Avsar, B. Wiegmann, W. Sommer, F. Ius, C. Kunze, J. Gottlieb, A. Varela, and A. Haverich, Normothermic perfusion of donor lungs for preservation and assessment with the Organ Care System Lung before bilateral transplantation: a pilot study of 12 patients. The Lancet 380 (2012) 24-30.

[210] C.Y. Watson, F. Damiani, S. Ram-Mohan, S. Rodrigues, P.d.M. Queiroz, T.C. Donaghey, J.H.R. Lichtenstein, J.D. Brain, R. Krishnan, and R.M. Molina, Screening for Chemical Toxicity Using Cryopreserved Precision Cut Lung Slices. Toxicological Sciences 150 (2016) 225-233.

[211] J. Wesley-Smith, C. Walters, N.W. Pammenter, and P. Berjak, Why is intracellular ice lethal? A microscopical study showing evidence of programmed cell death in cryo-exposed embryonic axes of recalcitrant seeds of Acer saccharinum. Annals of Botany 115 (2015) 991-1000.

[212] W.N. Wicomb, N.A. Halasz, and G.M. Collins, Damaging effect of subzero temperature (-4 degrees C) on rabbit renal function. Cryobiology 21 (1984) 6-12.

[213] P. Wierup, A. Haraldsson, F. Nilsson, L. Pierre, H. Schertsen, M. Silverborn, T. Sjoberg, U. Westfeldt, and S. Steen, Ex vivo evaluation of nonacceptable donor lungs. The Annals of Thoracic Surgery 81 (2006) 460-466.

[214] S.M. Wishnies, A.R. Parrish, I.G. Sipes, A.J. Gandolfi, C.W. Putnam, C.L. Krumdieck, and K. Brendel, Biotransformation activity in vitrified human liver slices. Cryobiology (1991).

[215] O.H. Wittekindt, Tight junctions in pulmonary epithelia during lung inflammation. Pflugers Archiv European Journal of Physiology 469 (2017) 135-147.

[216] B. Wowk, Thermodynamic aspects of vitrification. Cryobiology 60 (2010) 11-22.

[217] M.C. Wusteman, D.E. Pegg, L.H. Wang, and M.P. Robinson, Vitrification of ECV304 cell suspensions using solutions containing propane-1,2-diol and trehalose. Cryobiology (2003).

[218] J. Xiang, C. Wan, R. Guo, and D. Guo, Is Hydrogen Peroxide a Suitable Apoptosis Inducer for All Cell Types? BioMed Research International 2016 (2016).

[219] J.C. Yeung, T. Krueger, K. Yasufuku, M. de Perrot, A.F. Pierre, T.K. Waddell, L.G. Singer, S. Keshavjee, and M. Cypel, Outcomes after transplantation of lungs preserved for more than 12 h: a retrospective study. The Lancet Respiratory Medicine 5 (2017) 119-124.

[220] K.H. Yoo, S.H. Lee, H.J. Kim, K.W. Sung, H.L. Jung, E.J. Cho, H.K. Park, H.A. Kim, and H.H. Koo, The impact of post-thaw colony-forming units-granulocyte/macrophage on engraftment following unrelated cord blood transplantation in pediatric recipients. Bone Marrow Transplantation 39 (2007) 515-521.

[221] G. Yu, R. Li, and A. Hubel, Interfacial Interactions of Sucrose During Cryopreservation Detected by Raman Spectroscopy. Langmuir 35 (2019) 7388-7395.

[222] Z. Yu, and P.J. Quinn, The effect of dimethyl sulphoxide on the structure and phase behaviour of palmitoleoylphosphatidylethanolamine. Biochimica et Biophysica Acta (BBA) - Biomembranes 1509 (2000) 440-450.

[223] S. Zeerleder, T. Mauron, B. Lämmle, and W.A. Wuillemin, Effect of low-molecular weight dextran sulfate on coagulation and platelet function tests. Thrombosis Research 105 (2002) 441-446.

[224] M.A.J. Zieger, E.E. Tredget, and L.E. Mcgann, Cryomicroscopy of an in situ cell model of skin, Cryo-Letters, 1997.

[225] L. Zilli, J. Beirão, R. Schiavone, M.P. Herraez, A. Gnoni, and S. Vilella, Comparative proteome analysis of cryopreserved flagella and head plasma membrane proteins from sea bream spermatozoa: Effect of antifreeze proteins. PLoS ONE 9 (2014).

[226] B. Zobrist, C. Marcolli, T. Peter, and T. Koop, Heterogeneous ice nucleation in aqueous solutions: The role of water activity. Journal of Physical Chemistry A 112 (2008) 3965-3975.

[227] B. Zych, A.F. Popov, G. Stavri, A. Bashford, T. Bahrami, M. Amrani, F. De Robertis, M. Carby, N. Marczin, A.R. Simon, and K.C. Redmond, Early outcomes of bilateral sequential single lung transplantation after ex-vivo lung evaluation and reconditioning. Journal of Heart and Lung Transplantation 31 (2012) 274-281.